HUAZHONG AGRICULTURAL UNIVERSITY

COLLEGE OF LIFE SCIENCE AND TECHNOLOGY

AND

BURGUNDY UNIVERSITY

ÉCOLE DOCTORALE ENVIRONNEMENT-SANTÉ-STIC

State Key Laboratory of Agricultural Microbiology

and

Pôle IPM CNRS ERL 6300, Mixed Research Unit 1347 Agroecologie

THESIS

To obtain the grade of
Doctor of Huazhong Agricultural University
Discipline: Microbiology
and
Doctor of Burgundy University
Speciality: Biochemistry, Cellular and Molecular Biology

Presented by

LIU Yi

CALCIUM-RELATED FUNGAL GENES IMPLICATED IN ARBUSCULAR MYCORRHIZA

Defended publicly 10th December 2012

Professor Zixin Deng, Wuhan University, Wuhan	Reporter
Professor Philipp Franken, Leibniz Institute and Humboldt University, Berlin	Reporter
Professor Bin Zhao, Huazhong Agriculture University,Wuhan	Supervisor
Dr. Vivienne Gianinazzi-Pearson, Directeur de Recherche CNRS, Dijon	Supervisor
Dr. Diederik van Tuinen, Chargé de Recherche INRA, Dijon	Co-supervisor
Professor Daniel Wipf, Burgundy University, Dijon	Examiner
Professor Zhongming Zhang, Huazhong Agriculture University, Wuhan	Examiner
Professor Yucai Liao, Huazhong Agriculture University, Wuhan	Examiner

TABLE OF CONTENTS

ABBREVIATIONS **4**

ABSTRACT **5**

RESUME **6**

摘要 **7**

CHAPTER 1 ..... **8**

GENERAL INTRODUCTION **8**

1.1. The arbuscular mycorrhiza symbiosis 9
1.2. Molecular mechanisms regulating the AM symbiosis 12
1.3. Calcium-regulated signaling events in cells 16
1.4. Thesis objectives 21

CHAPTER 2 ..... **23**

MATERIAL AND METHODS **23**

2.1. Biological materials and growth conditions 24
2.2. Estimation of mycorrhizal root colonization 27
2.3. Laser Capture Microdissection (LCM) of arbuscule-containing cortical root cells 29
2.4. Nucleic acid preparation from spores and roots 30
2.5. Fungal gene selection and primer design 32
2.6. Polymerase chain reaction (PCR) 36
2.7. PCR amplification on genomic DNA 42
2.8. Yeast complementation 45
2.9. Statistical analysis 46

CHAPTER 3 ..... **48**

STUDIES OF *G. MOSSEAE* GENES EXPRESSED BEFORE ROOT CONTACT WITH *A. SINICUM* **48**

3.1. Fungal gene expression monitored by reverse-transcription (RT)-PCR 49
3.2. Full length gene sequences and analyses 50
3.3. Localization of *G. mosseae* Gm152 gene activity in mycorrhizal roots of *A. sinicus* 53
3.4. Discussion and conclusions 55

CHAPTER 4 ..... **57**

GROWTH AND MYCORRHIZA DEVELOPMENT IN WILD-TYPE AND MYCORRHIZA-DEFECTIVE MUTANT PLANTS **57**

4.1. *Medicago truncatula* wild-type J5 and the mutant TRV25 58
4.2. Wild type *Pisum sativum L.* cv Finale and the mutant *Pssym36* 60
4.3. Discussion and conclusions 61

CHAPTER 5 ..... **62**

SELECTION OF *G. INTRARADICES* GENES RELATED TO CALCIUM HOMEOSTASIS AND SIGNALLING IN ARBUSCULAR MYCORRHIZA INTERACTIONS **62**

5.1. Homology searches and primer design for fungal genes based on selected ESTs in *G. intraradices* DAOM 197198 (syn. *R. irregularis*) 63
5.2. Fungal gene expression monitored by reverse-transcription (RT)-PCR 67
5.3. Discussion and conclusions 71

CHAPTER 6 ..... **72**

EXPRESSION OF *G. INTRARADICES* GENES ENCODING CA^{2+}-RELATED PROTEINS IN INTERACTIONS WITH WILD-TYPE OR MYC- MUTANT ROOTS OF *MEDICAGO TRUNCATULA* **72**

6.1. Relative quantitative Real-time RT-PCR 73
6.2. Absolute quantitative Real-time RT-PCR 78
6.3. Discussion and conclusions 80

CHAPTER 7 84

LOCALIZATION OF GENE ACTIVITY IN *G. INTRARADICES* DURING PRESYMBIOTIC STAGES AND DEVELOPMENT WITH ROOTS 84

7.1. *In situ* RT-PCR 85
7.2. Laser cryo-microdissection 86
7.3. *G. intraradices* gene expression in *P. sativum L.* wild-type and mutant genotypes 88
7.4. Discussion and conclusions 90

CHAPTER 8 92

FUNCTIONAL CHARACTERIZATION OF THREE *G. INTRARADICES* BEG141 GENES 92

8.1. Full length gene sequencing and phylogenetic analyses 93
8.2. Yeast complementation assays 97
8.3. Discussion and conclusions 104

CHAPTER 9 106

GENERAL DISCUSSION AND CONCLUSIONS 106

REFERENCES 115

ACKNOWLEDGEMENTS 126

Abbreviations

AM	Arbuscular mycorrhiza
dai	Days after inoculation
bp	Base pair
CaM	Calmodulin
CCaMK	Ca^{2+}/calmodulin-dependent protein kinase
cDNA	Complementary deoxyribonucleic acid
cv.	Cultivar
DESAT	Stearoyl-CoA desaturase
DMI	Doesn't make infections
DNA	Deoxyribonucleic acid
dNTP	Deoxyribonucleoside triphosphate
ER	Endoplasmic reticulum
EST	Expressed sequence tag
LCM	Laser capture microdissection
LSU	Large subunit rRNA
Myc	Mycorrhiza
Nod	Nodule formation
PAM	Periarbuscular membrane
PAS	periarbuscular space
PCR	Polymerase chain reaction
PPA	Prepenetration apparatus
Q-PCR	Quantitative real-time RT-PCR
RNA	Ribonucleic acid
RT-PCR	Reverse transcription polymerase chain reaction
SSH	Suppressive subtractive hybridization
Taq	Thermophilus aquaticus
TEF	Translation elongation factor
SD	Synthetic defined
Sym	Symbiotic
YPD	Yeast Extract Peptone D-glucose

Chapter 1

General Introduction

1.1. The arbuscular mycorrhiza symbiosis

Arbuscular mycorrhiza (AM) are a unique example of a ubiquitous symbiosis between soil borne fungi (Glomeromycota) and plant roots which leads to reciprocal benefits to both partners. The mutualistic symbiotic associations that AM fungi form with the roots of more than 80% of land plant families facilitate plant mineral nutrient uptake (e.g. P, N, trace elements,..), enhance tolerance to environmental stresses (e.g. salinity, heavy metals, drought) and reduce root diseases caused by pathogenic fungi or nematodes (Smith and Read, 2008). In return, AM fungi obtain carbohydrates from their host plants. The mycorrhizal symbiosis impacts on plant survival, ecosystem variability and productivity, and is consequently a major factor contributing to the maintenance of plant biodiversity and to ecosystem functioning (Smith and Read, 2008).

AM fungi form an independent phylum, the Glomeromycota, where they are presently subdivided into four orders (Glomerales, Archaeosporales, Paraglomerales and Diversisporales) (Schüβler et al., 2001). Nowadays, new perspectives and new findings from gene-based studies are facilitating our understanding of the complex network of fungal-plant interections which regulate the AM symbiosis (Lanfranco and Young, 2012).

1.1.1. AM developmental stages

Because of their obligate biotrophy, AM fungi are incapable of completing their life cycle in the absence of a host root. Although they can persist in soil as spores (Smith and Read, 2008), asymbiotic spore germination and hyphal growth are important events which determine root colonization and the establishment of the mycorrhizal symbiosis. After spore germination, hyphal growth is very limited and the fungi must colonize root tissues of a host plant for their reproduction and long-term survival.

The different stages in the formation of the symbiosis between AM fungi and plant roots require a series of important morphological changes in each partner which can lead to structurally distinct types of AM (*Paris* vs *Arum*) depending on the plant and fungus involved. The *Paris*-type is characterized by the growth of hyphae directly from one root cell to the next whilst in the *Arum*-type, fungal spread along the root is by intercellular hyphae which grow in the spaces between plant cells (Smith and Smith, 1997).

Early interactions between AM fungi and plants begin when spore germination and hyphal growth are stimulated by host root exudates (Gianinazzi-Pearson et al., 1989) (Fig.

1.1). As hyphae from germinating soil-borne spores come into contact with the host root surface, they form a special type of appressorium called hyphopodium which is necessary for root penetration.

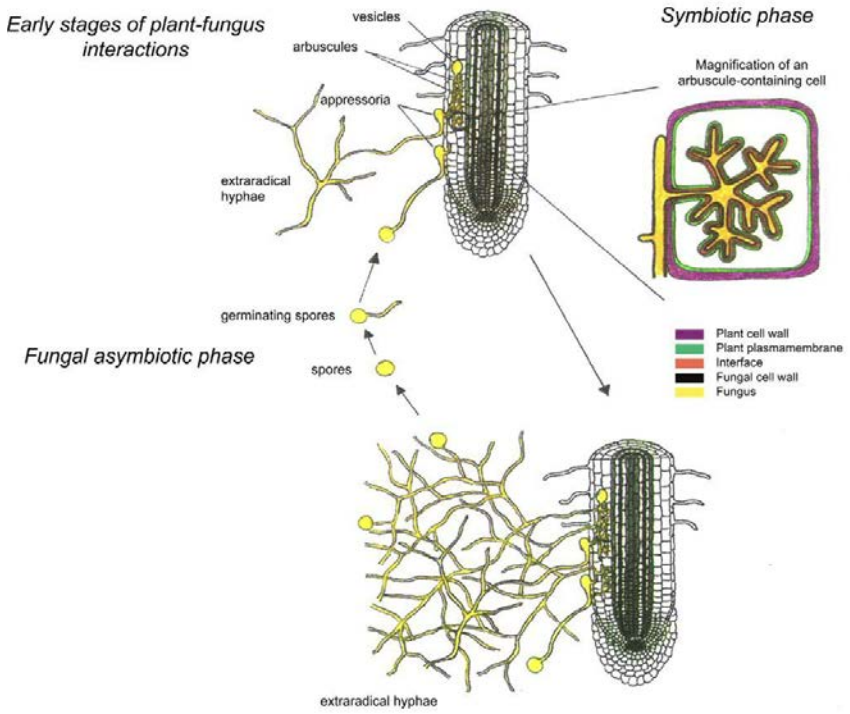


Fig. 1.1 Different stages of root colonization by an arbuscular mycorrhizal fungus (taken from Balestrini and Lanfranco, 2006).

Under a hyphopodium, plant cells produce a prepenetration apparatus (PPA) which guides the fungus through root cells towards the inner cortex. The plant cell nucleus moves ahead of the growing PPA and directs its orientation within the cell. After completion of the PPA, a fungal hypha extends from the hyphopodium, enters the PPA to cross the plant cell and, in the case of *Arum*-type AM, enters the intercellular space, where it grows laterally along the root axis between the root cells. The intercellular hyphae induce the development of PPA-like structures in the inner cortical cells, subsequently enter these cells and branch to form arbuscules (Fig.1.2) (Genre et al., 2008).

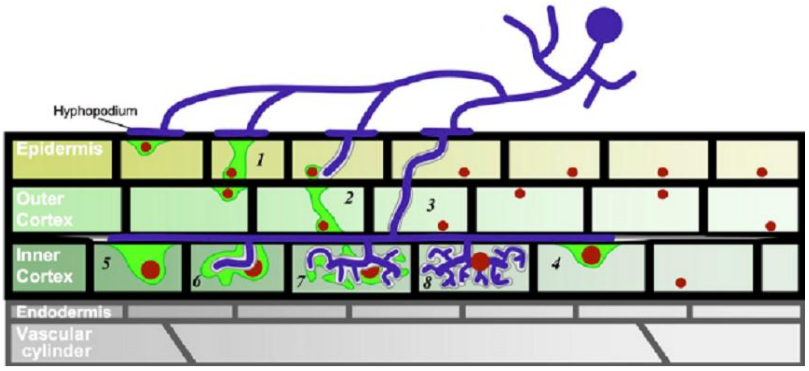


Fig. 1.2. Schema summarizing the *Arum*-type AM colonization pattern and associated cellular dynamics in *M. truncatula* (taken from Genre et al., 2008). (1) The adhesion of a fungal hyphopodium to the root surface triggers repositioning of the host nucleus and the assembly of a PPA in the contacted epidermal cell; (2) PPA formation in the underlying outer cortical cell; (3) Hypha crossing the outer root layers; (4) Nuclear reposition in inner cortical cells upon hyphal contact; (5) Formation of PPAs in the inner cortical cells; (6) Inner cortical cell penetration; (7) Arbuscule branch formation; (8) Completed arbuscule development.

The arbuscule branches within the plant cell are surrounded by a plant-derived periarbuscular membrane (PAM) that is continuous with the plant peripheral plasma membrane and which excludes contact of the fungus with the plant cytoplasm. The resulting surface of contact between the plant protoplast and the fungal cell creates the symbiotic interface, a specialized apoplastic zone for nutrient exchange between the mycorrhizal symbionts (Gianinazzi-Pearson, 1996). The apoplastic interface formed between the fungal plasma membrane and the plant-derived PAM is called the periarbuscular space (PAS) (Fig.1.3) Because of the cell-wall synthesizing potential of both the fungal membrane and the PAM, the PAS comprises fungal and plant cell-wall material.

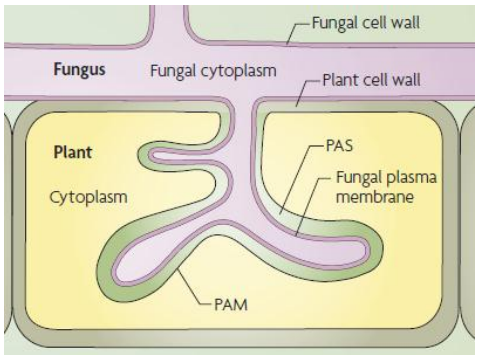


Fig. 1.3. Structure of the intracellular arbuscule (taken from Parniske, 2008). The periarbuscular memebrane (PAM) is continuous with the plant plasma membrane and excludes the fungus from the plant cytoplasm. The periarbuscular space (PAS) is the apoplastic interface between the fungal cell wall and the plant-derived PAM.

Once the fungus is established within the host roots and arbuscules are formed, a network of extraradical hyphae develops out into the soil which serves for nutrient uptake and the formation of resting spores, thus completing the fungal life-cycle (Fig. 1.1). Vesicles are also formed by the fungi, in roots or on soil mycelium, as storage organs.

1.2. Molecular mechanisms regulating the AM symbiosis

Interactions between plants and AM fungi begin with the recognition and the exchange of molecular signals which trigger the morphological changes necessary for symbiosis establishment (Gianinazzi‐Pearson et al., 2007). The resulting symbiosis is characterized by modifications in gene expression in both partners (Balestrini and Lanfranco, 2006; Massoumou et al., 2007).

1.2.1. Recognition and exchange of molecular signals for symbiosis establishment

Recent studies indicate that plants and AM fungi perceive each other prior to their physical interaction (Gianinazzi‐Pearson et al., 2007; Bonfante and Genre, 2010; Bonfante and Requena, 2011). There is much interest in the molecular identification of the plant and fungal signals involved. It was predicted that AM fungi can sense components from host root exudates in the rhizosphere and “branching factors” secreted from plant were found to be responsible for the induction of hyphal branching (Buee et al., 2000) and

alterations in fungal mitochondrial activity, thus leading to the developmental switch from asymbiosis to presymbiosis (Tamasloukht et al. 2003) . Flavonoids and strigolactones contained in host plant root exudates have been found to act as plant signals which enhance AM fungal activity, growth and root colonization (Steinkellner et al., 2007). Meanwhile, the fungus produces diffusible signal molecules, termed 'Myc factors' in analogy to the Nod factors produced by symbiotic rhizobia, which affect plant gene expression, induce signal perception Ca^{2+} spiking responses within host cells and stimulate lateral root formation (Kosuta et al., 2003; Weidmann et al., 2004; Navazio and Mariani, 2008; Chabaud et al., 2011). Recently, an AM fungal lipochitooligosaccharide was identified as stimulating M. truncatula root growth and branching through a Ca^{2+}-dependent symbiotic signalling pathway (Maillet et al., 2011).

1.2.2. Symbiosis-related transcriptional changes during AM formation

The plant partner

A large number of early and late mycorrhiza-induced genes have been identified in the plant partner (Parniske, 2008; Oldroyd et al., 2009; Bonfante and Requena, 2011). Molecular events associated with AM development and/or functioning include signal perception and transduction, plant defense responses, transmembrane nutrient transport and common properties between AM and the nodulation symbiosis (Dumas-Gaudot et al., 2004; Lévy et al., 2004; Siciliano et al., 2007). Modifications in plant gene expression have been studied before and during appressorium development. For example, expression of the *M. truncatula* gene *MtENOD11*, coding for a putative cell wall repetitive proline-rich protein (RPRP) in roots, is induced by the diffusible factor from AM fungi (Kosuta et al., 2003). A plant Clp serine protease is activated in pea roots induced by *Glomus mosseae* during hyphopodium formation which may have multiple functions related to the cross-talk between plant and fungal partners and/or controlling levels of key regulatory proteins within a signal-transduction pathway during early interactions in arbuscular mycorrhiza (Roussel et al. 2001). Also, suppressive-subtractive cDNA libraries have identified a number of plant genes that are up-regulated during these early stages of fungal interactions with roots (Weidmann et al., 2004; Siciliano et al., 2007).

Initial steps of root colonization by AM fungi or rhizobia are regulated by a number of common plant genes through a so-called common Sym pathway (Parniske, 2008). In *M.*

truncatula, the common Sym genes *DMI1*, *DMI2* and *DMI3* have been particularly well studied (Catoira et al., 2000; Oldroyd et al., 2005; Oldroyd et al., 2009). In silico and microarray-based transcriptome profiling approaches have been carried out to uncover the transcriptome of developing root nodules and AM roots of *Medicago truncatula*. Hundreds of genes have been found to be activated in different stages of either symbiosis, of which almost 100 are co-induced during nodulation and AM development (Küster et al., 2007). However, transcriptome studies have also indicated that the two symbioses involve independent recognition and signaling pathways, with early discrimination by plant roots between the different microbial symbionts (Weidmann et al., 2004; Küster et al., 2007).

Targeted and non-targeted approaches to search for differentially expressed genes have revealed the complexity of transcriptional changes also during late stages of the AM symbiosis, as well as the identification of plant genes exhibiting common responses to different AM fungi (see for example, Brechenmacher et al., 2004; Küster et al., 2007; Massoumou et al., 2007). Symbiosis-induced plant phosphate transporter genes have received particular attention. Several have been identified in different plant species, like potato, rice and *M. truncatula*, which are probably involved in the transfer of fungus-delivered phosphate into colonized plant cells (Karandashov and Bucher, 2005; Javot et al., 2007).

The fungal partner

Most of the effort put into identifying gene expression patterns in AM interactions has focused on plant genes. Research on AM fungi is hampered by their obligate biotrophic life style and the fact that they are so far not amenable to genetic manipulation, furthermore knowledge about fungal gene expression in the symbiosis has remained relatively limited (Balestrini and Lanfranco, 2006; Seddas et al., 2009; Bonfante and Genre, 2010; Kutznetsova et al., 2010), although recently published genome-wide transcriptomic data open new opportunities (Tisserant et al., 2012; Lanfranco and Young, 2012). Franken et al. (1997) first reported the identification of expressed arbuscular mycorrhizal fungal genes in spores during asymbiosis stage. In recent years, progress has been made in studies of the fungal genes involved in mycorrhiza development and/or function using different approaches (Gianinazzi-Pearson et al., 2007; Genre and Bonfante, 2007). For example, the construction of cDNA libraries and gene expression profiling during appressorium development by *Glomus mosseae* has identified some up-regulated genes related to Ca^{2+}-dependent signaling, suggesting that calcium may play a role in the early stages of

mycorrhiza formation (Breuninger and Requena, 2004). Also, the upregulation of a number of genes associated with increased cell activity has been detected in *Gigaspora rosea* during presymbiotic phase in the presence of plant root exudates (Tamasloukht et al. 2007). Using differential RNA display, Tamasloukht et al. (2003) showed that extensive hyphal branching observed by *Gigaspora rosea* spores in response to the increased expression of several genes encoding mitochondrial proteins. Plant mutants have also been used to investigate the symbiosis-associated fungal molecular responses. Genotypes of *M. truncatula* mutated for Ca^{2+}-dependent signalisation cascades can down-regulate gene expression of *G. intraradices* at early stages of fungal development (Seddas et al. 2009). In pea mutants where arbuscule formation is inhibited or fungal turnover modulated, most of the studied *G. intraradices* genes were down regulated when arbuscule formation was defective (Kuznetsova et al., 2010). Recent techniques like *in situ* RT-PCR and laser capture microdissection corroborate arbuscule-related fungal gene expression (Balestrini et al., 2007; Seddas et al., 2008; Kuznetsova et al., 2010), and heterologous complementation experiments are leading to the identification of gene function in systems using fungi other than yeast (Tollot et al., 2009; Kloppholz et al., 2011). These approaches offer new perspectives for the detailed analysis of fungal developmental processes that occur during functional differentiation in symbiotic arbuscular mycorrhiza interactions.

Research on the AM fungal partner has focused particularly on genes associated with nutrient uptake, and a number of related fungal genes that are up-regulated during the symbiosis have been identified (Govindarajulu et al., 2005; Karandashov and Bucher, 2005; López-Pedrosa et al., 2006; Balestrini et al., 2007; Cappellazzo et al., 2008). For example, an ammonium transporter *GintAMT1* from *G. intraradices* is expressed in the extraradical mycelium where NH_4^+ is taken up from the surrounding medium (López-Pedrosa et al., 2006). The expression of gene *GmosAAP1*, coding an amino acid permease from *G. mosseae*, was detected in the extraradical fungal structures, and transcript abundance increased upon exposure to organic nitrogen suggesting a role in the first steps of amino acid acquisition from the soil resources (Cappellazzo et al., 2008). Three AM fungal phosphate transporter genes have been identified so far: *GvPT*, *GiPT* and *GmosPT*, from *G. versiforme*, *G. intraradices* and *G. mosseae*, respectively (Harrison and van Buuren, 1995; Maldonado-Mendoza et al., 2001; Benedetto et al., 2005). The expression of the phosphate transporter genes from *G. versiforme* (*GvPT*) and *G. intraradices* (*GiPT*) has been detected predominantly in the extraradical mycelium, thus indicating a role in Pi acquisition from the soil (inport the Pi) (Harrison and van Buuren, 1995; Maldonado-Mendoza et al., 2001).

However, transcripts of *GvPT* were also weakly detected in *M. truncatula* roots colonized by *G. versiforme* (Harrison and van Buuren,1995), and the phosphate transporter gene from *G. mosseae* (*GmosPT*) showed activity in arbuscules (Benedetto et al., 2005). It was suggested that the presence of phosphate transporter transcripts in intraradical mycelium may indicate that, inside the root, the AM fungus somehow controls the amount of phosphate delivered to the plant by re-absorbing Pi released from neighboring plant cells (Benedetto et al., 2005; Balestrini et al., 2007; Tisserant et al., 2012).

1.3. Calcium-regulated signaling events in cells

Many cell processes depend on internal signals composed of small molecules which bind and activate protein kinases, ion channels, and other proteins, to initiate or continue signaling cascades (Borges-Walmsley and Walmsley, 2000; Mansilla et al., 2008; Dahan et al., 2010). These intracellular messengers include, amongst others, cyclic nucleotides (cAMP), inositol trisphosphate (IP_3), diacylglycerol (DAG) and calcium ions (Ca^{2+}) (Wakelam, 1998; Borges-Walmsley and Walmsley, 2000; Nash et al., 2001).

Ca^{2+} is an important signaling molecule in cell responses to various environmental stimuli, including abiotic stresses (e.g. salt, cold, drought, ozone, metals) as well as biotic elicitors from bacteria and fungi. The signature of Ca^{2+} responses is cell type and organ specific (Boudsocq and Sheen, 2010). Signaling occurs when the cell is stimulated to release calcium ions (Ca^{2+}) from intracellular stores, and/or when calcium enters the cell through plasma membrane ion channels (Clapham, 2007). Stimuli from the external medium or from subcellular compartments elevate cytosolic free Ca^{2+} concentrations in cells, often as repetitive oscillations or spiking (McAinsh and Pittman, 2009). Elevation of cytosolic Ca^{2+} levels functions as a major secondary messenger in cell physiology and signaling where Ca^{2+} channels and transporters, Ca^{2+} sensors, and signal transducers are conserved essential components of the cellular Ca^{2+} signaling machinery, named the "calciome" (Ton and Rao, 2004). This can underlie Ca^{2+} homeostasis in cells by regulating movement of ions between the extracellular environment, cells and subcellular compartments and so provide mechanisms for generating Ca^{2+} signals (Dodd et al., 2010).

Ca^{2+} entering cells can bind to and activate the universal Ca^{2+} sensor protein calmodulin (CaM). Many downstream transcriptional and translational events are controlled by such Ca^{2+}-mediated activation of CaM. A primary downstream interpreter of Ca^{2+} signals is phosphorylation which is regulated by Ca^{2+}-dependent kinases and

phosphatases following the activation of CaM. As a result, transcription factors are activated through reversible phosphorylation by these proteins, leading to downstream gene expression (Dodd et al. 2010).

In yeast, Ca^{2+} entering the cytosol via the plasma membrane channel complex Cch1/Mid1 binds to calmodulin and activates the CaM kinases CMK1 and CMK2 and the phosphatase calcineurin. Dephosphorylation by calcineurin activates the transcriptional regulator Crz1 (Calcineurin-Responsive Zinc Finger) /Tcn1, leading to nuclear translocation and transcription of target genes involved in cell physiological processes. Two Ca^{2+}-ATPases, located in the vacuolar (PMC1) and the Golgi (PMR1) membranes, and a vacuolar calcium ion transporter (vacuolar Ca^{2+}/H^{+} exchanger) (VCX1) are responsible for depleting the cytosolic Ca^{2+} to maintain low levels compatible for growth. Activation of calcineurin leads to the transcriptional induction of the *Pmc1* and *Pmr1* genes via Crz1 but inhibits the function of VCX1. Consequently, PMC1 and VCX1 independently transport cytosolic Ca^{2+} into vacuoles.

1.3.1 Ca^{2+} flux in organelles

Calcium elevation is not only induced in the cytosol but also in other cellular compartments, including the nucleus and mitochondria. Calcium influxes into the cytosol or organelles via ion channels in the plasma membrane and endomembranes, and Ca^{2+} effluxes via transporters which remove Ca^{2+} from the cytosol or organelles. This allows replenishment of internal and external stores in the cell, and a return to basal Ca^{2+} levels, which may contribute to shaping specific and distinct Ca^{2+} signatures in the different cell compartments (McAinsh and Pittman, 2009). Endoplasmic reticulum, vacuoles and mitochondria have important functions in Ca^{2+} homeostasis where Ca^{2+} pumps and/or exchangers are regulated to maintain cytoplasmic Ca^{2+} balance (Ton and Rao, 2004).

The large vacuole in fungi and plants serves as a major store for Ca^{2+}, for the purposes of both detoxification and signaling (Ton and Rao, 2004). A remarkable feature of yeast vacuoles is their ability to sequester large amounts of Ca^{2+} and release it in response to particular stimuli. The vacuole probably receives a small amount of Ca^{2+} through the fusion of vesicles derived from the Golgi complex, which acquires Ca^{2+} directly from secretory pathway Ca^{2+}-ATPases (SPCAs) or indirectly from the environment through endocytosis, but the large majority of vacuolar Ca^{2+} comes directly from the cytoplasm through the action of Ca^{2+} pumps and Ca^{2+}/H^{+} exchangers that are specifically localized in

the vacuole membrane (Cunningham, 2011).

Most of the Ca^{2+} in the fungal and plant vacuoles is immobilized in the form of complexes with inorganic polyphosphate (Cunningham, 2011). AM fungi are characterized by an extensive vacuolar system which is considered central for sequestering and transfering phosphate that accumulates within the hyphae after uptake from soil (Smith and Gianinazzi-Pearson, 1988). Ca^{2+} has been co-localized with polyphosphate in the vacuoles of the AM fungal cells, suggesting a role of Ca^{2+} in the phosphate metabolism in mycorrhizal tissues (Strullu et al., 1981). In this context, it has been proposed that the vacuolar H^+/Ca^{2+} transporters CAX1 and CAX3 in *Arabidopsis* may be involved in Pi homeostasis because a *cax*1/*cax*3 double mutant is affected in Ca^{2+} homeostasis and shows 66% more shoot Pi than the wild type (Cheng et al., 2005).

To maintain a low cytosolic Ca^{2+} concentration, cells also actively pump the ion from the cytosol into the endoplasmic reticulum (ER) or Golgi and also mitochondria, as well as into the extracellular space. During Ca^{2+}-signalling in animal cells, the sarco (endo) plasmic reticulum Ca^{2+}-ATPase (SERCA pump) regulates Ca^{2+} levels by effluxing the ion into the endoplasmic reticulum lumen which also serves as an intracellular Ca^{2+} store (Berridge et al., 2003). In *Arabidopsis*, the ER-type Ca^{2+}-ATPases (ECA) play an important role in regulating cytosolic cation levels. ECA1 and ECA3 also have an important role in tolerance to Mn^{2+} stress. ECA1 was found to be localized at the ER, while ECA3 was found associated with Golgi and post-Golgi vesicles (Dodd et al., 2010). Ca^{2+} is constantly seeping out of the ER into the cytoplasm and SERCAs pump it back into the ER. Specific signals can increase the cytoplasmic Ca^{2+} level by opening channels in the ERor the plasma membrane. The most common signaling pathway that increases cytoplasmic calcium concentration is the phospholipase C (PLC) pathway. Many cell surface receptors, including G protein-coupled receptors and receptor tyrosine kinases, activate the phospholipase C enzyme. PLC hydrolyses the membrane phospholipid PIP_2 to form two second messengers, IP3 and diacyglycerol (DAG). DAG activates the protein kinase C enzyme, while IP_3 diffuses to the endoplasmic reticulum, binds to its receptor (IP_3 receptor), which is a Ca^{2+} channel, and thus releases Ca^{2+} from the ER. After such store depletion, a Ca^{2+} entry mechanism, "Store-Operated Channels" (SOCs) is activated. The inflowing calcium current that results after ER calcium have been released is referred to as Ca^{2+}-release-activated Ca^{2+} current (CRAC). The four-transmembrane domain plasma-membrane protein, Orai1 and the EF-hand protein STIM 1 are required for CRAC activity, that is, Orail and STIM1 are possible mediators of CRAC (Clapham, 2007).

Mitochondria also regulate internal Ca^{2+} levels which are important for signaling and for driving mitochondrial function in cells. The main mechanism depends on the rapid sequestration of the ion from the cytoplasm via Ca^{2+}-binding mitochondrial carriers (Satrústegui et al., 2007). Mitochondria not only control their own intra-organelle Ca^{2+} concentration but they also influence the entire cellular network of cellular Ca^{2+} signaling, including the endoplasmic reticulum, the plasma membrane, and the nucleus. Ca^{2+} channeling between mitochondria and the endoplasmic reticulum collaborate in the regulation of Ca^{2+} influx and extrusion through the plasma membrane Ca^{2+} ATPases (PMCA). In addition, mitochondrial and nucleus communicate through a Ca^{2+} signal (Szabadkai and Duchen, 2008).

There is some evidence that the nuclei of plant cells may generate Ca^{2+} signals independently of the cytosol (Mazars et al., 2009). Studies of signaling events involved in the nodulation process in legumes have clearly shown that Nod factor-induced changes in intracellular Ca^{2+} are frequently observed as Ca^{2+} oscillations in the nuclear region (Oldroyd and Downie, 2006). It has been hypothesized that Ca^{2+}/CaM-dependent protein kinases (CaMKs) play pivotal roles in decoding nuclear Ca^{2+} signals. CaMKs co-ordinate and translate calcium fluxes into appropriate cellular responses via phosphorylation. The kinases CaMKI, CaMKII and CaMKIV are partially regulated by the intracellular calcium receptor calmodulin (CaM). Calcium/CaM binding alone produces maximal activity of CaM kinase II (CaMKII), whereas CaMKI and CaMKIV require phosphorylation of a threonine residue by CaMK kinase (CaMKK) for maximal activity. That is, Ca^{2+}-CaM can activate CaM kinase kinase (CaMKK), after that, CaM kinase I (CaMKI) and CaMKIV are activated by CaM kinase kinase (CaMKK), thus enable to phosphorylate various protein targets (Corcoran and Means, 2001). CaM regulates two CaMKK-encoding genes which in turn activate CaMKI and CaMKIV. In mammalian cells, CaMKI is cytoplasmic, CaMKII is cytoplasmic or nuclear whilst CaMKIV is predominantly in the nucleus (Kahl and Means, 2003). The CaMK cascade is thus well positioned to affect cytoplasmic events, but it is more difficult to explain its effects on transcription. Whether CaMKI enters the nucleus or affects transcription through a cytoplasmic intermediate has not been well studied, but it can stimulate transcription of reporters in transient transfection assays, and the molecular mechanisms that regulate the translocation of particular proteins into the nucleus are unknown (Kahl and Means, 2003; Dahan et al., 2010).

1.3.2. Ca^{2+}-related gene expression related to AM establishment

Calcium is a key secondary messenger in cell functional processes and changes in Ca^{2+} levels represent intracellular signaling events in biological systems, including mutualistic and pathogenic plant-microbe interactions (Vadassery and Oelmüller, 2009). Convincing evidence for the implication of plant genes regulating Ca^{2+} signaling in recognition responses of roots to symbiotic AM fungi has come from studies of various host plants and their symbiosis-defective genotypes mutated for Ca^{2+}-dependent signalisation cascades (Weidmann et al., 2004; Sanchez et al., 2005; Oldroyd and Downie, 2006; Gianinazzi‐Pearson et al., 2007). In *M. truncatula*, for example, three nodulation-related genes, *MtDMI1* (cation channel), *MtDMI2* (leucine-rich-repeat receptor kinase) and *MtDMI3* (calcium and calmodulin-dependent protein kinase), are also involved in the formation of arbuscular mycorrhiza. The non-symbiotic Nod^-/Myc^- mutants *dmi1* and *dmi2* of *M. truncatula* block Ca^{2+} spiking responses to Nod factors and mycorrhizal fungi, whereas the Nod^-/Myc^- mutant *dmi3* shows normal Ca^{2+} spiking. This indicates that *MtDMI1* and *MtDMI2* are directly involved in Ca^{2+} spiking whilst *MtDMI3* seems to act immediately downstream of calcium spiking and might have a role in perceiving the Ca^{2+} signal (Ané et al., 2004; Lévy et al., 2004; Mitra et al., 2004; Oldroyd and Downie, 2006). In fact, some putative signal transduction-related *M. truncatula* genes show activation during early stages of AM fungal interactions with wild-type *M. truncatula*, but none respond in the mycorrhiza-resistant *dmi3* mutant (Weidmann et al., 2004; Sanchez et al., 2005). Such non-symbiotic plant mutants can also down-regulate the expression of *G. intraradices* genes prior to and during appressorium formation by the AM fungus (Seddas et al., 2009). However, nothing is known about the regulation or role of Ca^{2+} in the fungal cells during the development and functioning of the AM symbiosis, apart from the reported up-regulation of one *Gigaspora rosea* P-type IIA ATPase by root exudates (Tamasloukht et al., 2007), and the reported activation of some *G. mosseae* genes with a potential role in Ca^{2+}-dependent signaling, in synchrony with appressorium formation on parsley roots (Breuninger and Requena, 2004).

1.3.3. Ca^{2+} involvement in plant-biotrophic pathogen interactions

Calcium signaling has been implicated in the induction of appressoria, development

and pathogenesis of leaf pathogenic fungi (Ebbole, 2007; Rho et al., 2009). Several Ca^{2+}-related proteins have been identified in biotrophic pathogens. For example, a P-type ATPase (PDE1) has a role in the development of penetration hyphae and pathogenicity in the rice blast fungus *Magnaporthe grisea* (Balhadère and Talbot, 2001). Also, a Ca^{2+}/calmodulin-dependent signaling system is involved in appressorium formation by *M. grisea* and calmodulin gene expression is induced concomitantly with appressorium formation (Lee and Lee, 1998; Liu and Kolattukudy, 1999). In addition, an endoplasmic sarcoplasmic/reticulum Ca^{2+}-ATPase (*Eca1*) has been identified in the fungal pathogen *Ustilago maydis* which restores growth of a yeast mutant defective for calcium homeostasis (Adamíková et al., 2004). These studies point to an importance of Ca^{2+}-dependent signaling processes in fungal events leading to interactions with plant tissues.

It has been hypothesized that pathogenic and symbiotic fungi may share some common regulatory mechanisms for the invasion of plant tissues (Genre and Bonfante, 2007), and evidence to support this hypothesis comes from recent investigations. It has been shown that transformation with the *G. intraradices* transcription factor gene *GintSTE12* restores pathogenicity of a *clste12*Δ mutant of the hemi-biotrophic pathogen *Colletotrichum lindemuthianum*, providing evidence for the possible existence of common genetic elements regulating the penetration of plant tissues by the two fungi (Tollot et al., 2009). Also, the expression of another *G. intraradices* gene, *SP7*, which interacts with a plant pathogenesis-related transcription factor, in the rice blast fungus *Magnaporthe oryzae* attenuates root decay symptoms caused by the biotrophic pathogen (Kloppholz et al., 2011). Furthermore, a gene (*Erl1*) encoding an Era (*Escherichia coli* Ras)-like GTPase which might be involved in the control of in planta growth of *M. oryzae* is orthologous to the mature amino terminal part of the Gin1 protein from *G. intraradices* (Heupel et al., 2010).

1.4. Thesis objectives

The aim of my thesis work was to provide a first insight into whether Ca^{2+} may also be an important intracellular component in fungal events leading to successful mycorrhizal interactions with plant tissues. In this context, Ca^{2+}-related genes were identified in isolates of the AM fungi *G. mosseae* and *G. intraradices*, expression was analysed at different stages of interactions with host roots and full-length cDNA sequences were obtained for candidate genes. Two *G. mosseae* genes were targeted based on sequences previously identified in an appressorium stage cDNA library (Breuninger and Requena, 2004), and

seven *G. intraradices* genes were selected from widescale transcriptome sequencing data covering different stages of fungal development (Tisserant et al., 2012). Based on the results obtained, a mechanism for Ca^{2+} homeostasis in AM fungal cells is proposed and the possible role of Ca^{2+}-related proteins in intracellular signaling during symbiotic mycorrhizal interactions is discussed.

Chapter 2

Material and Methods

2.1. Biological materials and growth conditions

2.1.1. *Astragalus sinicus L.* + *Glomus mosseae* (BEG225)

Spores of *Glomus mosseae* Nicol. & Gerd. (isolate BEG225), from the Bank of Glomales in China (BGC), were collected from pot cultures of mycorrhizal *Sorghum* by wet sieving. For pre-symbiotic stages, spores were washed several times with sterile distilled water and germinated in 3 ml of water in multiwell dishes (Fig. 2.1) at 25°C in the dark. After 7 days, the germinated spores were harvested and immediately frozen in liquid nitrogen for RNA extraction.

For experiments involving the early interactions of the symbiosis, 2000 spores of *G. mosseae* were germinated in water at 25 °C in the dark for 7 days and seeds of *Astragalus sinicus L.* (a legume used as rice field green manure in China) were surface sterilized (5 min in 75 % alcohol, 10 min in 3 % sodium hypochlorite), and germinated at 28 °C in the dark on 0.7% sterile water–agar plates for 3 days. Seedlings were then transferred to the sterile water containing the germinated spores in order to stimulate them by crude plant root exudates for 7 days (Fig. 2.1), then spores were frozen for RNA extraction.

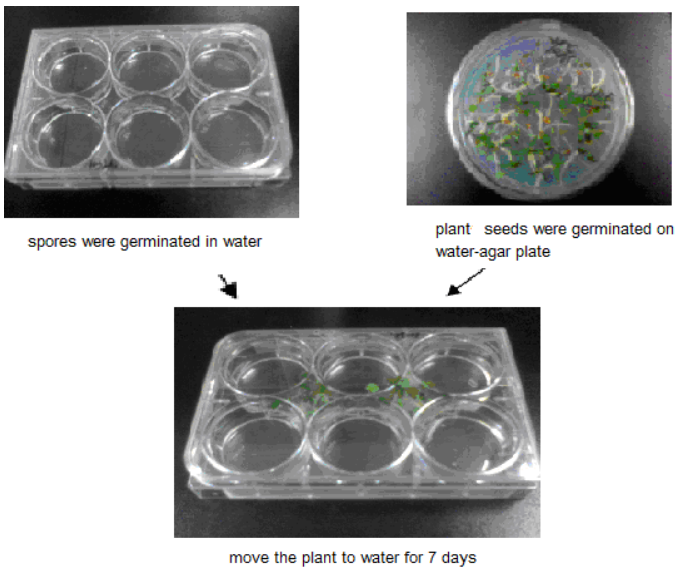


Fig. 2.1. Stimulation of germinated spores by root exudates of *A. sinicus*

Mycorrhizal root material was provided by the laboratory in Wuhan. *A. sinicus* seeds were surface sterilised for 5min in 5% NaClO, then rinsed in sterile demineralised water. They were germinated for 48 h on 0.7% sterile agar at 28 °C in the dark then transplanted into 400 ml plastic pots containing a mix (1:1 v/v) of soil (loam, pH 6.59, P: 11.83 mg/kg)

and sand with 10% soil-based inoculum (spores, roots and hyphae) of *G. mosseae* (BEG225, China) produced on Sorghum. Plants were grown for 40 days under controlled conditions (100-200Wm-2, 24 and 18 °C, 16 and 8 h, day and night, respectively) and watered each day with demineralised water and once a week with Hoagland nutrient solution (Hoagland and Arnon, 1950) (Table 2.1).

Table 2.1. Modified Hoagland nutrient solution with low phosphorus

Component	Concentration (mol / L)
KNO_3	2×10^{-3}
$Ca(NO3)_2$	5×10^{-4}
NH_4NO_3	1×10^{-3}
MgSO4	5×10^{-4}
$MnCl_2$	9×10^{-6}
$CuSO4 \times 5H_2O$	3×10^{-7}
$ZnSO_4 \times 7H_2O$	8×10^{-6}
H_3BO_3	4.6×10^{-5}
$CaCl_2$	2.5×10^{-4}
$(NH4)_2\ MoO_4$	3×10^{-7}
FeNa-EDTA	2×10^{-5}
KH_2PO4	6.5×10^{-5}

2.1.2. *Medicago truncatula* +*Glomus intraradices* DAOM197198 (syn. *Rhizophagus irregularis* Blaszk., Wubet, Renker & Buscot)

Mycorrhizal root material was kindly provided by A. Aloui (INRA, Dijon). *Medicago truncatula* Gaertn. cv. Jemalong wild-type (line J5) was inoculated with the *Glomus intraradices* isolate DAOM197198 (syn. *Rhizophagus irregularis*; Krüger et al., 2012) and plants were grown for 3 weeks according to Aloui et al. (2009). Roots were harvested, washed in ice-cold osmosed water and stored in liquid nitrogen until RNA extraction.

Spores (10,000) of *G. intraradices* DAOM197198, provided by P. Seddas (INRA, Dijon), were activated for 24h at 25 °C in sterile water and 2 % CO2 (IG150, Jouan incubator) and stored in liquid nitrogen until RNA extraction.

2.1.3. *Medicago truncatula* + *Glomus intraradices* BEG141

Wild-type *M. truncatula* (line J5) and the Myc$^-$ *dmi3/Mtsym13* mutant TRV25 (provided by G. Duc, INRA-Dijon, France) genotypes were used. The *M. truncatula* Myc–

dmi3/Mtsym13 mutant is mutated for the gene *DMI3/MtSYM13* encoding a calcium calmodulin-dependent protein kinase (Lévy et al., 2004). It presents a mycorrhiza-defective phenotype allowing only appressoria formation development of AM colonization (Morandi et al., 2005). The AM fungus *Glomus intraradices* Smith & Schenck, isolate BEG141, was provided by the International Bank of Glomeromycota (IBG, http://www.ukc.ac.uk/bio/beg/) (INRA-Dijon, France).

Glomus intraradices BEG141 spores were extracted by laceration of colonized leek roots (6-month-old leek pot culture) in sterile water using a blender. Two biological repetitions of spores (5,000) were activated for 24h at 25 °C in water and 2 % CO_2 (IG150, Jouan incubator). Root exudates of *M. truncatula* were collected according to Seddas et al (2009). Briefly, five germinated seedlings of *M. truncatula* per each well were incubated in 3 ml of sterile water in a six-well plate (Falcon Multiwell, BD Sciences, San Jose, CA, U.S.A.) for 7 days. After elimination of all plant residues, this crude plant root exudates were directly used with spores. Two biological repetitions of spores (5,000) were germinated in wild-type J5 or TRV25 mutant root exudates separately for 6 days and two biological repetitions of 5,000 spores were germinated in water for 6 days as control.

For a time-course study of gene expression during mycorrhiza development, surface sterilized seeds (6 min in 98 % sulphuric acid, 10 min in 3 % sodium hypochlorite) of *M. truncatula* line J5 and the Myc^- TRV25 mutant were germinated for 3 days on 0.7 % Bactoagar (Difco Laboratories, Detroit) at 25 °C in the dark and then transplanted into 50-ml or 75-ml pots containing a mixture (2:1, vol / vol) of Terragreen (OilDri-US special, Mettman, Germany) and a neutral clay soil-based inoculum (spores, roots, and hyphae) of *G. intraradices* BEG141 produced on leek. Inoculum was checked for the absence of rhizobia by growing with the hypernodulating *M. truncatula* genotype TR122 for 3 weeks. Plants were grown under constant conditions: 355 µE/m2/s, 16h-24 °C and 8h-21 °C, day and night, respectively, 70 % humidity. They were fertilized with 3 ml (50-ml pot) or 5 ml/pot (75-ml pot) of a modified Long Ashton solution (Hewitt et al., 1966) without phosphate, enriched in nitrogen (Table 2.2) twice a week, and received distilled water on other days. Plants were harvested at 4, 6, 17 or 21 days after inoculation (dai) for the J5 genotype, and 4 or 6 dai for the TRV25 mutant. Fresh roots from each harvest were washed in ice-cold water and immediately stored in liquid nitrogen for RNA extraction. At each time point, root systems of additional plants were stained for mycorrhizal root colonization (see below).

Table 2.2. Long Ashton solution without phosphorus

Component	Concentration (mg/l)
KNO_3	808
$Ca(NO3)_2 \times 4H_2O$	1888
$MgSO4 \times 7H_2O$	368
$MnSO4 \times H_2O$	2.23
$CuSO4 \times 5H_2O$	0.25
$ZnSO_4 \times 7H_2O$	0.29
H_3BO_3	3.10
NaCl	5.90
$H_{24}Mo_7N_5O_{24} \times 4H_2O$	0.088
FeNa-EDTA	22

2.1.4. *Pisum sativum L.* + *Glomus intraradices* BEG141

Wild-type pea (*P. sativum L.*) *cv.* Finale and the symbiotic mutant *Pssym36* (previously denoted RisNod24; provided by A. Borisov, ARRIAM, St. Petersburg, Russia) were used. The mutant *Pssym36* is defective for arbuscule formation (Gianinazzi-Pearson, 1996).

Seeds were surface-disinfected 10-min in a sodium hypochlorite solution (3 %) at room temperature, washed with distilled water and germinated in Petri dishes (12-cm diameter) on humid filter paper at 24 °C in the dark for 5 days. Seedlings were planted into pots containing 200 ml of a 1:1 mixture of quartz sand and mycorrhizal soil-based inoculum (spores, roots, and hyphae) of *G. intraradices* BEG141. Plants were grown under control conditions (326 µ mol m^{-2} s^{-1}, 24/22 °C, 16 h light, 70 % relative humidity), fertilized with 10 ml / pot of a modified Long Ashton solution without phosphorus, enriched in nitrogen (Table 2.2) three times a week, or 10 ml of distilled water on other days. Plants were harvested at 21 days after inoculation (dai). Root systems were washed in cold water, root and shoot fresh weights were recorded, and roots were stored in liquid nitrogen for RNA extraction or directly stained to determine the AM fungal development on randomly sampled root pieces (see below).

2.2. Estimation of mycorrhizal root colonization

To determine the number of appressoria and total root colonization for *M. truncatula*, fresh roots were washed under running tap water, cleared for 48 h in 10 % KOH at room temperature and stained overnight with 0.05 % trypan blue in glycerol (4 and 6 dai roots)

or 30 min in 10 % KOH at 90 °C and 15 min in 0.05 % trypan blue at 90 °C (17, 21 dai roots). For *P. sativum* roots were cleared 1 hour at 90°C in 10 % KOH and stained 15 min in 0.05 % trypan blue at 90 °C. Root systems were cut into 1 cm pieces and 30 root fragments/plant were observed microscopically according to Trouvelot et al. (1986) (Fig. 2.2). Mycorrhiza parameters were calculated using the MYCOCALC program (http://www.dijon.inra.fr/mychintec/Mycocalc-prg/download.html). The parameters used were F % (frequency of mycorrhizal colonization in the root system), M % (intensity of mycorrhizal colonization in the root cortex), m % (intensity of mycorrhizal colonization in mycorrhizal root fragments), A % (arbuscule abundance in the root system), a % (arbuscule abundance in mycorrhizal root fragments). Also the development of vesicles in roots was estimated as V % (vesicle abundance in the root system), v % (vesicle abundance in mycorrhizal root fragments), using the same scoring as for arbuscules

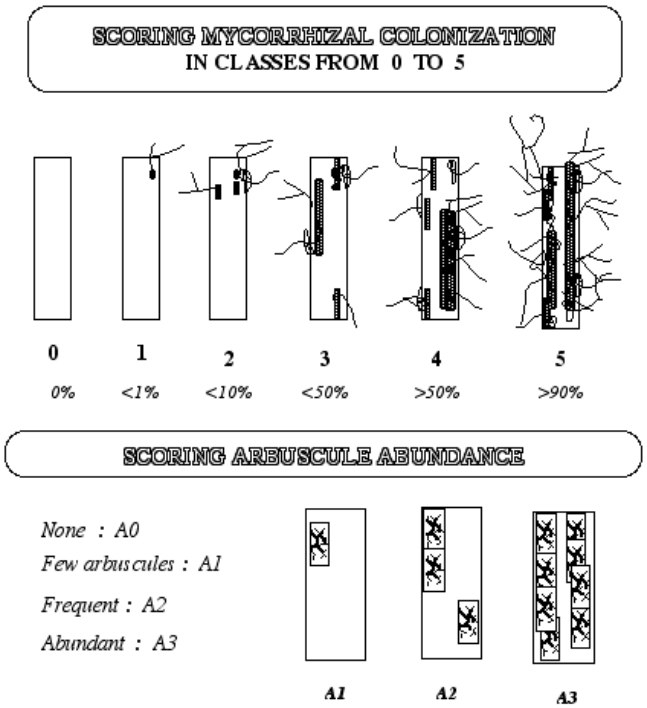


Fig. 2.2. Estimation of mycorrhiza development by scoring (Trouvelot et al. 1986). For each root fragment, mycorrhizal colonization is scored from 0 to 5 and arbuscule abundance is classed in 4 categories (A0, A1, A2 and A3).

2.3. Laser Capture Microdissection (LCM) of arbuscule-containing cortical root cells

2.3.1. Tissue preparation

Roots of *M. truncatula* J5 colonized by *G. intraradices* BEG141, harvested between 17 and 21 dai, were cut into 0.5-cm pieces and fixed in Tissue-Tek® O.C.T.™ Compound at -24 °C. Sectioning was performed at -24 °C using a CRYOCUT 1800 microtome (Leica, Germany) and RNAse-free tools. 35 µm thick sections were placed on RNA-free slides (Probe On Plus Microscope Slides, Fisher Scientific, France). To remove the medium, slides were incubated on ice as follows: 3 min in 70 % ethanol, then 40 min in DEPC-treated water and rinsed twice in 100 % ethanol for 2 min. After the last ethanol step, slides were kept on a warmer at 37 °C for 25 min. After that, the root tissues were used directly for microdissection or stored at -80 °C then placed in a desiccator before microdissection.

2.3.2. Dissection of arbuscule-containing cells

Dissection was performed using an Arcturus™ XT Microdissection instrument (Life Sciences / Roche Applied Biosystems, France). Sections on the slides were visualized under a computer monitor through a video camera, and selected cells were marked using graphical software, isolated using an infrared (IR) laser and captured automatically into CapSure HS laser capture microdissection caps (Arcturus Picopure isolation kit (Life Sciences / Roche Applied Biosystems, France). To prevent RNA degradation, dissection in one cap was performed within 30 min and then transferred into RNA extraction buffer provided in the Picopure RNA Isolation Kit.

2.3.3. RNA extraction from laser-dissected cells

Harvested laser-dissected cells were incubated in the RNA extraction buffer for 45 min at 42 °C, centrifuged at 800 × g for 2 min, and stored at –80 °C until use. RNA was extracted using the Picopure RNA Isolation Kit according to the manufacturer's protocol. The quantity and quality of RNA were checked with an Agilent Bioanalyzer 2100 (http://www.home.agilent.com/).

2.3.4. One-step RT-PCR

After RNA extraction, the RT-PCR experiments were performed using a One-Step RT-PCR kit (Qiagen, Valencia, CA, U.S.A.). Reactions were carried out in a final volume of 50 µl containing 10 µl of 5× buffer, 2 µl of 10mM dNTPs, 3 µl of each primer (10 µM), 2 µl of One-Step RT-PCR enzyme mix, 8 units of RNAse inhibitor, and 3 ng of total RNA from arbusculated cells and noncolonized cortical cells from mycorrhizal roots. The samples were incubated for 30 min at 58 °C, followed by 15-min incubation at 95 °C. Amplification reactions (the primers and conditions are indicated in Table 2.5 and 2.6) were run for 35 to 40 cycles. The PCR products were separated by agarose gel electrophoresis in a Trisacetate-EDTA 0.5× buffer, stained with ethyl bromide, and visualized using a VersaDoc Imaging System (Bio-Rad Laboratories, CA, U.S.A.). Experiments were repeated using arbusculated cells from two different biological repetitions (C1 and C2) and representative results are shown.

2.4. Nucleic acid preparation from spores and roots

2.4.1. RNA extraction

Total RNA was extracted from *G. mosseae* quiescent spores and spores germinated in water or stimulated by plant root exudates (2000 per treatment) using a E.Z.N.A. fungal RNA kit (Omega Bio-Tek Inc, USA) (E.Z.N.A., EaZy Nucleic Acid), and DNA removed by RNase-Free DNase (Omega Bio-Tek Inc, USA) according to the manufacturer's protocol. RNA quantity was estimated using an Eppendorf biophotometer (Eppendorf, Germany).

Total RNA was extracted from *G. intraradices* DAOM197198 spores, *G. intraradices* BEG141 spores and mycorrhizal (*G. intraradices* BEG141) *M. truncatula* roots using a SV Total RNA Isolation System (Promega, Madison, WI, USA), according to the manufacturer's protocol. The DNase-containing columns of the Promega kit for total RNA isolation (SV Total RNA Isolation System) were used to remove any DNA contamination.

Total RNA was isolated from mycorrhizal (*G. intraradices* DAOM197198) *M. truncatula* roots by A. Aloui using the phenol-chloroform method according to Franken and Gnadinger (1994). In order to test the specificity of the fungal primers, cDNA from

non-mycorrhizal *M. truncatula* root was used as control; total RNA was extracted from non-mycorrhizal *M. truncatula* roots using the Qiagen RNeasy Plant Mini Kit (74904) following the manufacturer's instructions (Qiagen, Hilden, Germany). RNA integrity, quantity and quality were controlled by 1.2 % denaturing agarose gel electrophoresis and photometric analysis (Eppendorp biophotometer).

2.4.2. cDNA synthesis

RNA from *G. mosseae* quiescent spores (0.030 µg/µl), from spores germinated in water (0.028 µg/µl) and from spores stimulated by crude plant root exudates (0.083 µg/µl) (Eppendorf biophotometer) were used to synthesize cDNA according to the protocol of the Superscript III Reverse Transcriptase kit (Invitrogen, USA). 0.2 µg DNA-free RNA from spores were reverse transcribed with 1 µg oligo(dT)18 (Promega, USA) and 200 U M-MLV Reverse transcriptase RNase H Minus (Promega) according to the Promega protocol. cDNA was amplified via the protocol as follows: 42 °C for 1 h and 70 °C for 2 min and stored at -20 °C until use.

RNA from two batches of spores and three biological repetitions of mycorrhizal *M. truncatula* roots and non-mycorrhizal *M. truncatula* were used to synthesize cDNA with Superscript III Reverse Transcriptase according to the Invitrogen protocol. 0.15 µg or 1 µg DNA-free RNA from spores and mycorrhizal roots were separately reverse transcribed into first-strand cDNA. The reaction mix containing RNA, 1 µg oligo$(dT)_{15}$ (Promega) and 0.5 mM dNTPs (Final concentration) was preheated at 70 °C for 5 min and cooled on ice for 3 min. 40 U RNasine RNA inhibitor (Promega), 300 U M-MLV Reverse transcriptase RNase H Minus (Promega) and reaction buffer were added to obtain a final mix volume of 25 µl and amplified using the following programme: 25 °C for 15 min, 42 °C for 1 h and 96 °C for 2 min. cDNA was stored at -20 °C until use.

2.4.3 Genomic DNA extraction from fungal spores

G. mosseae genomic DNA was extracted from 2000 spores using the protocol described by Zézé et al. (1994). Briefly, spores were gently crushed in TE buffer containing 2 % mercaptoethanol, the suspension was centrifuged and nuclei were resuspended in lysis buffer. After centrifugation, the supernatant was collected and proteins

were precipitated with potassium acetate. Nucleic acids contained in the supernatant were treated with DNAse-free RNAse A, and then purified with phenol-chloroform. The purified DNA was precipitated in ethanol at -70 °C, centrifuged, washed with 70 % ethanol, air dry and resuspended in TE buffer or sterile water.

2.4.4. Plasmid DNA preparation

Amplified fragments of cDNA (see below) were cloned into a plasmid vector using the TOPO TA Cloning kit (Invitrogen Corporation, Carlsbad, CA, USA). The plasmids were recuperated by white-blue selection and PCR. Recombinants (white colonies) were multiplied in liquid LB culture containing ampicillin (50 µg / ml), and plasmid DNA was isolated using the NucleoSpin®Plasmid kit (Macherey-Nagel, Düren, Germany) following the manufacturer's instructions. The yield and purity of plasmid DNA were estimated using an Eppendorp BioPhotometer. Cloned PCR products were sent for sequencing to MWG-Biotech (Ebersberg, Germany).

2.5. Fungal gene selection and primer design

2.5.1. Gene selection

ESTs of two calcium-related *G. mosseae* genes (Gm2 and Gm152) were selected from amongst those reported to be up-regulated with appressorium formation; these putatively code for a MAP3k-like protein kinase and a P-type ATPase respectively (Breuninger and Requena, 2004). The *G. mosseae* gene coding for the H^+-ATPase PMA1, whose expression was previously shown not to vary during appressorium formation, was used for comparison as described by Breuninger and Requena (2004). EST sequences and similarity to genes in other eukaryotes are given in Table 2.3.

Table 2.3. Putative function and primer design of selected *G. mosseae* genes

Selected ESTs	Primer	Sequence 5'-3'	Putative function	Organism	E-value
Gm2	F-2	TTCCGACATAGCTTACGTGACG	MAP3k-like protein kinase	*Arabidopsis thaliana*	3e-16
	R-2	GAATGGTTCCATCAGAAGAGGG			
Gm152	152-9	AACATCAGTCGTTCCACCAG	P-type ATPase, SPF1p, Ca^{2+}-transporting ATPase	*S. cerevisiae*	5e-07
	gmr4	AAGCTTCCATTCCAACGCTTC			

Seven fungal ESTs encoding Ca^{2+}-related proteins were selected from the transcriptome sequencing programme of *G. intraradices* DAOM197198 (syn. *R. irregularis*) according to the microarray expression analysis results, on the basis of their putative function and expression profile in microarray analyses. Most of the selected genes were up-regulated in mycorrhizal roots as compared to the spores at least 2.5 fold with a *p value* <0.05 (Tisserant et al., 2012). Homology searches were carried out using NCBI and Swissprot databases by blastx. Six ESTs putatively encoded proteins involved in membrane transport (two vacuolar Ca^{2+} ion transporters, three Ca^{2+}ATPases, one mitochondrial Ca^{2+}-binding carrier) and one Ca^{2+}/calmodulin-dependent protein kinase (CCaMK). Six of the corresponding genes encoded proteins involved in membrane transport: plasma membrane/tonoplast, endoplasmic reticulum, golgi reticulum, mitochondria, and one is a nuclear protein (Table 2.4). Two symbiosis–related *G. intraradices* genes, stearoyl-CoA desaturase (*DESAT*) and a phosphate transporter (*GiPT*), were used as controls to monitor fungal activity; *G. intraradices* large-subunit (*LSU*) rRNA was used to confirm the presence of fungal RNA for transcript analyses, and α subunit of translation elongation factor 1 (*TEF*) as the fungal reference house-keeping gene (Maldonado-Mendoza et al., 2001; Seddas et al., 2009). EST sequences and similarity to genes in other eukaryotes are given in Table 2.4.

Table 2.4. Putative function of studied *G. intraradices* genes

ESTs	Putative function	Organism	E-value
Glomus_c17763	Vacuolar Ca/Mn transporter (1)	*Saccharomyces cerevisiae*	7e-20
Glomus_lrc1694	Vacuolar Ca/Mn transporter (2)	*Saccharomyces cerevisiae*	3e-53
Glomus_c3514	Vacuolar Ca^{2+}-transporting ATPase II	*Schizosaccharomyces pombe*	9e-21
	Plasma membrane Ca^{2+}-transporting ATPase II	*Oreochromis mossambicus* (*Mozambique tilapia*)	2e-12
Glomus_c2781	Sarcoplasmic/endoplasmic reticulum calcium ATPase II	*Rana esculenta* (edible frog)	2e-40
Glomus_c10704	Golgi reticulum P-type Ca^{2+} ATPase II	*Pongo abelii* (Sumatran orangutan)	1e-10
Glomus_c23149	Mitochondria membrane Ca^{2+}-dependent carrier	*Homo sapiens* (human)	5e-92
Glomus_lrc995	Nuclear CCaMK	*Mus musculus* (house mouse)	4e-69

2.5.2. Primer design

Primers were manually designed for Gm2 and Gm152 sequences and checked by the programme DNAMAN (Lynnon Biosoft, USA). They were tested by PCR on cDNA synthesized from *G. mosseae* spores by gel RT-PCR at 60 °C and with 33 amplification cycles. PCR products were sequenced (AuGCT biotechnology, Beijing, China) and EST sequence homology verified by blastx (Table 2.3).

Primers were also manually designed for the selected ESTs of *G. intraradices* DAOM197198 (Glomus_c17763, Glomus_lrc1694, Glomus_c3514, Glomus_c2781, Glomus_c23149, Glomus_995) (Table 2.5) and checked by the programme Amplify 3X (http://engels.genetics.wisc.edu/amplify/). They were tested on cDNA synthesized from equal amounts of total RNA from mycorrhizal (*G. intraradices* DAOM197198 or BEG141) *M. truncatula* roots and from spores by gel RT-PCR at 58 °C and with 30 amplification cycles. PCR products were sequenced (MWG-Biotech, Ebersberg, Germany) and EST sequence homology verified by blastx (Table 2.4). Previously published primers from *G. intraradices* BEG141 and other fungi described as *G. intraradices* were used for the control genes *LSU*, *TEF*, *DESAT* and *GiPT* (Maldonado-Mendoza et al., 2001; Farmer et al., 2007; Seddas et al., 2009) (Table 2.6).

Table 2.5. Primer design for *G. intraradices* genes

Gene	Primer name	Sequence 5'-3'	Size[1] (bp)
Vacuolar calcium ion transporter 1	C17763_F2	GATGGTATAACGAAAAGCGGAC	331
	C17763_R2	AATAGCGGTAACAAACTCAGCA	
Vacuolar calcium ion transporter 2	1694_F2	CGTCTTCTCATATCATTCTAACTAAAG	114
	1694_R3	TTGGTTTGAAGGTGCTATGTTGC	
Plasma membrane /vacuolar calcium transporting ATPase II	C3514_F	TGGAGGATTAGATGGATTGGT	247
	C3514_R2	GAATAGACTTTGTTTTCTTTACTGG	
Endoplasmic reticulum calcium ATPase II	C2781_F	CGACGAATACTCTGCTCACG	249
	C2781_R3	TCAATGCCACTAATTCTCTTAGC	
Golgi reticulum calcium transporting ATPase II	10704_F3	GGAGCTGAAATTGTCCTGATGC	198
	10704_R3	CGTTGCATATTTACCAAGCACAGG	
Mitochondria membrane calcium-binding carrier	23149F5	TAAGAGATGTACCATTTTCAGCCA	249
	23149R5	TCCGCTAATATCCTTCTTCCTGC	
Nuclear calcium/calmodulin-dependent protein kinase (CCaMK)	lrc995_F4	ATTATGTGGATACACTCCATTCTG	195
	lrc995_R2	AACCAAGGGTGTTTCAATGCTTC	

1) Amplicon size

Table 2.6. Primer design for control *G. intraradices* genes

Gene	Primer name	Sequence 5'-3'	Size[1] (bp)	Target organism	Reference
Stearoyl-CoA-desaturase (*DESAT*)	DESAT for	TCGTGTTCCTGAAAATGAAG	269	*G. intraradices* BEG141	Seddas et al. (2009)
	DESAT rev	GCTTTAGTGGAGTCTTTACC			
Phosphate transporter (*GiPT*)	GiPT1	CTCCTGCAAATATCGACTTGGGT	243	*G. intraradices* (AF359112)	Maldonado-Mendoza et al. (2001)
	GiPT2	GATAATCTCCTCCAATACCGACA			
Large subunit rRNA (*LSU*)	FLR3	TTGAAAGGGAAACGATTGAAGT	300	*Glomeromycota*	Gollotte et al. (2004)
	8.24	CGATCAGAGACCAGACAGGT		*G. intraradices*	Farmer et al. (2007)
Translation elongation factor (*TEF*)	Gi-TEFfor	AGCCGAACGTGAACGTGG	144	*G. intraradices* BEG141	Seddas et al. (2009)
	Gi-TEFrev	GCACAATCGGCCTGAGAAGTAC			

1) Amplicon size

2.6. Polymerase chain reaction (PCR)

2.6.1. Reverse-transcription (RT-PCR)

Transcripts of each selected gene were amplified by RT-PCR. Reactions were carried out in 20 µl PCR mix containing 0.2 U of Taq polymerase and 2 µl 10X buffer with 1.5 mM $MgCl_2$ (Invitrogen, USA), 125 µM dNTPs, 0.5 µM of each gene-specific primer pair (Table 2.3, 2.5 and 2.6), and 1:10 diluted cDNA from spores or roots. Reactions were conducted in a T3000 thermocycler (Biometra, Germany). For the *G. mosseae* genes, the amplification programme was 60 °C with 33 amplification cycles, and for *G. intraradices* genes the following program was used: 94 °C for 3 min, 30 cycles (94 °C for 1 min, 58 or 60 °C for 1 min, 72 °C for 1 min), 10 min at 72 °C. PCR products were separated by 1.2 % agarose gel electrophoresis for 25 min at 100 volts, gels were stained 10 min in ethidium bromide and documented under UV light using GelDoc EQ apparatus (BioRad, USA).

2.6.2. Relative quantitative real-time PCR

Targeted genes of *G. intraradices* DAOM197198

Relative real-time PCR reactions were carried out to quantify gene transcripts using an ABI PRISM 7900 real-time cycler (Applied BioSystems, Foster City, CA, USA), and

the ABsolute SYBR green ROX MIX (ABsoluteTM QPCR® SYBR Green ROX Mix 2x; Thermo Scientific, UK) as fluorescent dye. The gene specific primers are described above (see tables 2.5, 2.6). Each reaction (15 µl) contained 2 µl of 1:20 diluted cDNA from spores and root-extracted RNA, 7.5 µl SYB green mix (from Absolute QPCR SYBR Green kit), 1 pM of each primer and sterile water. The amplification program was performed as follows: 95 °C for 15 min, 40 cycles (95 °C for 15 s, 58 °C for 30 s, 72 °C for 20 s, 75 °C for 15 s). A melting curve (95 °C for 15 s, 55 °C for 15 s, 95 °C for 15 s) was recorded at the end of every run to verify the specificity of amplification. Primer efficiency (E) was calculated using the formula: $E=10^{(-1/slope)}-1$ (Invitrogen guide for important parameters of quantitative PCR analysis). cDNA amplifications were quantified using 5 cDNA dilutions to produce a linear slope. Three biological repetitions, each with two technical repetitions, were analyzed for each treatment. The threshold was set at 0.2 and Ct (threshold cycle) values were automatically calculated by the SDS 2.3 program (Applied Biosystems, Foster City, USA). To compare to microarray data, the relative expression ratio between mycorrhizal *M. truncatula* roots and water-activated spores was calculated according to the formula of Pfaffl (2001) using the reference gene *GiTEF*:

$$\text{ratio}= \frac{(E_{target})^{\Delta Ct\ target\ (control-\ sample)}}{(E_{ref})^{\Delta Ct\ ref\ (control-\ sample)}}$$

E_{target}: efficiency of target gene transcript

E_{ref}: efficiency of reference gene transcript

Control: activated spores

Sample: mycorrhizal roots

Targeted genes of *G. intraradices* BEG141

Gene expression was monitored by relative Q-PCR on the Step One Plus Real-Time PCR System Thermal Cycling Block (Applied Biosystems, USA) using the ABsolute SYBR green ROX MIX (ABgene, Epsom, UK), and the gene specific primers described above (see tables 2.5, 2.6). Assays were performed on cDNA from two biological repetitions of differently treated spores and three biological repetitions of mycorrhizal *M. truncatula* roots for each time point. For each sample, PCR reactions were carried out in technical duplicates using 2 µl of 1:20 diluted cDNA from spores and 1:4 of diluted cDNA from mycorrhizal root as template. PCR was performed as follows: 95 °C for 15 min, 40 cycles (95 °C for 15 s, 58 °C for 30 s, 72 °C for 30 s, 75 °C for 15 s) and for the melting curve: 95 °C for 15 s, 72 °C for 1 min, 95 °C for 15 s. Amplification efficiency of each

primer pair was determined using a serial dilution of cDNA. The generated data were analysed by StepOne software v2.1 (Applied Biosystems, USA) using a threshold set at 0.2. The *GiTEF* gene served as reference, and relative gene expression was calculated using the formula $R=2^{\Delta CT(reference-target)}$.

Ct_{target}: the threshold cycle of target gene transcript

$Ct_{reference}$: the threshold cycle of reference gene transcript

2.6.3. Absolute quantitative real-time PCR

Transcript abundance of genes corresponding to BEG141_c2781, BEG141_c10704, BEG141_lrc1694 and BEG141_lrc995 was quantified by absolute Q-PCR, using the Step One Plus Real-Time PCR System Thermal Cycling Block (Applied Biosystems, USA) and the ABsolute SYBR green ROX MIX (ABgene, Epsom, UK). The expression of each gene was assayed in two technical repetitions and analyzed by the StepOne software v2.1 (Applied Biosystems, USA). To calculate the absolute number of transcripts present in the original samples, plasmid DNA containing each amplicon was quantified by UV absorbance spectroscopy and linearized by digestion with the restriction enzyme *BamH1*. A standard curve of each primer pair was determined using a serial dilution of linearized plasmid DNA at dilutions of 10, 10^2, 10^3, 10^4, 10^5, 10^6, and 10^7 copies for each assay. To verify the specificity of each amplification, a melting-curve analysis was included at the end of each PCR run. Relative number of transcripts for each gene was calculated as a ratio to the amount of the reference gene *TEF* transcripts.

2.6.4. *In situ* RT-PCR

In situ RT-PCR was performed according to Seddas et al. (2008) on spores from pot cultures or roots prepared as follows. Surface sterilized seeds of *M. truncatula* line J5 were germinated as described above, and half the seedlings were transplanted into 75-ml pots containing the Terragreen/soil-based *G. intraradices* BEG141 inoculum mix for inoculated plants. The other half of the seedlings were grown as controls with autoclaved inoculum and 1ml bacterial filtrate for each pot (15ml inoculum in 15ml water filtered with Whatman 2v filter paper). Plants, grown under constant conditions as described above, were harvested from 17 to 21 dai, root systems were washed in ice-cold water and fresh

roots were immediately fixed for *in situ* RT-PCR.

Spores or roots were fixed in 67 % (v / v) ethanol and 23 % (v / v) acetic acid containing 10 % (v / v) DMSO. After 1 h incubation at 4 °C under vacuum, samples were placed in 200 µl fresh fixative solution during 16 h at 4 °C. Samples of fixed materials were washed twice in 67 % (v / v) ethanol and 23 % (v / v) acetic acid then once in DEPC-treated water. Cell walls were permeabilised by digestion with chitinase from *Streptomyces griseus* (Sigma) and pectinase from *Aspergillus nige*r (Sigma). After washing in the same buffer, samples were digested with proteinase K. Genomic DNA was digested with Hae III (Promega) and Hpa II (Promega) in presence of RNAsin (Promega), then eliminated with DNAse. RNA controls were carried out with RNase before performing the DNAse treatment.

The large ribosomal subunit gene (*LSU rRNA*) of *G. intraradices* BEG141 was used to standardize the *in situ* RT-PCR methodology. Genes putatively encoding two P-type Ca^{2+} ATPases (BEG141_c2781, BEG141_c10704) and one tonoplast Ca/Mn transporter (2) (BEG141_lrc1694), as well as the control genes *DESAT*, *TEF* and *GiPT*, were chosen to localize gene activities in spores and mycorrhizal roots. Gene-specific primers (Table 2.5 and 2.6) were labeled with Texas Red (MWG-Biotech). Controls were provided by omission of primers in the reverse transcription reaction.

Following amplification, the PCR-mix was removed and samples were post-fixed in 100 % ethanol during 10 min at room temperature then quickly wash in 70 % ethanol. Each sample was deposited on a microscope slide in anti-fading medium (DAKO) and stored at 4 °C in the dark until observation. Fluorescence was observed using a confocal microscope (LEICA TCS SP2 AOBS; Leica Microsystems, Germany). Excitation was carried out with a 594 nm laser used at 27 % of its maximum power with a photomultiplicator at 687 V. The resulting signal was collected between 606 and 640 nm. Autofluorescence of plant and fungal tissues was avoided under these conditions of excitation and signal collection. A 40× oil objective was used to seize images. Each fluorescent image corresponded to the maximum projection of optical sections from a z series, using Leica Confocal software. The resultant depth (z) of each projection was about 300 nm. The optical section number of each projection was between 20 and 40. A Nomarski image was taken in parallel each time.

The same treatment was also done on the 40 day old *G. mosseae*-inoculated *A. sinicus* roots (see chapter 2.1.1) to locate gene expression of Gm152. The Gm152 gene-specific primers (Table 2.3) were labeled with TET (Tetrachlorofluorescein, a fluorescent dye

labeling) (Sangon Shanghai, China). Fluorescence was observed using a confocal microscope (Zeiss LSM510 META, Germany); a 488 nm laser was used for excitation and the resulting signal was collected at 514 nm for the mycorrhizal root tissues.

2.6.5. Rapid Amplification of cDNA Ends (RACE)

Since the 5′end cDNA sequence of Gm152 was available in the *G. mosseas* SSH library database, only the 3′end cDNA sequence was obtained using rapid amplification of cDNA ends (RACE) according to Scotto–Lavino et al., 2007. Briefly, to generate the 3' end, mRNA was reverse transcribed using a primer QI-QO that terminates in two mixed bases (GATC / GAC) followed by 17 Ts and a unique primer sequence. The end was amplified using the primer QO that contains part of this sequence and that binds to these cDNAs at their 3'ends, and a primer that matches the gene of interest, 152GSP1. A second amplification series was then performed using internal primers QI and 152GSP2 to suppress the amplification of non-specific products. Primers were listed in Table 2.7. A LA Taq DNA Polymerase (TaKaRa, Japan) was used for this LA (Long and Accurate) PCR amplification from *G. mosseas* cDNAs according to the manufacturer's instructions.

PCR products were visualized by electrophoresis on 1.0% agarose gels stained with ethidium bromide. Bands were excised and purified using the TIANgel Midi Purification Kit (Tiangen Biotech, Beijing, China). PCR products were sequenced (AuGCT Biotechnology, Beijing, China) and homology searches were carried out using NCBI databases by BLAST search. Multiple sequence alignments of translated gene sequences were carried out with the program CLUSTALW (http://www.ebi.ac.uk/clustalW/).

Table 2.7. 3′ RACE primers for Gm152

Primer name	Sequence 5'-3'	Temp[1] (°C)
QI-QO	CCAGTGAGCAGAGTGACGAGGACTCGAGCTCAAGCTTTTTTTTTTTTTTTT	68
QO	CCAGTGAGCAGAGTGACG	60
QI	GAGGACTCGAGCTCAAGC	60
152GSP1	GCGGGGACAGGTTTATAAATTTC	60
152GSP2	TGTTTTGGCATGGATACGTATGG	60

1) Annealing temperature.

The complete cDNA sequence of three selected *G. intraradices* BEG141 ESTs was obtained after 3′ and 5′ rapid amplification of cDNA ends (3′, 5′ RACE) using the Generacer kit (Invitrogen Corporation, Carlsbad, CA, USA) according to the manufacturer's instructions. The gene-specific primers for 3' and 5' RACE, used in conjunction with GeneRacer primers for PCR amplification, are listed in Table 2.8. These primers were used for PCR amplification from *G. intraradices* BEG141 cDNAs with a proofreading DNA polymerase (Platinum® *Taq* DNA polymerase High Fidelity; Invitrogen Corporation, Carlsbad, CA, USA). For the RACE amplification results, homology searches were carried out using NCBI databases by BLAST search (http://blast.ncbi.nlm.nih.gov/). Multiple sequence alignments of translated gene sequences were carried out with the program CLUSTALW2 (http://www.ebi.ac.uk/clustalW/). The amino acid sequences of orthologs from *Saccharomyces cerevisiae*, *Schizosaccharomyces pombe*, *Coprinopsis cinerea*, *Cryptococcus neoformans*, *Aspergillus fumigatus*, *Magnaporthe grisea*, *Ustilago maydis*, *Arabidopsis thaliana* and *Medicago truncatula* were aligned and the program Mega4 was used for phylogenetic analysis.

Table 2.8. 3′ and 5′ RACE primers for the selected ESTs of *Glomus intraradices* BEG141

ESTs	Primer name	Sequence 5'-3'		Temp[1] (°C)
BEG141_ lrc1694	1694_R3	TTGGTTTGAAGGTGCTATGTTGC	3′ end RACE	58
	1694-F6	TAACAGCAAAATTAAAAGCAGC	5′ end RACE	58
BEG141_c2781	R-2781-F5	AATTCGTGAGCAGAGTATTCGTCG	3′ end RACE	65
	R2781R5	CTCATTTTCGCTAAGAGAATTAGTGGC	5′ end RACE	65
	R2781-R22	AGCTGGAGCATCATTAACACC	5′ end RACE	60
	R2781-R32	CAGGAATTTTATCACCCACAGC	5′ end RACE	58
BEG141_ lrc995	lrc995_F6	ATTGATAAAATGTTAGCTTATGATGCTG	3′ end RACE	62
	lrc995_R3	CTT GAGCATAATCACTAATATTTGACC	5′ end RACE	60

1) Annealing temperature.

2.7. PCR amplification on genomic DNA

The full genomic sequence of Gm152 was obtained by PCR amplification of *G. mosseae* genomic DNA using Inverse PCR (Molecular Cloning: A Laboratory Manual) and TAIL-PCR (Liu and Chen, 2007). Based on a known (429bp) cDNA sequence, specific primers were designed for Gm152 and a series of PCR reactions were carried out using primers listed in Table 2.9 and Table 2.10.

2.7.1. Inverse PCR

Inverse PCR, which is a method used to amplify DNA with only one known sequence, involves restriction digestion and ligation resulting in a looped fragment that can be primed for PCR from a single section of the known sequence.

Genomic DNA was digested into fragments using the restriction enzyme *EcoR1* (Promega, USA) according to the manufacturer's instructions. After, self-ligation with T4 DNA ligase (Promega, USA) was induced to give a circular DNA product. PCR was carried out with the primer pair 152f-2/152AR and 152f-3/152AR (Table 2.9), which are complementary to sections of the known internal sequence. PCR was done in a 20 µl volume containing 5 µg circularized DNA, 0.2 U LA Taq (TaKaRa, JAPAN), 2µl 10×PCR buffer (Mg^{2+}), 2.5 mM dNTP and 10 µM primers. The amplification program was performed as follows: 94°C for 3 min, 30 cycles (94°C for 1 min, 58 or 60°C for 1 min, 72°C for 3 min), 72°C for 5 min. PCR products were sequenced (AuGCT Biotechnology, Beijing, China) and homology searches were carried out using NCBI databases by BLAST search. Finally, the sequence was verified by comparing with the sequence available in the data base.

Table 2.9. Primers designed for Gm152 PCR amplification

Primer name	Sequence 5'-3'	Temp[1] (°C)
Inverse PCR		
152f-2	ACTGCTTGTCATGTGGCTCG	60
152f-3	ATGGGTATATGCTCGCGTGTC	60
152AR	GGAAACAGCATCGTCCTTCAG	60
TAIL-PCR		
152f1	TGGTTCGGGCTTTGATGGGTTG	60
152f2	TTGAGGTGTCATGATATCTTGCGG	60
152f3	GTTTTGGCATGGATACGTATGG	58
F1	CTGCCAGTAAGGATCAAGTTTGC	60
F2	CGCAAATATTATACGTCAAGGTCG	60
F3	GCAAACGACGACCACAAACC	60
AD1	NTCGA(G/C)T(A/T)T(G/C)G(A/T)GTT	45

2.7.2. TAIL-PCR

The Thermal Asymmetric Interlaced PCR (TAIL-PCR) method is a technique for genomic walking which does not require any restriction or ligation steps as compared to inverse PCR. It utilizes nested known long sequence-specific primers with high melting temperature in combination with short (15–16 nucleotides) degenerate primers of arbitrary sequences (AD primer). A thermal cycling program composed of low-stringency and high-stringency cycles, allows only sequence-specific fragments to be exponentially amplified. AD primers with higher degrees of degeneracy in the low-stringency PCR cycle may have more chances to bind to the target sequences. In the high-stringency PCR cycles with high annealing temperatures, only the specific primer with the higher melting temperature can efficiently anneal to target molecules (Liu and Chen, 2007). Primers used for TAIL-PCR of Gm152 are given in Table 2.9 and the PCR conditions are listed in Table 2.10.

The protocol for TAIL-PCR was as follows:

-Primary reaction

Each primary reaction mixture (20 µl) consisted of 2 µl 10×PCR buffer, 200 µM each of dNTPs, 0.2 µM specific primer (152f1 or F1), 1.2 µM AD primer, 1.25 unit of Taq DNA polymerase, and 1–10 ng of DNA.

-Secondary reaction

The secondary PCR mixtures (20µl) contained 2 µl 10×PCR buffer, 200 µM each of dNTPs1, 0.2 µM internal specific primer (152f2 or F2),1.2 µM the same AD primer, 1.25 units of Taq DNA polymerase and 1 µl of the 40 time diluted PCR product from the primary reaction.

-Tertiary reaction

The tertiary PCR mixtures (20 µl) contained 2 µl 10×PCR buffer, 200µM each of dNTPs, 0.5 µM the innermost specific primer (152f3 or F3), 3µM the same AD primer, 1.25 units of Taq DNA polymerase and 1 µl of the 10 time diluted PCR product from the secondary reaction.

The secondary and tertiary PCR products were visualized by electrophoresis on 1.0% agarose gels stained with ethidium bromide. The specificity of the products was confirmed by the expected differences of size between the secondary and tertiary products.

Table2.10 . Amplfication conditions used for TAIL-PCR

Reaction	File no.[a]	Cycle no.	Thermal condition[b]
Primary	1	1	92°C (3min)
	2	1	94°C (3min)
	3	2	94°C (1min),60℃(1min),72℃(3min)
	4	1	94°C (1min)
	5	1	25°C (2min)
	6	1	72°C (3min)
	7	30	94°C (30s), 60°C (1min),72°C (3min)
	8	15	94°C (30s), 43°C (1min),72°C (3min)
	9	1	72°C (5min)
Secondary	10	24	94°C (30s), 60°C (1min),72°C (3min)
	11	12	94°C (30s), 45°C (1min),72°C (3min)
	12	1	72°C (5min)
Tertiary	13	20	94°C (30s), 45°C (1min),72°C (3min)
	14	1	72°C (30s)

2.8. Yeast complementation

2.8.1. Yeast strains

The homology searches for three selected genes were carried out by BLASTX in the Saccharomyces Genome Database (SGD; Stanford University, Stanford, CA), available on line (http://www.yeastgenome.org) (Table 2.11). Three yeast strains YGL167C, YDL128W and YFR014C, respectively knocked out for PMR1, VCX1 and CMK1 and the parental wild type strain MATa W303 were obtained from Open Biosystems (Thermo Scientific). The triple mutant K667 (Cagnac et al., 2010), was generously provided by O. Cagnac (Estación Experimental del Zaidin, CSIC, Grenada, Spain). All yeast strains used in this study are listed in Table 2.12.

Table 2.11. Comparison with the amino acid sequence databases of *Saccharomyces cerevisiae* (S288C)

Genes	Putative protein	Location	E-value
BEG141_lrc1694	YDL128W (VCX1)	Vacuolar membrane	6.2e-79
BEG141_c2781	YGL167C (PMR1)	Golgi reticulum	3.1e-120
BEG141_lrc995	YFR014C (CMK1)	Nucleus	1.9e-68

Table 2.12. Strains used in this study

Strain	Genotype	Source
W303	MATa, ura3-52, trp1-Δ2, leu2-3_112, his3-11, ade2-1, can1-100	Open Biosystems (Thermo Scientific)
YGL167C	MATa, ura3-52, trp1-Δ2, leu2-3_112, his3-11, ade2-1, can1-100, *pmr1*Δ	Open Biosystems (Thermo Scientific)
YDL128W	MATa, ura3-52, trp1-Δ2, leu2-3_112, his3-11, ade2-1, can1-100, *vcx1*Δ	Open Biosystems (Thermo Scientific)
YFR014C	MATa, ura3-52, trp1-Δ2, leu2-3_112, his3-11, ade2-1, can1-100, *cmk1*Δ	Open Biosystems (Thermo Scientific)
K667	MATa, ura3-1, trp1-1, leu2-3, his3-11, ade2-1, can1-100,*cnb*Δ::*LEU2*, *pmc1*Δ::*TRP1*, *vcx1*Δ	Cagnac et al 2010

2.8.2. Plasmid construction and yeast transformation

The yeast complementation vectors were constructed with Gateway technology with Clonase™ II (Invitrogen Corporation, Carlsbad, CA, USA) according to the manufacturer's instructions. Destination vector *pDRf1-GW* used for gateway was from

Loqué et al. (2007). The complete gene coding sequences were amplified using proofreading DNA polymerase (Platinum® *Taq* DNA polymerase High Fidelity; Invitrogen Corporation, Carlsbad, CA, USA). The primers used are listed in Table 2.13. All the plasmids were multiplied in *E. coli* grown at 37 °C in LB broth or on agar supplemented with 50 μg / ml of kanamycin or ampicillin according to the manufacturer's instructions. Yeast transformations were performed using a protocol adapted from Gietz et al. (1995). Mutant strains received either the *pDRf1-GW* -gene vector or the *pDRf1-GW* empty vector, both containing a URA3 auxotrophic marker.

Table 2.13. Primers for the complete gene coding sequences with the attB adaptor

Genes	Primer name	sequences
BEG141_lrc1694	1694_attB_F	*GGGGACAAGTTTGTACAAAAAAG* CAGGCTTCATGGCAGAGGGACAACCACTGGTCTTAAAC
	1694_attB_R	*GGGGACCACTTTGTACAAGAAAG* CTGGGTCTTACAATTTATCGGGATATAAAAAGAAAGC
BEG141_c2781	2781_attB_F	*GGGGACAAGTTTGTACAAAAAAG* CAGGCTTCATGGATGACGCATTTACAAAAAGTCC
	2781_attB_R	*GGGGACCACTTTGTACAAGAAAG* CTGGGTCCTAATCAACTTTAATTTTTGTTGGTGG
BEG141_lrc995	995_attB_F	*GGGGACAAGTTTGTACAAAAAAG* CAGGCTTCATGCGTAAATATTATAGAAATACTCCG
	995_attB_R	*GGGGACCACTTTGTACAAGAAAG* CTGGGTCTTAAACCGGTATAACTTTGTTTTTCG

2.8.3. Growth media and tests

Transformants were selected on a SD media (0.67 % yeast nitrogen base, 2 % glucose) with the appropriate amino acids and lacking uracil. The medium for growth tests were YPD medium (1 % yeast extract, 2 % peptone, 2 % glucose) or SD medium with / without uracil. The medium adding a series of concentration of $CaCl_2$ were used for knockout strain phenotypic selection according to Szigeti et al. (2005) and Kmetzsch et al. (2010). Cells were grown at 30 °C and 37 °C for 2 d.

2.9. Statistical analysis

All data were statistically compared between treatments using one-way ANOVA using the Systat version 10 program (Systat Software 2000). Significant differences between means were established by the Tukey's pairwise comparison test at $P \leq 0.05$.

Where ANOVA gave P values just above 0.05 between wild type and mutant root data, gene expression was also compared separately for different time points using the Student's t-test at $P \leq 0.05$.

CHAPTER 3

Studies of *G. mosseae* genes expressed before root contact with *A. sinicum*

Evidence for the implication of calcium in early recognition responses of roots to the symbiotic fungi has been obtained from gene expression studies, but little is known for the molecular mechanism on fungal partner. Breuninger and Requena (2004) reported that gene expression in *G. mosseae* during appressorium development was up-regulated. In their work, the expression of genes (named Gm2 and Gm152), putatively encoding a MAP3k-like protein kinase (clone 2) and a P-type ATPase (clone 152), were up-regulated with appressorium formation on parsley roots and could potentially be involved in cellular Ca^{2+} homeostasis and signaling. Consequently, we targeted these two genes for further study. This work (the 1st year of my PhD research) was carried out at Huazhong Agriculture University, Wuhan, China. *A. sinicus* was used as host plant since much work about AM fungi - *A. sinicus* interactions has been carried out in the laboratory in Wuhan.

3.1. Fungal gene expression monitored by reverse-transcription (RT)-PCR

Transcript analyses of the two selected *G. mosseae* genes and *PMA1* by RT-PCR indicated significant activation of Gm2 and slight up-regulation of Gm152 in germinated spores stimulated by crude *A. sinicus* root exudates as compared to spores germinated in water (Fig. 3.1). *PMA1* expression did not appear to be affected by root exudates; this gene is highly expressed during asymbiotic growth but is down-regulated during the symbiotic phase of fungal growth in roots (Requena et al., 2003).

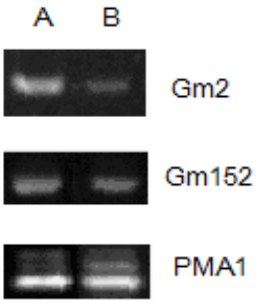


Fig. 3.1 Transcript levels of *G. mosseae* genes in germinated spores treated with *A. sinicus* root exudates (A) or not (B) (RT-PCR 33cycles, 60 °C)

3.2. Full length gene sequences and analyses

A total 7498bp genomic sequence of Gm152 was obtained by PCR amplification of G. mosseae genomic DNA using TAIL-PCR, and the upstream regulating sequence was obtained by Inverse PCR. It has 22 exons and 21 introns (Fig. 3.2); a promoter region was predicted in 1484 to 1734bp (http://www.ncbi.nlm.nih.gov/Class/NAWBIS/Modules/DNA/dna21b.html).

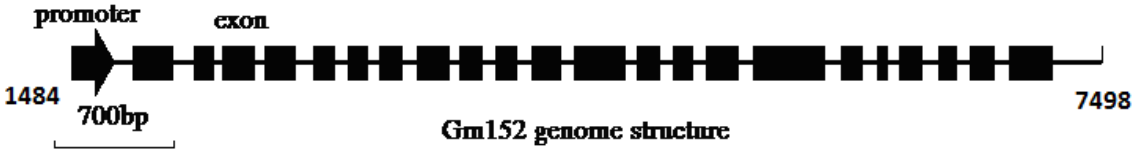


Fig. 3.2 Predicted genome structure of Gm152 containing 22 exons and 21 introns. The promoter region is indicated by ➡, exon positions are indicated by ▮

The final full-length cDNA, named Gm152, covers 3907bp and includes an open reading frame encoding 1188 amino acids, a 160 bp 3'-untranslated region (UTR), and a polypeptide with a predicted molecular weight of 134.81kDa. It was predicted to be a P-ATPase, member of the E1-E2_ATPase superfamily. A hydrolase domain, a protein tyrosine phosphatase and twelve transmembrane regions were also predicted (http://www.isrec.isb-sib.ch/ftp-server/tmpred/www/TMPRED_form.html) (Fig. 3.3). Multiple sequence alignments with amino acid sequences in databases showed that Gm152 is closely related to various fungal P-type ATPases (Fig. 3.4): *Ajellomyces dermatitidis* (54% identities), *Aspergillus nidulans* (56% identities), *Pichia stipitis* (52% identities), *Schizosaccaromyces pombe* (50% identities). In particular, it shows 58% identity to an endoplasmic reticulum Ca^{2+}-transporting P-type ATPase from the ectomycorrhizal fungus *Laccaria bicolor* (XP_001889526).

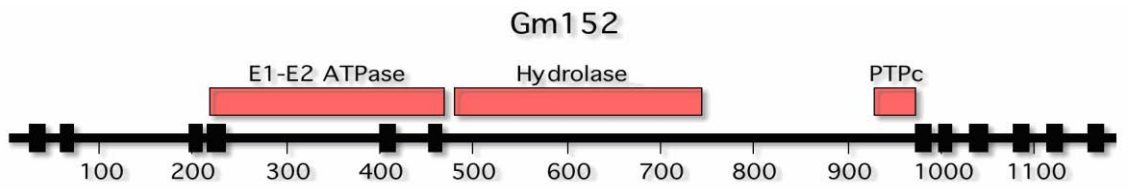
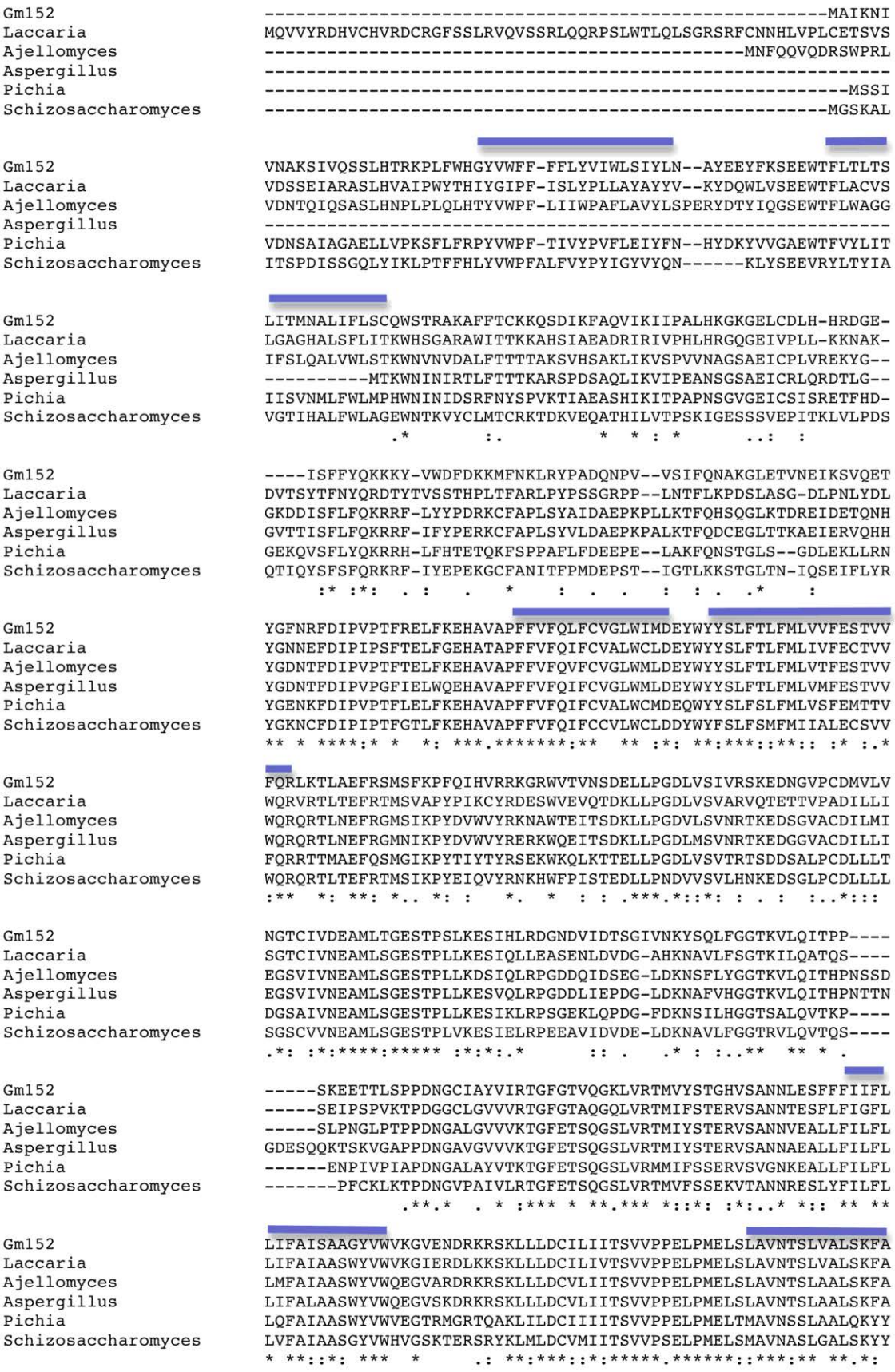


Fig. 3.3 Predicted topology model of Gm152 containing predicted functional regions: E1-E2_ATPase, hydrolase and tyrosine phosphatase (PTPc) and twelve putative transmembrane regions (▮).


Gm152 ----------MAIKNI
Laccaria MQVVYRDHVCHVRDCRGFSSLRVQVSSRLQQRPSLWTLQLSGRSRFCNNHLVPLCETSVS
Ajellomyces ----------MNFQQVQDRSWPRL
Aspergillus ----------
Pichia ----------MSSI
Schizosaccharomyces ----------MGSKAL
Gm152 VNAKSIVQSSLHTRKPLFWHGYVWFF-FFLYVIWLSIYLN--AYEEYFKSEEWTFLTLTS
Laccaria VDSSEIARASLHVAIPWYTHIYGIPF-ISLYPLLAYAYYV--KYDQWLVSEEWTFLACVS
Ajellomyces VDNTQIQSASLHNPLPLQLHTYVWPF-LIIWPAFLAVYLSPERYDTYIQGSEWTFLWAGG
Aspergillus ----------
Pichia VDNSAIAGAELLVPKSFLFRPYVWPF-TIVYPVFLEIYFN--HYDKYVVGAEWTFVYLIT
Schizosaccharomyces ITSPDISSGQLYIKLPTFFHLYVWPFALFVYPYIGYVYQN------KLYSEEVRYLTYIA
Gm152 LITMNALIFLSCQWSTRAKAFFTCKKQSDIKFAQVIKIIPALHKGKGELCDLH-HRDGE-
Laccaria LGAGHALSFLITKWHSGARAWITTKKAHSIAEADRIRIVPHLHRGQGEIVPLL-KKNAK-
Ajellomyces IFSLQALVWLSTKWNVNVDALFTTTTAKSVHSAKLIKVSPVVNAGSAEICPLVREKYG--
Aspergillus ----------MTKWNININRTLFTTTKARSPDSAQLIKVIPEANSGSAEICRLQRDTLG--
Pichia IISVNMLFWLMPHWNINIDSRFNYSPVKTIAEASHIKITPAPNSGVGEICSISRETFHD-
Schizosaccharomyces VGTIHALFWLAGEWNTKVYCLMTCRKTDKVEQATHILVTPSKIGESSSVEPITKLVLPDS
Gm152 ----ISFFYQKKKY-VWDFDKKMFNKLRYPADQNPV--VSIFQNAKGLETVNEIKSVQET
Laccaria DVTSYTFNYQRDTYTVSSTHPLTFARLPYPSSGRPP--LNTFLKPDSLASG-DLPNLYDL
Ajellomyces GKDDISFLFQKRRF-LYYPDRKCFAPLSYAIDAEPKPLLKTFQHSQGLKTDREIDETQNH
Aspergillus GVTTISFLFQKRRF-IFYPERKCFAPLSYVLDAEPKPALKTFQDCEGLTTKAEIERVQHH
Pichia GEKQVSFLYQKRRH-LFHTETQKFSPPAFLFDEEPE--LAKFQNSTGLS--GDLEKLLRN
Schizosaccharomyces QTIQYSFSFQRKRF-IYEPEKGCFANITFPMDEPST--IGTLKKSTGLTN-IQSEIFLYR
Gm152 YGFNRFDIPVPTFRELFKEHAVAPFFVFQLFCVGLWIMDEYWYYSLFTLFMLVVFESTVV
Laccaria YGNNEFDIPIPSFTELFGEHATAPFFVFQIFCVALWCLDEYWYYSLFTLFMLIVFECTVV
Ajellomyces YGDNTFDIPVPTFTELFKEHAVAPFFVFQVFCVGLWMLDEYWYYSLFTLFMLVTFESTVV
Aspergillus YGDNTFDIPVPGFIELWQEHAVAPFFVFQIFCVGLWMLDEYWYYSLFTLFMLVMFESTVV
Pichia YGENKFDIPVPTFLELFKEHAVAPFFVFQIFCVALWCMDEQWYYSLFSLFMLVSFEMTTV
Schizosaccharomyces YGKNCFDIPIPTFGTLFKEHAVAPFFVFQIFCCVLWCLDDYWYFSLFSMFMIIALECSVV
Gm152 FQRLKTLAEFRSMSFKPFQIHVRRKGRWVTVNSDELLPGDLVSIVRSKEDNGVPCDMVLV
Laccaria WQRVRTLTEFRTMSVAPYPIKCYRDESWVEVQTDKLLPGDLVSVARVQTETTVPADILLI
Ajellomyces WQRQRTLNEFRGMSIKPYDVWVYRKNAWTEITSDKLLPGDVLSVNRTKEDSGVACDILMI
Aspergillus WQRQRTLNEFRGMNIKPYDVWVYRERKWQEITSDKLLPGDLMSVNRTKEDGGVACDILLI
Pichia FQRRTTMAEFQSMGIKPYTIYTYRSEKWKQLKTTELLPGDLVSVTRTSDDSALPCDLLLT
Schizosaccharomyces WQRQRTLTEFRTMSIKPYEIQVYRNKHWFPISTEDLLPNDVVSVLHNKEDSGLPCDLLLL
Gm152 NGTCIVDEAMLTGESTPSLKESIHLRDGNDVIDTSGIVNKYSQLFGGTKVLQITPP----
Laccaria SGTCIVNEAMLSGESTPLLKESIQLLEASENLDVDG-AHKNAVLFSGTKILQATQS----
Ajellomyces EGSVIVNEAMLSGESTPLLKDSIQLRPGDDQIDSEG-LDKNSFLYGGTKVLQITHPNSSD
Aspergillus EGSVIVNEAMLSGESTPLLKESVQLRPGDDLIEPDG-LDKNAFVHGGTKVLQITHPNTTN
Pichia DGSAIVNEAMLSGESTPLLKESIKLRPSGEKLQPDG-FDKNSILHGGTSALQVTKP----
Schizosaccharomyces SGSCVVNEAMLSGESTPLVKESIELRPEEAVIDVDE-LDKNAVLFGGTRVLQVTQS----
Gm152 -----SKEETTLSPPDNGCIAYVIRTGFGTVQGKLVRTMVYSTGHVSANNLESFFFIIFL
Laccaria -----SEIPSPVKTPDGGCLGVVVRTGFGTAQGQLVRTMIFSTERVSANNTESFLFIGFL
Ajellomyces -----SLPNGLPTPPDNGALGVVVKTGFETSQGSLVRTMIYSTERVSANNVEALLFILFL
Aspergillus GDESQQKTSKVGAPPDNGAVGVVVKTGFETSQGSLVRTMIYSTERVSANNAEALLFILFL
Pichia ------ENPIVPIAPDNGALAYVTKTGFETSQGSLVRMMIFSSERVSVGNKEALLFILFL
Schizosaccharomyces -------PFCKLKTPDNGVPAIVLRTGFETSQGSLVRTMVFSSEKVTANNRESLYFILFL
Gm152 LIFAISAAGYVWVKGVENDRKRSKLLLDCILIITSVVPPELPMELSLAVNTSLVALSKFA
Laccaria LIFAIAASWYVWVKGIERDLKKSKLLLDCILIVTSVVPPELPMELSLAVNTSLVALSKFA
Ajellomyces LMFAIAASWYVWQEGVARDRKRSKLLLDCVLIITSVVPPELPMELSLAVNTSLAALSKFA
Aspergillus LIFALAASWYVWQEGVSKDRKRSKLLLDCVLIITSVVPPELPMELSLAVNTSLAALSKFA
Pichia LQFAIAASWYVWVEGTRMGRTQAKLILDCIIIITSVVPPELPMELTMAVNSSLAALQKYY
Schizosaccharomyces LVFAIAASGYVWHVGSKTERSRYKLMLDCVMIITSVVPSELPMELSMAVNASLGALSKYY

```
Gm152                   IYCTEPFRIPYAGKVDVCAFDKTGTLTRANLVVEGVAGIHPE----------DSKKLVKP
Laccaria                IFCTEPFRIPFAGRVDVCCFDKTGTITAENLVLEGVAGVNVV----------DPRKLVGV
Ajellomyces             IFCTEPFRIPYAGRIDIACFDKTGTLTGEDLLVDGIAGLTLGHAGAKTDKHGAHTDITPV
Aspergillus             IFCTEPFRIPFAGRVDVACFDKTGTLTGEDLVVDGVAGLALGQPGAKVEKDGAHTELSKG
Pichia                  VYCTEPFRIPLAGRIDVCCFDKTGTLTAEDLVFEGLAGFNLN----------DIHHLFKC
Schizosaccharomyces     IYCTEPFRIPLSGHLDICCFDKTGTLTEEHMVVQGIAGVNRK----------DPYSLEKL
                        ::******** :*:::*:..******:*  .:::.:*:**.                :

Gm152                   PDALRDTIQTLAAAHALARLDDDDDI--VVGDPMEKVTLEALEWKLDKNKRDTVIPQS--
Laccaria                KETSRETTLCLAAAHALVQLDDG--T--VVGDPMEKTTLDSLEWTLGKG--NVISPSS--
Ajellomyces             EKVANETTLVLATAHALVKLDEGE----IVGDPMEKATLTSLGWVLGRN--DILTSKATG
Aspergillus             SSIPVDTTLVLASAHALVKLDEGE----VVGDPMEKATLQWLGWTLGKN--DVLTSKS-G
Pichia                  EDAPETTSLVLGSAHALVRLDDGD----IVGDPMEQATLKAAHWNVGNN--DTVERDI--
Schizosaccharomyces     SDASNDAILAIATAHTLVLLEQEGETPKVVGDPMEKATVENLGWSIEKK--NFVSAPE--
                         .    :   :.:**:*. *::      :******:.*:    * : .   : :

Gm152                   ---QRFQSRSQLQIHRRFLFSSALKRMSSVSTVTTP------RGKKTFIAVKGAPETLRQ
Laccaria                ---NVAPHRTHLTIRRRFQFSSALKRMSTLSSLPN---------GKIIAAVKGAPETIKG
Ajellomyces             VSRQPGRALDSVQIKRRFQFSSALKRQSAIATVVSTDRQTSKKLKGTFVGVKGAPETIRA
Aspergillus             LATGAARSPESVQVKRRFQFSSALKRQSTIATVVIQDRKTSKKVKSTFVGVKGAPETIET
Pichia                  ---GKGKS-EKIKILRRFQFSSALKRSSAISSINTVPGKN-------FVAAKGAPETIRN
Schizosaccharomyces     ---GSVFYKGKVQIIRNFQFSSALKRQSSVSNVRVSGGS-----FKTFVSVKGAPEVIAT
                                : : *.* ******* *:::.:             : ..*****.:

Gm152                   MYLYVPDDYEETFKFFTRRGSRVLALGYKYLEDNMTIDK--INGLLREDVESELNFAGFL
Laccaria                MLDVVPENYDQTYKWFTRKGSRVLALGMKDMEP-MNADK--INKLPRDQVESKLVFAGFL
Ajellomyces             MLVSTPPHYEETFKYFTRNGARVLALGYKYLSTESELGQGRINNLKREDVESDLHFAGFL
Aspergillus             MLVNTPPNYEETFKYFTRNGARVLALAYKYLSSEAELSQGRINNYTREEIESELIFAGFL
Pichia                  MIIDAPENYEDIYKSFTRSGSRVLALAYKYLDANVN-----VNKVAREEIESKLHFAGFI
Schizosaccharomyces     MLREVPKDYEKIYKDYGRKGSRVLALGYKYFKNYIPENQ--VSDLSRESIESDLVFAGFL
                        *   .* .*:. :* : * *:*****. * :.         :.   *:.:**.* ****:

Gm152                   VFHCPLKDDAVSTLQMLNESSHRVIMITGDNPLTACHVAREVKIIERDVLILDIQEDAKS
Laccaria                VFHCPLKIDAVETLKMLADSSHRCIMITGDNPLTAVHVARDVEIVDREAMILDLAENPRH
Ajellomyces             VLQCPLKDDAVKALRMLNESSHRVVMITGDNPLTAAHVARQVEIVDREVLILDAPENDNS
Aspergillus             VLQCPLKDDAIKAVRMLNESSHRVVMITGDNPLTAVHVARQVEIVDREVLILDAPEHDTS
Pichia                  VFHCPLKDDAVETIKMLNESSHRSVMITGDNPLTACHVAKQVAITTKDVLILDAPEEHHD
Schizosaccharomyces     IFTSPLKEDARQTVQMLNNSSHRCMMITGDNPLTAVYVAEQVGIVEKPTLVLDIKHENEK
                        :: .*** ** .:::** :**** :********** :**.:* *  : .:::**  ..

Gm152                   PDELVWKSVDEKIMIPVNPIEPIERSVFRDYDICVTGAALSQYENKPSVRELLRNTWVYA
Laccaria                DGDLVFRTVDESKIIPVDPSEPFDLSVFDQYDICVTGAAMKQFVSKPSWNDLVQNTWVYA
Ajellomyces             GTKLVWRTIDDTFSVDVDPTQPLDREILATKDLCVTGYALAKFKNQKGFSDLLRHTWVYA
Aspergillus             GTKVVWRSIDDKINIDVDPTKPLDKEILKTKDICITGHALAKFKDQKALPDLLRHTWVYA
Pichia                  -QNLVWRNVTESIVIPFKSSDEINTELFKKYDVCITGYALGYLADHEQILDLLKHTWVYA
Schizosaccharomyces     --ILEWKSTDDTINLPMNPHKSLEASLYEKYDLCITGRALSQIINPDVIMSIFTHAWVYA
                           : ::.  :.  : ... . :: .:    *:*:** *:    .     .:. ::****

Gm152                   RVSPGQKEFILTELKKAGYTTLMVGDGTNDVGALKQAHVGVALLNGTPEDLKKIAERRRM
Laccaria                RVSPSQKEHILTTLKTLGYITLMAGDGTNDVGALKQAHIGVALLDGTPEDLQKIAERQRL
Ajellomyces             RVSPKQKEDILLGMKDAGYTTLMCGDGTNDVGALKQAHVGVALLNGSQDDLNKIAEHWRN
Aspergillus             RVSPKQKEDILLGLKDAGYTTLMCGDGTNDVGALKQAHVGVALLNGSPEDLTRIAEHYRT
Pichia                  RVSPNQKEFILTSLKEAGYNTLMCGDGTNDVGALKQAHIGVALLNGTEDGLKKIAENRKI
Schizosaccharomyces     RVSPSQKEFMISTLKHNGYITLMCGDGTNDVGALKQAHVGVALLNASEEDMLEMQERARN
                        **** *** ::  :*  ** *** **************:*****:.: :.: .: *. :

Gm152                   ITLKDMYENQLKFTARFNMPPPPPPPAIAHLFP----------------------------
Laccaria                ERIKKVYESQLKISARFGQVPPPVPPAIAHLLP----------------------------
Ajellomyces             NKMKEIYEKQVSLMQRFNQPAPPVPANVAHLYPPGPNNPHYEKAMIREAQRKGITGPAAT
Aspergillus             TKMKEIYEKQVNMMQRFNQPPPPVPAQIAHLYPPGPGNPHYQKAMEREAAKRGAK-DAAN
Pichia                  EAMTRVYEKQVEIFTNWGKNPPPVPPQLAHVYPPGPNNPKYLEALQ----KRGVEITDEM
Schizosaccharomyces     QKLMGVYEKQIQLAKRFNLPTPPVPPALCHAFPPGPNNPHREKTQEG-------------
                          :  :**.*:.:  .:.  .** *. :.*  *

Gm152                   ---HITQQQQ--------------------QQNNPARHAPRVDQIAEQLLQDFDD-EPPS
Laccaria                ---DAVQAQQRVAADLQVA-----------RQRNPMEKFDLNSITEKMAEMEGEE-DVPK
Ajellomyces             EGNGVPTVTSPGAQAIQQSNANLTPQQRQQQQASLAAAGFADKLTATMMEQELDDSEPPT
Aspergillus             QPEAIPTITSPGAQALQQS--NLTPQQQRQQQAQQAAAGFADKLTSTMMEQELDDNEPPT
Pichia                  R-RAVAIANRGGLPKIKAK------------EGKQSASSIADSLMASLNDPEGED-EAPV
Schizosaccharomyces     LNKVLEDLETKKASDVQLT---------EAEKAAERRANLANKMFDTLANASDDE--APK
                                                    :          .         . ::   *

Gm152                   IKFGDASVASHFTSKLSNVSAIANIIRQGRCTLVATIQMYKILALNCLISAYSLSVLYLD
Laccaria                IKLGDASCAAPFTSKLSHVSAITHIIRQGRCTLVATIQMYKILALNCLITAYSLSVQYLD
Ajellomyces             IKLGDASVAAPFTSKLANVIAIPNIIRQGRCTLVATIQMYKILALNCLISAYSLSVIYLD
Aspergillus             IKLGDASVAAPFTSKLANVIAIPNILRQGRCTLVATIQMYKILALNCLISAYSLSVIYLD
Pichia                  LKLGDASVAAPFTSKLANVSTVTNIIRQGRCALVSTIQMYKILALNCLISAYSLSVLYLA
Schizosaccharomyces     LKLGDASVAAPFTSKLAVVSSITNIVRQGRCTLVALVQMHKILALNCLITAYSLSVLHLD
                        :*:**** *: *****: * ::.:*:*****:**: :**:*********:****** :*
```

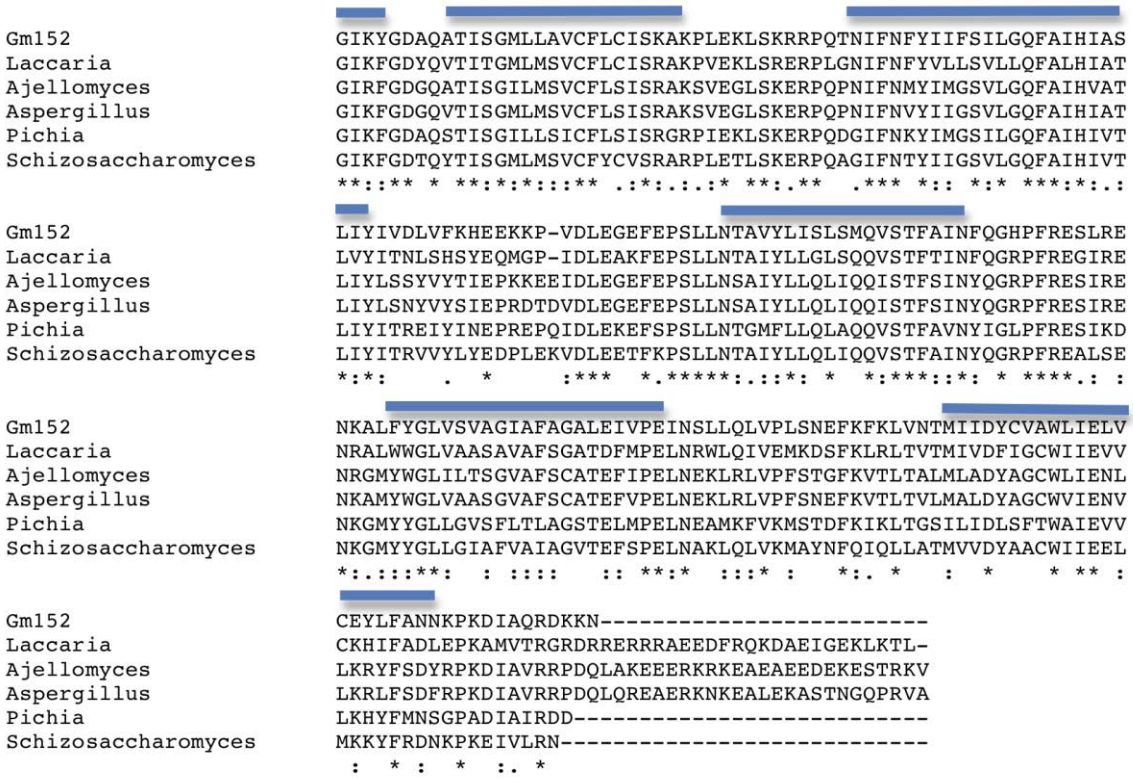


Fig. 3.4 Amino acid sequence alignment of Gm152 with P-type ATPase protein sequences from other organisms. Identical residues in all the sequences are marked with an asterisk. The putative transmembrane regions are indicated (▮). The GenBank accession numbers of the P-type ATPase proteins are: *Laccaria bicolor* (XP_001889526), *Schizosaccharomyces pombe* (NP_593971), *Pichia stipitis* (XP_001385220), *Ajellomyces dermatitidis* (XP_002623160) and *Aspergillus nidulans* (CBF83315).

3.3. Localization of *G. mosseae* Gm152 gene activity in mycorrhizal roots of *A. sinicus*

Results from in situ RT-PCR of Gm152 transcripts are given as Nomarski images, confocal fluorescence images, and a superposition of fluorescence and Nomarski images (Figs. 3.5, 3.6). Samples with RNAse digestion served as negative controls (Fig. 3.5). Autofluorescence of plant and fungal tissues was eliminated by analysing autofluorescence under different wavelength regions; where wavelength regions gave strong fluorescence in the negative control samples, these regions were avoided and only regions where autofluorescence in the negative controls was weaker were used to observe samples.

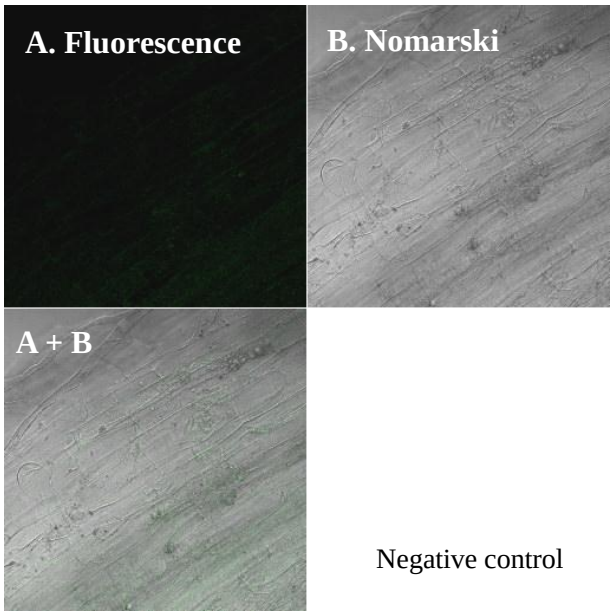


Fig. 3.5 Negative control for direct fluorescent *in situ* RT-PCR in *A. sinicus* roots after RNAse digestion to eliminate RNA.

When green fluorescent-labeled amplified cDNA was observed in situ, only a weak signal was detected in extraradical mycelium, whereas no signal was detected in the any cells of mycorrhizal *A. sinicus* root tissues (Fig. 3.6). Gm152 appears to be expressed in extraradical mycelium but it was not possible to conclude to the localization of Gm152 expression in intraradical fungal structures as the in situ RT-PCR gave a very weak signal or important background.

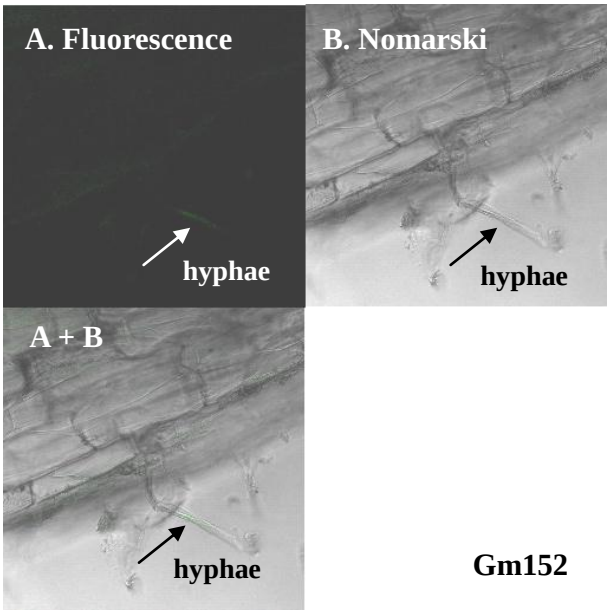


Fig. 3.6 Detection of Gm152 gene activity by direct fluorescent *in situ* RT-PCR in *G. mosseae* hyphae associated with *A. sinicus* roots after DNAse digestion to eliminate genomic DNA.

3.4. Discussion and conclusions

In a first step to investigate the role of Ca^{2+} in the molecular responses of the fungal partner during processes leading to the establishment of the mycorrhizal symbiosis, we selected two *G. mosseae* genes, Gm2 and Gm152, which had previously been reported to be up-regulated at the early stage of appressoria formation on parsley roots (Breuninger & Requena, 2004). The putative function and expression profiles of these two genes suggested that they may be involved in Ca^{2+}-regulated processes related to mycorrhiza interactions. Following the expression pattern observed by RT-PCR for Gm2 and Gm152 in root exudates of *A. sinicus*, both fungal genes appear to be activated also prior to contact with the host plant.

The full-length sequence obtained for Gm152 confirmed a probable function of P-type ATPase for this *G. mosseae* gene. ATPases carry out many energy-driven fundamental processes in biology, and P-type ATPases are members of a large family of biological energy transducers that utilize the chemical energy of ATP hydrolysis to generate transmembrane electrochemical ion gradients. The Gm152 protein contains two functional regions, E1-E2_ATPase and a hydrolase, and it shows high similarity to the endoplasmic reticulum Ca^{2+}-transporting P-type ATPase from the ectomycorrhizal fungus *L. bicolor*. Consequently, this gene product might be involved in pumping Ca^{2+} across the membrane to produce ion fluxes for Ca^{2+}-dependent signaling processes. Furthermore, a *Gigaspoara rosea* gene, *Gros(ASP)1*, putatively encoding a Type IIB calcium ATPase was up-regulated during the developmental switch from asymbiosis to presymbiosis (Tamasloukht et al. 2007). In this case, Gm152 could be one component of Ca^{2+}-related proteins that play a role in the adaptation of the cell to variations in Ca^{2+} concentrations (homeostasis) during symbiotic interactions.

However, further investigations of *G. mosseae* Ca^{2+}-related genes that could be involved in cellular Ca^{2+} homeostasis and signaling during successful mycorrhizal interactions are hampered by the lack of sequence information for this fungus. It was therefore decided to continue this work using another AM fungus, *G. intraradices*, for which a large amount of genome and transcriptome data has recently become available (Martin et al., 2008; Tisserant et al., 2012). A preliminary search showed the presence of a gene (Glomus_c14022) homologous (84% similarities) to *Gm152* in the *G. intraradices* genome. However, the microarray analysis showed that gene Glomus c14022 was down-

regulated with fungal development within roots as compare to spores (P value > 0.05).

CHAPTER 4

Growth and mycorrhiza development in wild-type and mycorrhiza-defective mutant plants

4.1. *Medicago truncatula* wild-type J5 and the mutant TRV25

Fresh shoot and root weights and fungal development were determined at each time point after inoculation with *G. intraradices* BEG141. Plant growth (Table 4.1) and appressoria formation by the AM fungus (Table 4.2) did not differ significantly (t-test) between wild-type *M. truncatula* J5 and the symbiosis-defective mutant TRV25 at 4 and 6 days after inoculation (dai).

Table 4.1. Development of the two *Medicago truncatula* genotypes at 4 dai and 6 dai

	***M. truncatula* genotype**	**Fresh shoots (g)**	**Fresh roots (g)**
4 dai	**J5**	0.039 a	0.022 a
	TRV25	0.041 a	0.022 a
6 dai	**J5**	0.064 a	0.059 a
	TRV25	0.053 a	0.057 a

Values followed by the same letter are not significantly different ($P \geq 0.05$) (ANOVA, Tukey test).

Table 4.2. Number of appressoria formed by *Glomus intraradices* BEG141 on the two *Medicago truncatula* genotypes 4 and 6 days after inoculation

***M. truncatula* genotype**	**Appressoria per cm root**	
	4 dai	**6 dai**
J5	0.86 a	1.66 a
TRV25	0.94 a	0.76 a

Values followed by the same letter are not significantly different ($P \geq 0.05$) (ANOVA, Tukey test).

At later stages of interactions with (17, 21 dai), hyphae had penetrated the roots of wild-type *M. truncatula*, forming arbuscules within cortical cells and vesicles (Fig. 4.1), whilst root penetration beyond the epidermis did not occur on the mutant roots. Time-course results of mycorrhiza colonization showed that *G. intraradices* developed well in wild-type *M. truncatula* roots (Table 4.3).

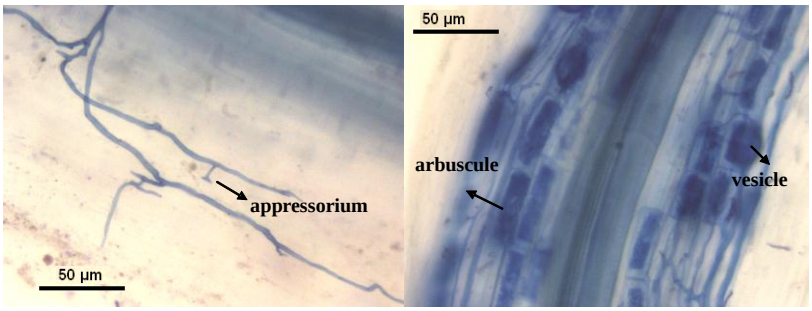


Fig. 4.1. Light micrographs of *G. intraradices* BEG141 development in wild-type *M. truncatula* J5 roots. Bars= 50 µm

Table 4.3. Development of *G. intraradices* BEG141 in *Medicago truncatula* wild-type J5 roots (F – frequency of the AM fungus in the root system; M - intensity of mycorrhizal colonization in the root system; m – intensity of mycorrhizal colonization in mycorrhizal root fragments; A - arbuscule abundance in the root system; a - arbuscule abundance in mycorrhizal root fragments; V - vesicle abundance in the root system; v - vesicle abundance in mycorrhizal root fragments).

Mycorrhiza colonization	4 dai	6 dai	17 dai	21 dai
F%	0.9	4.70±0.19	94.5±2.22	98.9±1.11
M%	n.d.	0.24±0.01	58.3±3.83	80.4±5.65
A%	n.d.	0.09±0.03	35.2±6.70	67.5±8.04
V%	n.d.	n.d.	25.2±6.95	34.9±3.12
m%	n.d	5	61.8±4.22	81.2±4.86
a%	n.d	10	59.5±7.90	83.3±4.48
v%	n.d	n.d	47.5±10.3	43.3±2.25

Data presented are mean values with standard errors from three biological repetitions; n.d.= not detected.

The AM fungus had penetrated wild-type J5 roots forming rare arbuscules (A % = 0.09) at 6 dai, and by 21 dai, most of the root system of wild-type *M. truncatula* was colonized (M % = 80.4) and arbuscules were abundant (A% = 67.5) (Fig. 4.2).

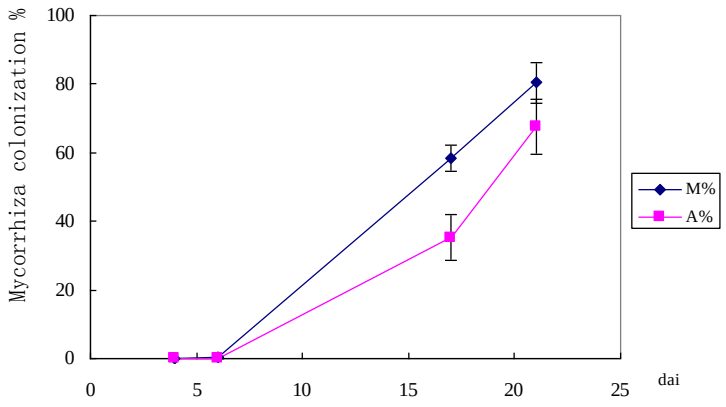


Fig 4.2. *Glomus intraradices* BEG141 development in *M. truncatula* wild-type (J5) roots (M %: intensity of the mycorrhizal colonisation; A %: arbuscule abundance). Bars = standard errors

4.2. Wild type *Pisum sativum L.* cv Finale and the mutant *Pssym36*

No significant difference (t-test) in the weight of roots or shoots was observed between the two pea genotypes (Tables 4.4), indicating that the mutation in the *Pssym36* gene did not affect biomass accumulation at 21dai as compared with wild type cv Finale plants.

Table 4.4. Development of the two *P. sativum L.* genotypes at 21 days after inoculation

Genotypes	Fresh shoots (g)	Fresh roots (g)
Finale	1.83 a	4.49 a
Pssym36	2.01 a	4.22 a

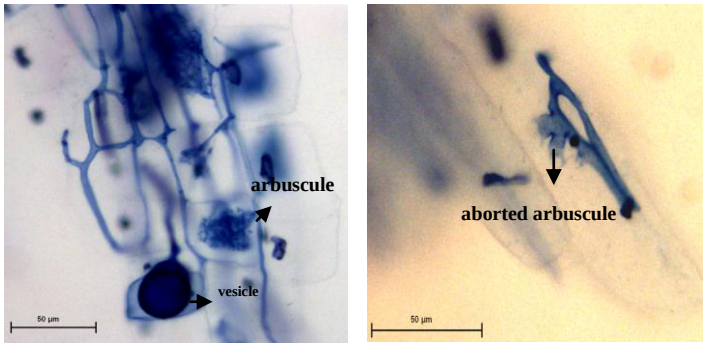
Values followed by the same letter are not significantly different ($P \geq 0.05$) (ANOVA, Tukey test).

G. intraradices developed less in *Pssym36* mutant roots than in wild type cv Finale according to the mycorrhization parameters (Tables 4.5). The AM fungus penetrated mutant *Pssym36* roots but rarely formed vesicles, and only aborted arbuscules with stumpy branches were observed within root cortical cells at 21 dai as compared to wild type cv Finale (Fig. 4.3).

Table 4.5. Mycorrhization parameters of the wild type Finale and mutant *Pssym36* at 21 dai with *G. intraradices* BEG141 (F – frequency of the AM fungus in the root system; M - intensity of mycorrhizal colonization in the root system; m – intensity of mycorrhizal colonization in mycorrhizal root fragments; A - arbuscule abundance in the root system; a - arbuscule abundance in mycorrhizal root fragments; V - vesicle abundance in the root system; v - vesicle abundance in mycorrhizal root fragments).

Genotypes	F %	M %	A %	V %	m %	a %	v %
Finale	71.1 ± 2.2	35.2 ± 2.3	21.9 ± 2.7	15.7 ± 3.1	49.8 ± 4.6	61.7 ± 3.6	43.9 ± 6.1
Pssym36	56.7 ± 8.4	13.0 ± 6.7	1.43 ± 0.9	0.20 ± 0.2	20.7 ± 7.6	9.87 ± 1.3	0.81 ± 0.7

Data presented are mean values with standard errors from three biological repetitions.



Wild type cv Finale ***Pssym36* mutant**

Fig. 4.3. Light micrographs of *G. intraradices* BEG141 development in roots of wild type and *Pssym36* mutant *P. sativum* plants. Bars=50 µm

4.3. Discussion and conclusions

Microscope observations of *G. intraradices* BEG141 development confirmed that the *M. truncatula* and *P. sativum* mutants have modified AM phenotypes as compared to the wild type plants. AM colonization of roots in the *M. truncatula* mutant TRV25 (mutated for the *DMI3/MtSYM13* gene) was blocked after the appressorium stage and characterized by the absence of intraradical mycelium, as already described (Catoira et al., 2000; Morandi et al., 2005). Mutation in the *PsSym36* gene of *P. sativum* influenced arbuscule formation and limited it to aborted branches after the penetration of root cortical cells. The production of vesicles was also blocked which may result from insufficient carbon transfer from the plant to the AM fungus in the absence of functional arbuscules (Kuznetsova et al., 2010). However, the mutations in the *DMI3/MtSYM13* and *PsSym36* genes did not affect plant development (shoot and root biomass accumulation) at 4, 6, 17 and 21 dai respectively.

The biological systems developed for *M. truncatula* and *P. sativum* were used in the studies that follow to investigate the role of *G. intraradices* genes related to calcium homeostasis and/or signalling in arbuscular mycorrhiza interactions.

CHAPTER 5

Selection of *G. intraradices* genes related to calcium homeostasis and signalling in arbuscular mycorrhiza interactions

5.1. Homology searches and primer design for fungal genes based on selected ESTs in *G. intraradices* DAOM 197198 (syn. *R. irregularis*)

Seven ESTs encoding Ca^{2+}-related proteins were selected from the transcriptome sequencing programme of *G. intraradices* DAOM197198 (syn. *R. irregularis*) (Tisserant et al., 2012). Six of the corresponding genes putatively encode proteins involved in membrane transport (two vacuolar Ca^{2+} ion transporters, three Ca^{2+}ATPases, one mitochondrial Ca^{2+}-binding carrier) and one Ca^{2+}/calmodulin-dependent protein kinase (CCaMK) (Table 5.1).

Table 5.1. Putative functions of selected *G. intraradices* DAOM197198 genes

ESTs	Putative function	Organism	E-value
Glomus_c17763	Vacuolar Ca/Mn transporter (1)	*Saccharomyces cerevisiae*	7e-20
Glomus_lrc1694	Vacuolar Ca/Mn transporter (2)	*Saccharomyces cerevisiae*	3e-53
Glomus_c3514	Vacuolar Ca^{2+}-transporting ATPase II	*Schizosaccharomyces pombe*	9e-21
	Plasma membrane Ca^{2+}-transporting ATPase II	*Oreochromis mossambicus* (*Mozambique tilapia*)	2e-12
Glomus_c2781	Sarcoplasmic/endoplasmic reticulum calcium ATPase II	*Rana esculenta* (edible frog)	2e-40
Glomus_c10704	Golgi reticulum P-type Ca^{2+} ATPase II	*Pongo abelii* (Sumatran orangutan)	1e-10
Glomus_c23149	Mitochondria membrane Ca^{2+}-dependent carrier	*Homo sapiens* (human)	5e-92
Glomus_lrc995	Nuclear CCaMK	*Mus musculus* (house mouse)	4e-69

More detailed homology searches were carried out by Blast p (Tables 5.2 and 5.3) for the three genes putatively encoding P-type ATPases, that is, the ESTs Glomus_c3514, Glomus_c2781 and Glomus_c10704. According to comparisons with data from Corradi and Sanders (2006), Glomus_c2781 and Glomus_c10704 are closely related to P-type II A ATPases (SERCA ATPase) whilst Glomus_c3514 is closely related to a P-type II B ATPase (PMCA ATPase).

Table 5.2. Comparison with the amino acid sequence databases of Type IIA ATPase (SERCA ATPase) according to Corradi and Sanders (2006)

Type IIA (SERCA ATPase)		E-value (Blast p)		
Organism	**Putative protein**	**Glomus_ c 2781**	**Glomus_ c 10704**	**Glomus_ c 3514**
Fungi				
Neurospora crassa	Putative calcium P-type ATPase	2.00E-52	4.00E-10	3.00E-05
Magnaporthe grisea	Hypothetical protein MG04550.4	1.00E-52	2.00E-12	3.2
Aspergillus fumigatus	Endoplasmic reticulum calcium ATPase	1.00E-57	4.00E-11	5.00E-04
Aspergillus nidulans	Hypothetical protein AN5743.2	1.00E-52	4.00E-12	0.013
Gibberella zeae	Conserved hypothetical protein	2.00E-50	3.00E-12	2.5
Glomus intraradices	Partial serca gene for P-type II A ATPase, exons 1-2		0.62	0.89
Glomus diaphanum	Partial serca gene for P-type II A ATPase, exons 1-2			8.9
Glomus proliferum	Partial serca gene for P-type II A ATPase, exons 1-2			
Ustilago maydis	Eca1 gene for endoplasmic reticulum calcium transporter	2.00E-41	3.00E-11	9.00E-05
Cryptococcus neoformans	Hypothetical protein CNBL2380	8.00E-62	7.00E-11	3.00E-09
Metozoa				
Danio rerio	Novel protein similar to vertebrate ATPase, Ca2+ , transporting,cardiac muscle, slow twitch 2 (ATP2A2)	2.00E-35	1.00E-10	1.2
Rana sylvatica	Ca^{2+}-ATPase	8.00E-40	8.00E-12	3.00E-06
Gallus gallus	Sarcoendoplasmic reticulum calcium ATPase	3.4	4.00E-13	4.00E-05
Viridiplantae				
Arabidopsis thaliana	ER-type calcium pump protein	9.00E-33	7.00E-13	3.00E-06
Hordeum vulgare	Partial CA7 gene for P-type ATPase	3.00E-27	4.00E-12	1.4

Blank: no significant similarity found.

Table 5.3. Comparison with the amino acid sequence databases of Type IIB ATPase (PMCA ATPase) according to Corradi and Sanders (2006)

Type IIB (PMCA ATPase)		E-value (Blast p)		
Organism	**Putative protein**	**Glomus_ c 2781**	**Glomus_ c 10704**	**Glomus_ c 3514**
Fungi				
Blakeslea trispora	Partial bca1 gene for putative calcium ATPase, exon 1	4.8		0.15
Phycomyces blakesleeanus	Partial pca1 gene for putative calcium ATPase, exon 1	3.1	1.8	
Schizosaccharomyces pombe	Vacuolar calcium transporting P-type ATPase, Pmc1	0.021	2.00E-07	7.00E-32
Neurospora crassa	Putative calcium p-type ATPase NCA-3	0.006	5.00E-07	9.00E-45
Gibberella zeae	Hypothetical protein FG09515.1		2.00E-06	1.00E-38
Magnaporthe grisea	Hypothetical protein MG04890.4	2.00E-04	4.00E-07	6.00E-42
Aspergillus nidulans	Hypothetical protein AN1189.2	0.021	2.00E-06	4.00E-43
Glomus intraradices	Partial pmca1 gene for P-Type II B ATPase	2.2	0.12	4.8
	Partial pmca2 gene for P-Type II B ATPase	0.48	0.13	
Glomus diaphanum	Partial pmca gene for P-type II B ATPase	1.8	0.12	
Glomus proliferum	Partial pmca gene for P-type II B gene	2.5	0.12	1.8
Cryptococcus neoformans	Hypothetical protein CNBD2820	0.01	5.00E-08	3.00E-36
Ustilago maydis	Signal peptide, repeats, gene anchored to telomere	0.65		
Metazoa				
Homo sapiens	Hypothetical protein	0.003	1.00E-08	2.00E-22
Rana catesbiana	PMCA2av	0.003	5.00E-08	8.00E-14
Viridiplantae				
Arabidopsis thaliana	Putative Ca2+-ATPase	1.00E-05	8.00E-08	2.00E-20
Brassica oleracea	Calmodulin-stimulated calcium-ATPase	0.011	6.00E-08	3.00E-20

Blank: no significant similarity found.

Primers were manually designed from the ESTs Glomus_c17763, Glomus_lrc1694, Glomus_c3514, Glomus_c2781, Glomus_c10704, Glomus_c23149 and Glomus_995 (Table 5.4). PCR performed on cDNA from mycorrhizal roots or spores of *G. intraradices* DAOM197198 and sequencing of PCR products confirmed their specificity (data not shown).

Table 5.4. Primer design for *G. intraradices* DAOM197198 genes

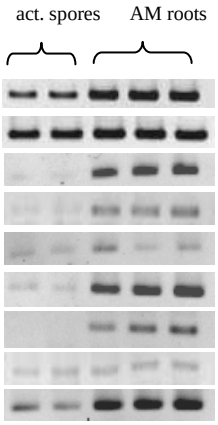
Gene	Primer name	Sequence 5'-3'	Size[1] (bp)
Vacuolar calcium ion transporter 1	C17763_F2	GATGGTATAACGAAAAGCGGAC	331
	C17763_R2	AATAGCGGTAACAAACTCAGCA	
Vacuolar calcium ion transporter 2	1694_F2	CGTCTTCTCATATCATTCTAACTAAAG	114
	1694_R3	TTGGTTTGAAGGTGCTATGTTGC	
Plasma membrane /Vacuolar calcium transporting ATPase II	C3514_F	TGGAGGATTAGATGGATTGGT	247
	C3514_R2	GAATAGACTTTGTTTTCTTTACTGG	
Endoplasmic reticulum calcium ATPase II	C2781_F	CGACGAATACTCTGCTCACG	249
	C2781_R3	TCAATGCCACTAATTCTCTTAGC	
Golgi reticulum calcium transporting ATPase II	10704_F3	GGAGCTGAAATTGTCCTGATGC	198
	10704_R3	CGTTGCATATTTACCAAGCACAGG	
Mitochondria membrane calcium-binding carrier	23149F5	TAAGAGATGTACCATTTTCAGCCA	249
	23149R5	TCCGCTAATATCCTTCTTCCTGC	
Nuclear calcium/calmodulin-dependent protein kinase (CCaMK)	lrc995_F4	ATTATGTGGATACACTCCATTCTG	195
	lrc995_R2	AACCAAGGGTGTTTCAATGCTTC	

1) Amplicon size

5.2. Fungal gene expression monitored by reverse-transcription (RT)-PCR

5.2.1. Gene expression in *G. intraradices* DAOM197198 spores and mycorrhizal roots of *M. truncatula*

Transcript analyses by RT-PCR showed that most of the *G. intraradices* DAOM197198 genes were expressed in spores activated by incubation in water and that the expression of five of the genes was clearly enhanced in mycorrhizal roots (Fig. 5.1). The latter putatively encode the endoplasmic reticulum P-type ATPase, Golgi reticulum P-type ATPase, two vacuolar Ca/Mn transporters and the nuclear CCaMK. For most of the genes, their expression profile observed by RT-PCR corresponded to results from hybridisation experiments (asterisks), using the Nimblegen microarray (Tisserant et al., 2012).



	µarray expression AM roots/ act. spores	RT-PCR	
LSU			
TEF			
Vacuolar Ca/Mn transporter 1 (Glomus_c17763)	7.99	↑	*
Vacuolar Ca/Mn transporter 2 (Glomus_lrc1694)	0.79	↑	
Plasma membrane / Vacuolar Ca^{2+}-transporting ATPase II (Glomus_c3514)	1.61	=	*
Endoplasmic reticulum P-type Ca^{2+} ATPase II (Glomus_c2781)	2.66	↑	*
Golgi reticulum P-type Ca^{2+} ATPase II (Glomus_c10704)	2.97	↑	*
Mitochondria membrane Ca^{2+}-dependent carrier (Glomus_c23149)	0.41	=	
Nuclear CCaMK (Glomus_lrc995)	1.88	↑	*

Fig. 5.1. Expression analyses by RT-PCR of *G. intraradices* DAOM197198 genes: amplification signals from cDNA of activated (act.) spores and mycorrhizal (AM) roots. Gene expression profiles from microarray hybridisation experiments are given for comparison.

In order to use *G. intraradices* BEG141, which is a highly effective isolate, as a model AM fungus for the molecular work, the primers designed for the ESTs of *G. intraradices* DAOM197198 were also used to amplify *G. intraradices* BEG141 cDNA. Corresponding transcripts were monitored in mycorrhizal *M. truncatula* roots 17 dai with *G. intraradices* BEG141 cDNA, compared to cDNA from non-mycorrhizal *M. truncatula* roots as control, by gel RT-PCR using specific primers (see Tables 5.4) for each gene at

58°C and with 35 amplification cycles. *DESAT* and *GiPT* were included as symbiosis marker genes. Transcripts of all the genes were detected in mycorrhizal *M. truncatula* roots and none was detected in non-mycorrhizal *M. truncatula* roots (Fig. 5.2), which demonstrated the specificity of the fungal primers also for *G. intraradices* BEG141.

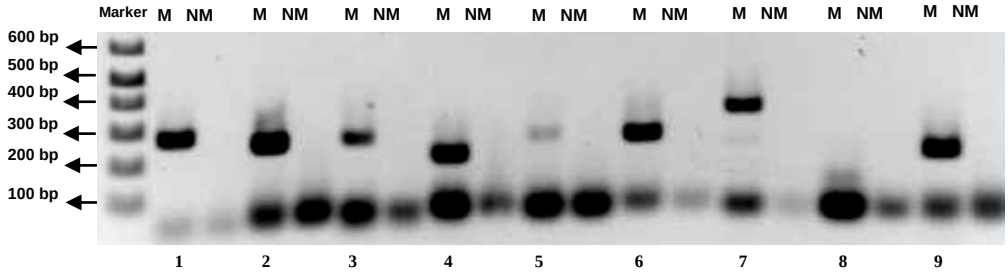


Fig. 5.2. Transcripts of *Glomus intraradices* BEG141 genes detected in mycorrhizal *M. truncatula* roots (M) and not in non-mycorrhizal roots (NM). Marker: 1 KB plus DNA ladder; 1. DESAT; 2. GiPT; 3. BEG141_c2781; 4. BEG141_c10704; 5. BEG141_c23149; 6. BEG141_c3514; 7 BEG141_c17763; 8. BEG141_lrc1694; 9. BEG141_lrc995.

After sequencing, the amplification products from *G. intraradices* BEG141 genes were compared to those from the isolate DAOM 197198, used to design the primers. High similarities between the nucleotide sequences indicated that the same genes were detected in the two fungal isolates (Table 5.5).

Transcript accumulation of the seven *G. intraradices* BEG141 ESTs was then monitored in quiescent spores, water-activated spores (24h) and mycorrhizal roots (17 dai) of the AM fungal isolate. *G. intraradices* large-subunit (*LSU*) rRNA was included in the analyses to ensure equivalent levels of fungal RNA at the different developmental stages.

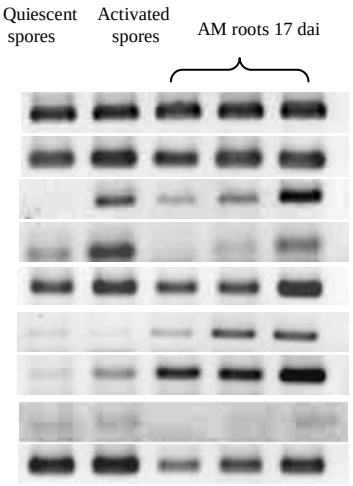
Table 5.5. Similarities of the selected ESTs between the two *G. intraradices* isolates

Putative protein	ESTs DAOM197198*	ESTs BEG141	Identities (blastn)
Vacuolar calcium ion transporter (1)	Glomus_c17763	BEG141_c17763	97 %
Vacuolar calcium ion transporter (2)	Glomus_lrc1694	BEG141_lrc1694	96 %
Plasma membrane /Vacuolar calcium transporting ATPase (P-type II B)	Glomus_c3514	BEG141_c3514	100 %
Endoplasmic reticulum calcium ATPase (P-type II A)	Glomus_c2781	BEG141_c2781	97 %
Golgi reticulum P-type Ca^{2+} ATPase (P-type II A)	Glomus_c10704	BEG141_c10704	97 %
Mitochondria membrane calcium-binding carrier	Glomus_c23149	BEG141_c23149	95 %
Nuclear calcium/calmodulin-dependent protein kinase (CCaMK)	Glomus_lrc995	BEG141_ lrc995	98 %

*) Accession number from the Glomus Genome Resource (http://mycor.nancy.inra.fr/IMGC/GlomusGenome/index.html)

Gel analysis of RT-PCR products of the *TEF* gene indicated similar transcript levels of the housekeeping gene at each stage of *G. intraradices* development. All the other genes presented expression profiles which appeared to vary between quiescent spores, activated spores and mycorrhizal roots. Expression of the *G. intraradices* genes were detected in spores and intraradical mycelium in AM roots but to different extents (Fig. 5.3). Expression of the two genes putatively encoding an endoplasmic reticulum P-type ATPase (BEG141_c2781) and Golgi reticulum P-type ATPase (BEG141_c10704) was clearly enhanced in mycorrhizal roots. The expression pattern observed by RT-PCR was in agreement with the results from the NimbleGen analyses for the DAOM isolate (asterisks), except for the vacuolar Ca/Mn transporter 1 (BEG141_c17763) and the nuclear CCaMK (BEG141_lrc995) (Fig. 5.3).

The RT-PCR results from mycorrhizal roots showed expression of most of the genes by the two *G. intraradices* isolates, DAOM 197198 and BEG141, in intraradical mycelium (Fig. 5.4).



	µarray expression AM roots/ act. spores DAOM 197198	RT-PCR BEG 141	
LSU			
TEF			
Vacuolar Ca/Mn transporter 1 (BEG141_c17763)	7.99	=	
Vacuolar Ca/Mn transporter 2 (BEG141_lrc1694)	0.79	↓	*
Plasma membrane / Vacuolar Ca^{2+}-transporting ATPase II (BEG141_c3514)	1.61	=	*
Endoplasmic reticulum P-type Ca^{2+} ATPase II (BEG141_c2781)	2.66	↑	*
Golgi reticulum P-type Ca^{2+} ATPase II (BEG141_c10704)	2.97	↑	*
Mitochondria membrane Ca^{2+}-dependent carrier (BEG141_c23149)	0.41	↓	*
Nuclear CCaMK (BEG141_lrc995)	1.88	↓	

Fig. 5.3. RT-PCR of transcripts of *Glomus intraradices* BEG141 genes in quiescent spores, activated spores and mycorrhizal roots (17 dai). Gene expression analyses from microarray hybridisation of the DAOM 197198 isolate are given for comparison.

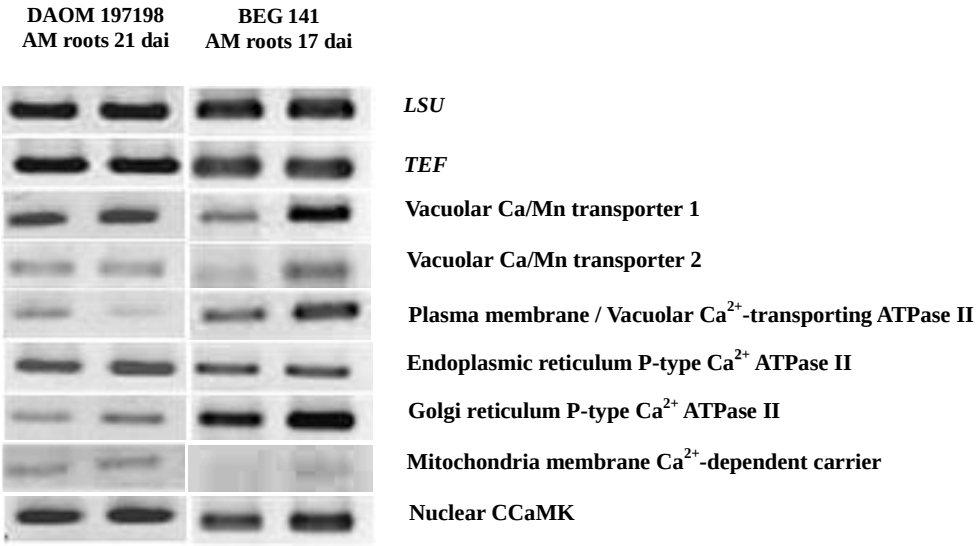


Fig. 5.4. RT-PCR of transcripts of *Glomus intraradices* genes in mycorrhizal roots in the two isolates

5.3. Discussion and conclusions

In order to identify calcium-dependent processes that may be important in fungal events leading to mycorrhizal interactions with plant tissues, we selected seven fungal Ca^{2+}-related proteins from the AM fungus *G. intraradices* DAOM 197198 according to their expression profiles in microarray analyses (Tisserant et al., 2012). Two genes encode SERCA ATPases and one is related to PMCA ATPase. SERCA, or sarco/endoplasmic reticulum Ca^{2+}-ATPases transfer Ca^{2+} from the cytosol of the cell into the endoplasmic reticulum lumen (Berridge et al., 2003), whilst the plasma membrane Ca^{2+} ATPase (PMCA) is a transport protein in the plasma membrane of cells that removes calcium from the cell, that is, transports Ca^{2+} into the extracellular space (McAinsh and Pittman, 2009). Thus these proteins regulate the amount of Ca^{2+} within cells to maintain low concentrations of Ca^{2+} for proper cell signaling. Attempt to also design primers for a Gm152 (in chapter 3, which encoding an endoplasmic reticulum Ca^{2+}-transporting P-type ATPase) homologue (Glomus _c14022) in *G. intraradices* have been unsuccessful.

Most of the selected genes were up-regulated in mycorrhizal *M. truncatula* roots as compared to spores, indicating an eventual role in the establishment or functioning of the mycorrhizal symbiosis. Six of these genes encoded membrane proteins which are potentially involved in calcium homeostasis necessary for intracellular signaling, via the regulation of Ca^{2+} transport between different cell compartments.

Gene specific primers were designed and tested on cDNA from *G. intraradices* DAOM197198 and *G. intraradices* BEG141. The high similarities between the nucleotide sequences indicated the presence of the same genes in these two fungal isolates. Detection of transcripts by RT-PCR confirmed expression of all the targeted genes in the spores and intraradical mycelium of the two fungal isolates, but to different extents. In order to gain a more precise insight into the eventual role of the different Ca^{2+}-related *G. intraradices* genes in mycorrhizal interactions, further research was carried out by monitoring gene expression during fungal development (Chapter 6), localizing transcripts in different fungal structures (Chapter 7) and functional analysis using yeast complementation systems (Chapter 8).

CHAPTER 6

Expression of *G. intraradices* genes encoding Ca^{2+}-related proteins in interactions with wild-type or Myc- mutant roots of *Medicago truncatula*

6.1. Relative quantitative Real-time RT-PCR

6.1.1 Gene expression in *G. intraradices* DAOM197198 spores and mycorrhizal *M. truncatula* roots

Fungal transcripts were quantified in mycorrhizal roots of wild-type *M. truncatula* as compared to water-activated spores by relative quantitative real-time RT-PCR (Q-PCR), using the constitutively expressed α subunit of the fungal translation elongation factor 1 (*TEF*) as the reference gene. With the exception of the vacuolar Ca/Mn transporter 2, the expression pattern observed by Q-PCR confirmed the results from the NimbleGen analyses (asterisks) (Table 6.1).

Table 6.1. Relative quantification of *G. intraradices* DAOM197198 transcripts

ESTs	Q-PCR expression AM roots/act. spores	µarray expression AM roots/act. spores	
Glomus_c17763	24.9 ±1.38	7.99	*
Glomus_lrc1694	1.85 ± 0.21	0.79	
Glomus_c3514	0.88 ± 0.28	1.61	*
Glomus_c2781	1.76 ± 0.14	2.66	*
Glomus_c10704	2.24 ± 0.32	2.97	*
Glomus_c23149	0.54 ±0.04	0.41	*
Glomus_lrc995	2.07 ±0.18	1.88	*

Data presented from Q-PCR are mean values with standard errors from three biological repetitions.

Taken together with the RT-PCR results, slight discrepancies in gene expression may be expected compared to the microarray analysis since microarray hybridizations may provide data for the overall expression of multigene families, with members having different expression levels, while the primers used in Q-PCR are more discriminatory. Moreover, the *M. truncatula* mycorrhizal roots used for microarray and Q-PCR analyses were produced in different laboratories under different conditions.

6.1.2 Gene expression in *G. intraradices* BEG141 spores

At the asymbiosis stage (spores in absence of root exudates) and pre-symbiotic stage (spores in presence of root exudates), the relative expression of all the genes remained low

as compared to the reference *TEF* gene, except for *DESAT* in quiescent spores. Most of the fungal genes showed no significant variation in gene expression between treaments and none of the genes were activated by root exudates, as compared to quiescent spores (Fig. 6.1). Expression of two Ca^{2+}-related genes decreased with spore germination. The gene encoding a plasma membrane/vacuolar Ca^{2+}-transporting ATPase (BEG141_c3514) was down-regulated during spore germination and no transcripts were detected after 6 days in water or root exudates, whilst the mitochondrial membrane Ca^{2+}-dependent carrier (BEG141_c23149) gene was inhibited by root exudates from wild-type *M. truncatula*. Only one gene was activated after incubation of spores 24h in water, the vacuolar Ca/Mn transporter 1 (BEG141_c17763), but expression decreased with spore germination after 6 days in water or root exudates (Fig. 6.1).

6.1.3 Gene expression in *G. intraradices* BEG141 associated with wild-type and mutant *M. truncatula* roots

The expression profiles of all the studied genes varied between early (4, 6 dai) and late (17, 21 dai) stages of development of *G. intraradices* with wild-type *M. truncatula* roots (Fig. 6.2). Expression of the symbiosis-related marker genes *DESAT* and *GiPT* relative to the reference *TEF* gene increased to high levels as *G. intraradices* developed arbuscules in roots of wild-type *M. truncatula*, indicating the formation of an active symbiosis. Very little expression of these genes was associated with appressoria formation on roots of either the wild-type or mutant genotypes.

Five of the seven selected Ca^{2+}-related *G. intraradices* genes had very low levels of expression relative to the reference *TEF* gene during fungal development with *M. truncatula* roots. Expression was highest for the two P-type Ca^{2+} ATPases (BEG141_c2781 and BEG141_c10704) and lowest for the plasma membrane/vacuolar Ca^{2+}-transporting ATPase (BEG141_c3514). Most of the Ca^{2+} related fungal genes were more weakly or not expressed when *G. intraradices* came into contact with roots of the *dmi3/Mtsym13* mutant, as compared to wild-type roots (Fig. 6.2). Exceptions were the vacuolar Ca/Mn transporter 1 (BEG141_c17763) and the nuclear CCaMK (BEG141_lrc995) genes.

Expression of four genes followed fungal development from appressoria formation (4, 6 dai) on both *M. truncatula* genotypes, and to root colonization (17, 21 dai) of the wild-type genotype; these encode the endoplasmic reticulum and Golgi reticulum P-type Ca^{2+}

ATPases (BEG141_c2781 and BEG141_c10704), the vacuolar Ca/Mn transporter 1 (BEG141_c17763) and the nuclear CCaMK (BEG141_lrc995). For the first three genes, expression tended to decrease but not significantly from 17 to 21 dai. In contrast, expression of three fungal genes was only detected during arbuscule development after root colonization (17, 21 dai) and none of them were active during appressorium formation on wild-type or mutant roots; these encode the mitochondria Ca^{2+}-dependent carrier (BEG141_c23149), the plasma membrane/vacuolar Ca^{2+}-transporting ATPase and the vacuolar Ca/Mn transporter 2 (BEG141_lrc1694). Expression of the mitochondria Ca^{2+}-dependent carrier and the plasma membrane/vacuolar Ca^{2+}-transporting ATPase increased significantly from 17 to 21 dai whilst that of the vacuolar Ca/Mn transporter 2 remained constant (Fig. 6.2).

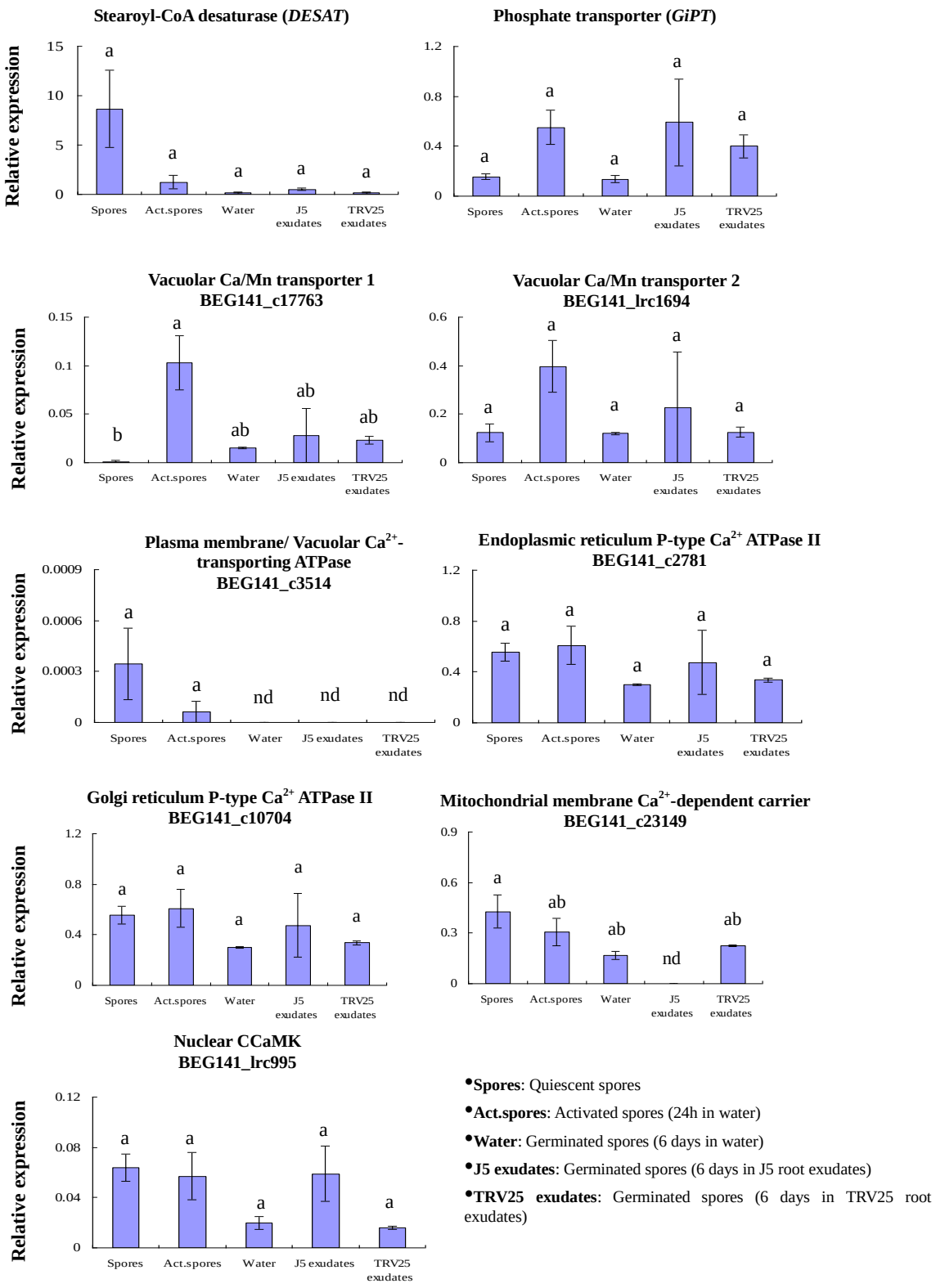


Fig. 6.1. Expression of selected *G. intraradices* BEG141 genes (relative to *TEF*) profiled by Q-PCR. Experiments were carried out on RNA extracted from spores. Data represent means of values from two independent biological experiments. Bars indicate standard errors of means and different letters indicate significant differences between treatments ($P \geq 0.05$) using one-way analysis of variance (Tukey's pairwise comparisons test); n.d. = not detected

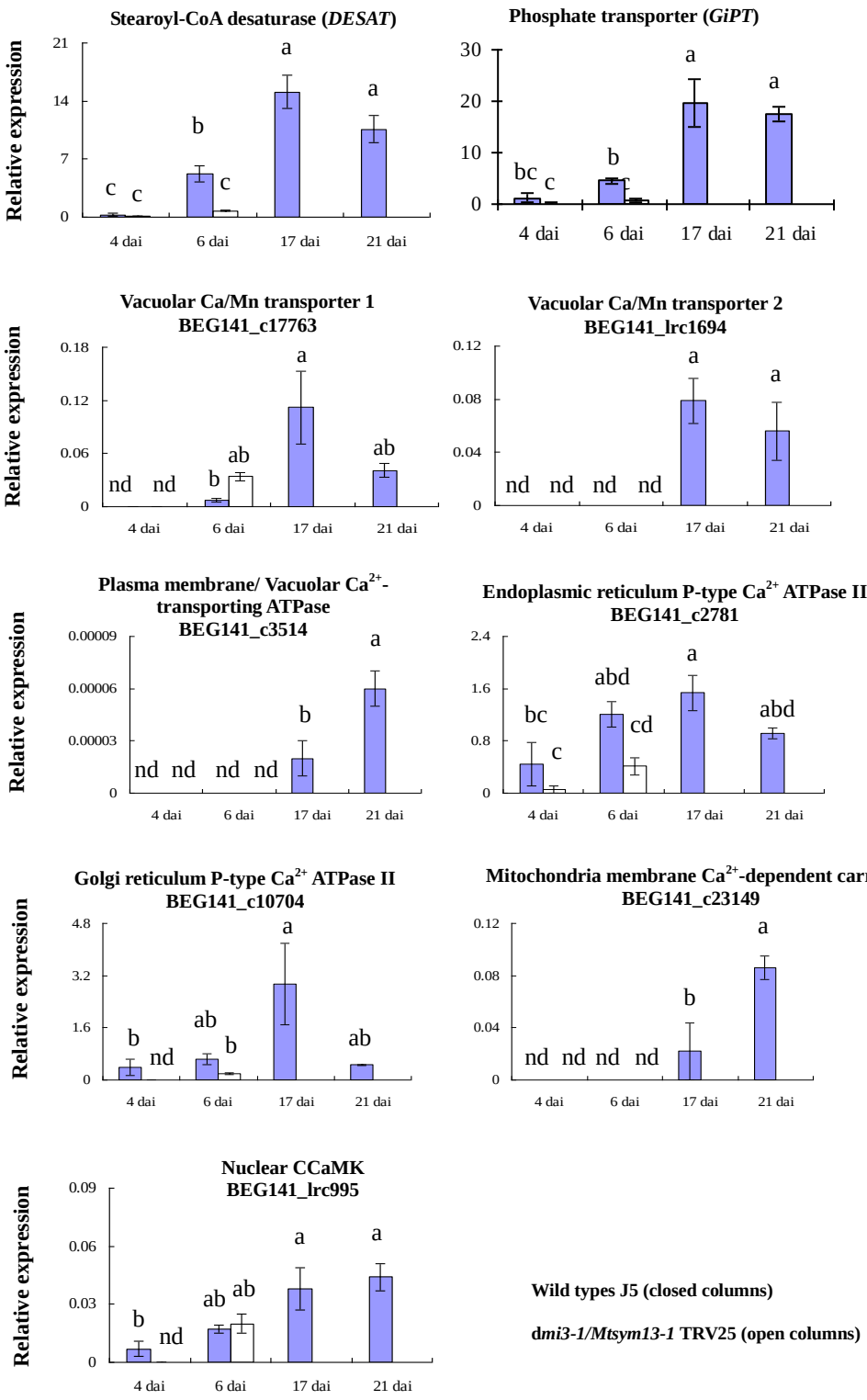
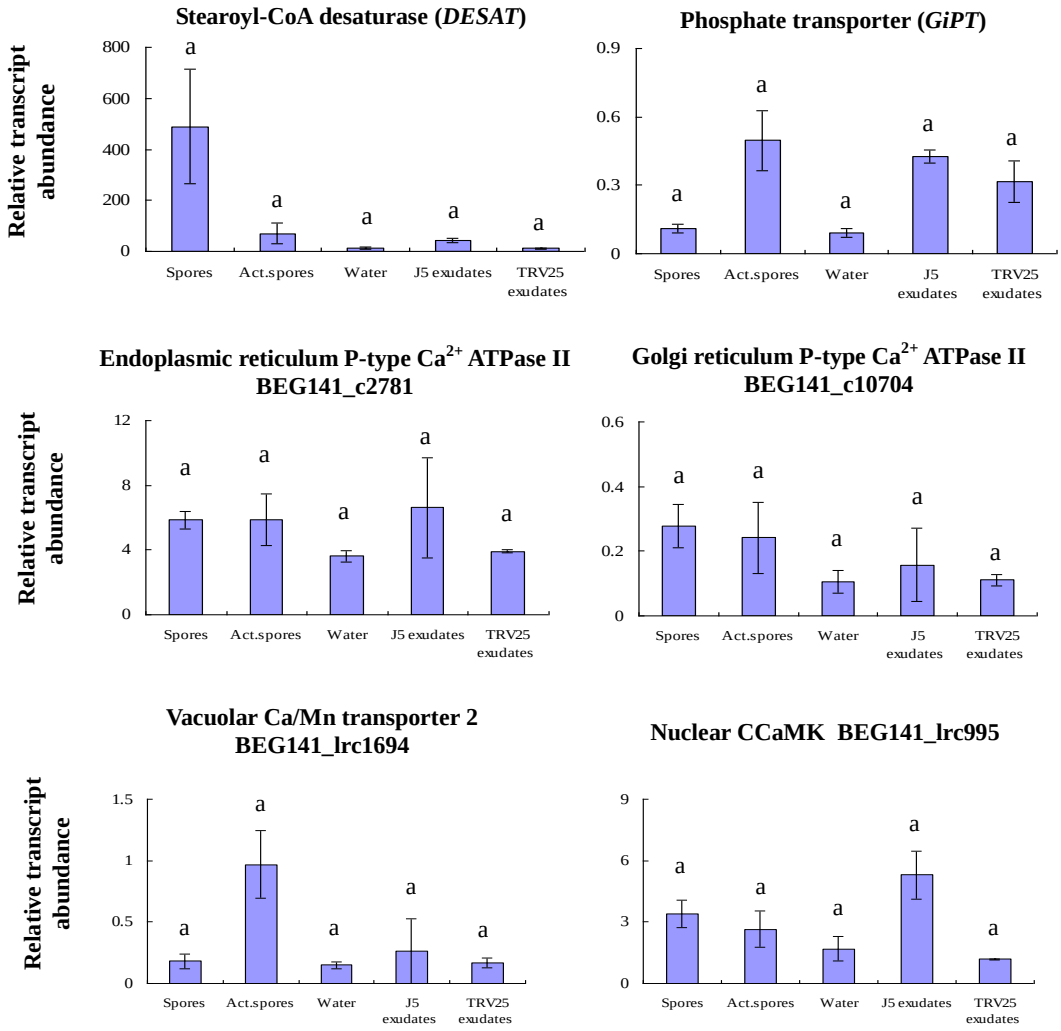


Fig. 6.2. Expression of selected *G. intraradices* BEG141 genes (relative to *TEF*) profiled by Q-PCR. Experiments were carried out on RNA extracted from mycorrhizal roots 4, 6, 17 and 21 dai. Data represent means of values from three independent biological experiments. Bars indicate standard errors of means and different letters indicate significant differences between time points ($P \geq 0.05$) detected using one-way analysis of variance (Tukey's pairwise comparisons test); n.d. = not detected.

6.2. Absolute quantitative Real-time RT-PCR

Expression of the *G. intraradices* genes was validated by measuring transcript abundance relative to that of the *TEF* gene using absolute Q-PCR. For this, the two symbiosis-related marker genes *DESAT* and *GiPT,* and four Ca^{2+}-related genes showing different expression profiles during colonization of *M. truncatula* roots (endoplasmic reticulum P-type ATPase, Golgi reticulum P-type ATPase, vacuolar Ca/Mn transporter 2, nuclear CCaMK), were selected. Transcripts of all of the selected genes were detected in spores and mycorrhizal roots. Expression profiles at the asybiosis and pre-symbiotic stage of all the genes were similar to those from the relative Q-PCR analysis, with no significant variation in relative transcript abundance during spore germination in the different treatments (Fig. 6.3).

Increasing expression of the *DESAT* and *GiPT* genes with mycorrhiza formation in wild-type *M. truncatula* roots was confirmed by absolute Q-PCR (Fig. 6.4). Likewise, the golgi reticulum P-type ATPase and vacuolar Ca/Mn transporter 2 genes were weakly or not expressed in contact with roots of either *M. truncatula* genotype then up-regulated in mycorrhizal roots, whilst the vacuolar Ca/Mn transporter 1 (BEG141_c17763) and the nuclear CCaMK (BEG141_lrc995) genes were active throughout fungal development.



- **Spores**: Quiescent spores
- **Act.spores**: Activated spores (24h in water)
- **Water**: Germinated spores (6 days in water)
- **J5 exudates**: Germinated spores (6 days in J5 root exudates)
- **TRV25 exudates**: Germinated spores (6 days in TRV25 root exudates)

Fig. 6.3. Transcript accumulation, relative to *TEF*, of *G. intraradices* BEG141 genes quantified by absolute Q-PCR. Experiments were carried out on RNAs extracted from spores. Data are represent means of values from two independent experiments. Bars indicate standard errors of means and different letters indicate significant differences between values ($P \geq 0.05$) detected using one-way analysis of variance (Tukey's pairwise comparisons test).

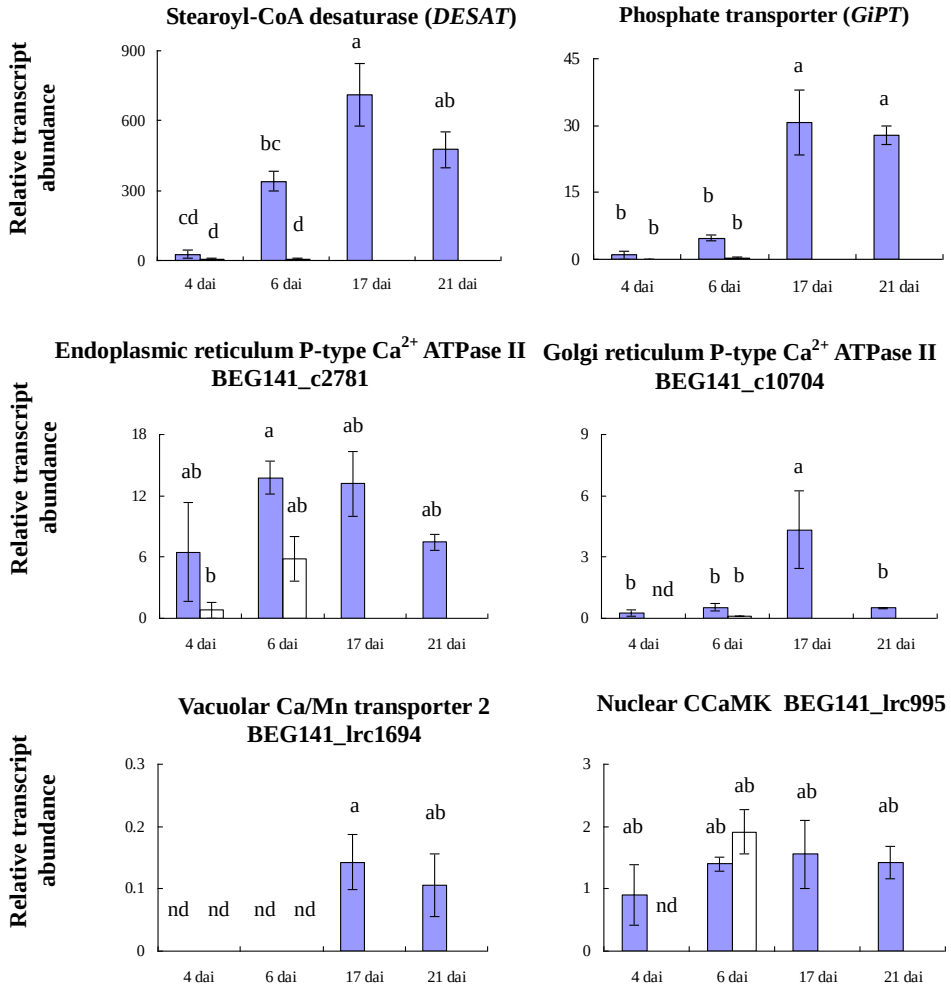


Fig. 6.4. Transcript accumulation, relative to *TEF*, of *G. intraradices* BEG141 genes quantified by absolute Q-PCR. Experiments were carried out on RNAs extracted from roots of the *M. truncatula* genotypes J5 (closed columns) and d*mi3-1/Mtsym13-1* (open columns) 4, 6, 17 and 21 dai. Data are represent means of values from three independent experiments. Bars indicate standard errors of means and different letters indicate significant differences between values ($P \geq 0.05$) detected using one-way analysis of variance (Tukey's pairwise comparisons test).

6.3. Discussion and conclusions

The relative and absolute Q-PCR analyses showed that the *G. intraradices* genes encoding Ca^{2+}-related proteins vary in their expression profiles between pre-symbiotic and symbiotic stages, suggesting different functions in fungal development. None of the genes were significantly activated by root exudates and maximum expression for them all was clearly linked to the functional symbiosis in wild-type *M. truncatula* roots, which was

reflected by the high fungal *DESAT* and *GiPT* gene activity at 17-21 dai. Stearoyl-CoA desaturase catalyses the biosynthesis of mono-unsaturated fatty acids (UFAs) from saturated fatty acids, and UFA homeostasis in many organisms is achieved by feedback regulation of fatty acid desaturase gene transcription (Mansilla et al., 2008). The *DESAT* gene also showed high activity in quiescent spores**.** As lipids are the major form of carbon storage in spores of AM fungi, *DESAT* may be involved in regulation of fatty acid at this stage as well as in lipid synthesis from host derived carbon in intraradical structures.

Calcium signaling involves calcium spiking which stimulates several Ca^{2+}-binding proteins and elicits downstream signaling pathways. The calcium signal is terminated when cytosolic-free Ca^{2+} concentrations are reduced to basal levels by moving calcium between cell components (McAinsh and Pittman, 2009). Vacuoles, endoplasmic reticulum, and mitochondria have important functions in Ca^{2+} homeostasis. Vacuolar calcium ion transporters have a role in promoting intracellular calcium ion sequestration via the exchange of calcium ions for hydrogen ions across the vacuolar membrane; they can also be involved in manganese ion homeostasis via its uptake into the vacuole and belong to the sodium/potassium/calcium exchanger family (Geisler et al., 2000). The two vacuolar calcium ion transporters 1 and 2 of *G. intraradices* showed significant differences in gene expression during spore germination and fungal development. Expression of the calcium ion transporter 1 gene was significantly increased with spore activation in water but show little response with spore germination to plant root exudates. Nevertheless, expression was detected with appressorium development on wild-type or *myc*$^{-}$ mutant *M. truncatula* roots, and it increased when arbuscules formed in roots. In comparison, expression of the calcium ion transporter 2, which also showed no variation with spore germination, was only detected with arbuscule formation. Accordingly, these two genes could be putatively involved in different symbiotic processes. *G. intraradices* vacuolar calcium ion transporter 1 showed 49% identities and calcium ion transporter 2 showed 44% identities (blast p) to the membrane protein CrCAX1_CAR92574, a cation antiporter of the CAX (cation exchanger) family in *Chlamydomonas reinhardtii* (Pittman et al., 2009). In *Arabidopsis*, the calcium–proton exchangers CAX1 and CAX3 appear to play a prominent role in Ca^{2+} homeostasis. Mutants for *cax1*, *cax3* or *cax1*/*cax3* have significantly severe phenotypes including leaf tip necrosis and ionic content. Also CAX1 and CAX3 may be involved in Pi homeostasis (Cheng et al., 2005), which could be relevant to the AM symbiosis since high concentrations of Ca^{2+} and polyphosphate have been co-localized in vacuoles of arbuscules

suggesting a role of Ca^{2+} in phosphate metabolism in mycorrhizal tissues (Strullu et al., 1981).

ATPases carry out many energy-driven fundamental processes in biology. The P-type II ATPase gene family codes for proteins with an important role as ion pumps in adaptation of the cell to variations in external K^+, Ca^{2+} and Na^{2+} concentrations. During Ca^{2+}-signalling in animal cells, for example, the SERCA pump regulates Ca^{2+} levels by effluxing the ion into the endoplasmic reticulum which serves as an intracellular Ca^{2+} store (Berridge et al., 2003). From the present gene expression analysis, the two P-type ATPases (endoplasmic reticulum P-type ATPase and Golgi reticulum P-type ATPase) of *G. intraradices* showed low activity in the pre-symbiotic stage as compared to their expression levels during fungal development within roots of the wild-type *M. truncatula* genotype. The expression profiles of these two genes suggest that they may regulate the intracellular Ca^{2+} homeostasis when *G. intraradices* comes into contact with plant cell, and thus be involved in a Ca^{2+}-based signaling process. In this context, a P-type ATPase has been reported to have a role in penetration hypha development and pathogenicity in the rice blast fungus *Magnaporthe grisea* (Balhadère and Talbot, 2001). Also, an endoplasmic sarcoplasmic/reticulum Ca^{2+}-ATPase (*Eca1*) has been identified in the plant pathogenic fungus *Ustilago maydis* which restores growth of a yeast mutant defective in calcium homeostasis (Adamíková et al., 2004).

In contrast, the vacuolar Ca^{2+}-transporting ATPase was inhibited with spore germination and specifically activated at the arbuscule stage during intraradical development. In this case, the Ca^{2+}-transporting ATPase could be putatively linked to cation mediation in the functional symbiosis.

The *G. intraradices* gene encoding the mitochondrial Ca^{2+}-dependent carrier protein showed decreased expression with spore germination and activation in intraradical mycelium at the late stage of arbuscule formation. Consequently this gene may be linked to symbiosis functioning. Two human mitochondrial carrier genes with calcium-binding domains, *ARALAR1* and *ARALAR2*, have been proposed to be involved in calcium-regulated metabolite transport in mitochondria and/or participate in calcium-modulated mitochondrial functions (Del Arco et al., 2000). Mitochondria not only control their own intra-organelle Ca^{2+} concentration but also influence the entire cellular network of cellular Ca^{2+} signaling, including the endoplasmic reticulum, the plasma membrane, and the nucleus. Ca^{2+} channeling between the endoplasmic reticulum and mitochondria collaborate in the regulation of Ca^{2+} influx and extrusion through the plasma membrane Ca^{2+} ATPases

(PMCA). In addition, mitochondrial and nucleus communicate through a Ca^{2+} signal (Szabadkai and Duchen, 2008).

Expression of the *G. intraradices* nuclear CCaMK was unaffected during presymbiotic fungal development; the gene was active during root colonization in the symbiotic stage suggesting a possible role in Ca^{2+} perception related to this process. CCaMK proteins are involved in signalling pathways leading to gene regulation. The calmodulin-binding domain and calcium-binding EF hand motifs of CCaMK allow the protein to sense calcium (Oldroyd and Downie, 2006). A calcium/calmodulin-dependent signaling system is involved in appressorium formation in the plant pathogenic fungus *Magnaporthe grisea* and calmodulin gene expression is induced concomitantly with appressorium formation (Ebbole, 2007). Moreover, a plant CCaMK is a prime candidate for the response to calcium signatures that are induced by AM fungi or Nod factors (Lévy et al., 2004; Mitra et al., 2004).

CHAPTER 7

Localization of gene activity in *G. intraradices* during presymbiotic stages and development with roots

7.1. *In situ* RT-PCR

Results from in situ RT-PCR are given as Nomarski images, confocal fluorescence images and a superposition of fluorescence and autofluorescence images in Fig. 7.1. Transcripts of the *G. intraradices* BEG141 genes were detected in spores and mycorrhizal roots of *M. truncatula*. Red fluorescent-labeled amplified transcripts of the *LSU*, *DESAT* and *TEF* genes were observed in situ in spores of *G. intraradices* BEG141. However, only LSU transcripts could be clearly localized in the fungus in mycorrhizal roots (in arbuscules) (Fig. 7.1).

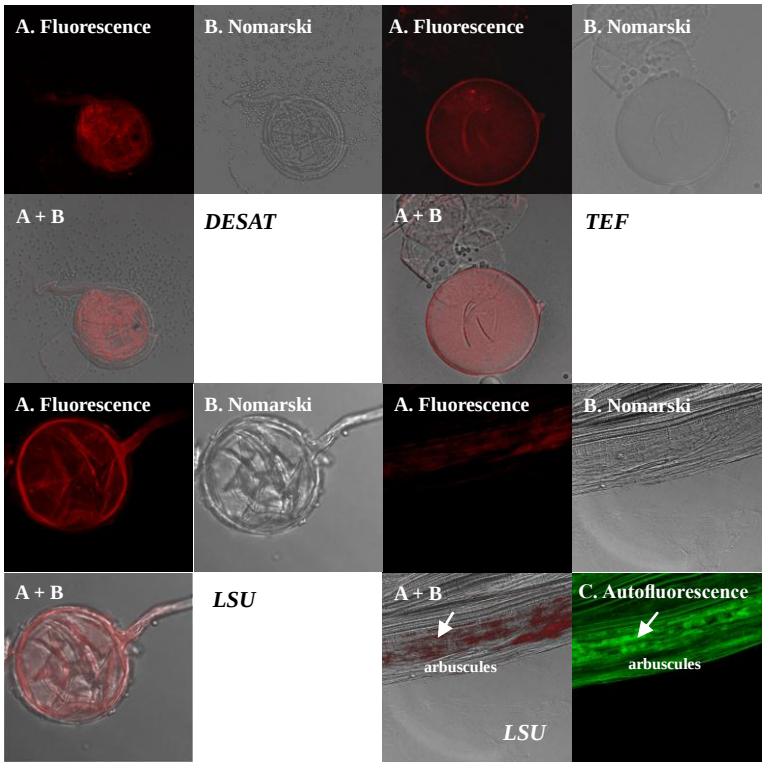


Fig. 7.1. Localization of *LSU*, *DESAT* and *TEF* transcripts by direct fluorescent *in situ* RT-PCR in spores and mycorrhizal roots of *G. intraradices* BEG141

It was not possible to conclude for the other studied genes (*DESAT*, *GiPT*, BEG141_c2781, BEG141_c10704 and BEG141_lrc1694) as the *in situ* RT-PCR gave no signal or an important background. However, the *DESAT* gene has previously been detected in arbuscules of *G. intraradices* BEG141 by *in situ* RT-PCR (Seddas et al., 2008). Several experiments performed to improve the experimental conditions did not give satisfactory results. It was therefore decided to use targeted cryo-microdissection to localize fungal gene expression.

7.2. Laser cryo-microdissection

Samples of mycorrhizal roots of *M. truncatula* were visualized on a computer monitor (Fig. 7.2 A, B); the targeted cells were marked using graphical software and cut out using an infrared (IR) laser (Fig. 7.2 C, D). Dissected cells were captured automatically into the CapSure HS LCM Caps (Fig. 7.2 E, F).

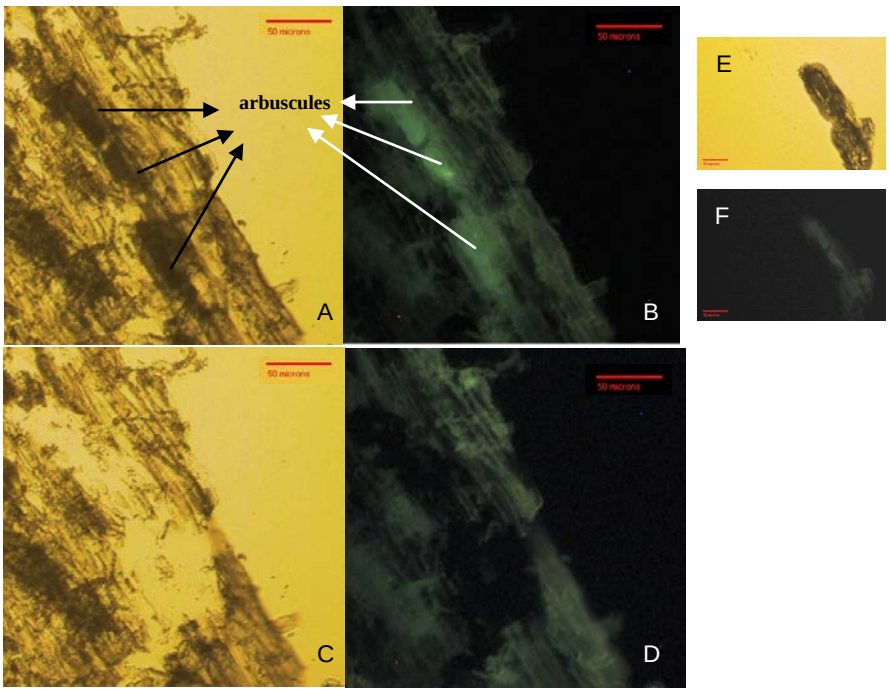


Fig. 7.2. Laser cryo-microdissection of *M. truncatula* root cortical cells containing arbuscules of *G.intraradices* BEG141. A and B (autofluorescence), before dissection; C and D (autofluorescence), tissue remaining after dissection; E and F (autofluorescence), collected arbuscule-containing cells. Bars = 50 µm

Three cell populations were chosen for transcript analyses: arbusculated cells, cells in non-arbusculated and vesicle-free cortical tissue from mycorrhizal roots, and vesicles. Between 1,000 and 2,000 cells of each cell population were collected and processed for RNA extraction. RNA from the same cell population was combined to give four samples (C1, C2, C3 and V1) (Table 7.1).The quantification and quality of RNA were checked by Agilent Bioanalyzer 2100 (Table 7.1). Experiments were repeated two times using arbusculated cells from different biological experiments (C1 and C2) and representative results are shown.

Table 7.1. Microdissected cell populations and RNA yield

RNA samples	Number of cells	RNA yield (ng)	RNA (ng/µl)	RIN
Arbusculated cells	C1 ≈ 11,400	50.658	1.6886	3.3
	C2 ≈ 4,900	192.384	8.016	3.5
Non-arbusculated tissues	C3 ≈ 6,540	127.782	4.122	3.7
Vesicles	V1 ≈ 28	10.504	1.313	3.6

RT-PCR was performed on the extracted RNA by a One-Step RT-PCR and compared to whole mycorrhizal root extracts. PCR products are presented in Fig. 7.3. An *LSU* rRNA probe was used to confirm the presence of fungal tissue in the samples and the *G. intraradices* genes *TEF*, *DESAT* and *GiPT* were used as controls to monitor fungal activity. As expected, cells with arbuscules contained transcripts of these four marker genes; in addition, they were detected in non-arbusculated, vesicle-free tissues (Fig. 7.3A), indicating the presence of RNA from intercellular hyphae. The *DESAT* gene was also expressed in vesicles (Fig. 7.3C).

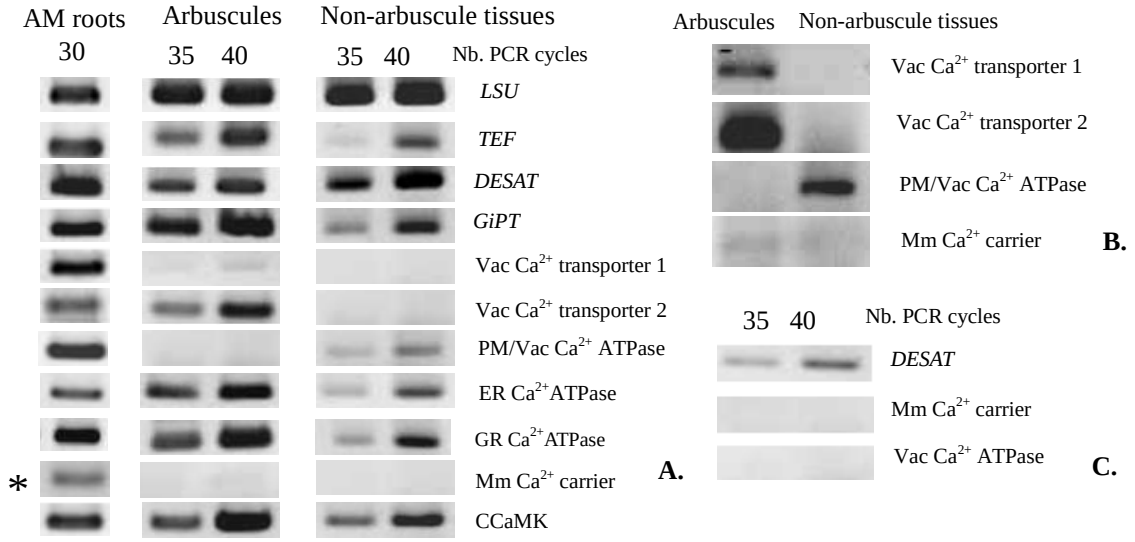


Fig. 7.3. (A) Transcripts of *G. intraradices* BEG141 genes in mycorrhizal roots (AM roots), arbuscule-containing cortical root cells (Arbuscules) and non-arbuscule tissues. PCR was run for 35 to 40 cycles for microdissected cells and 30 cycles for AM roots (*except for Mm Ca^{2+} carrier where 40 PCR cycles were necessary for detection). (B) Increased amounts of PCR products (40 cycles) from transcripts of arbuscules and non-arbuscule tissues loaded onto gels. Vac Ca^{2+} transporter 1 = vacuolar Ca^{2+} ion transporter 1; Vac Ca^{2+} transporter 2 = vacuolar Ca^{2+} ion transporter 2; PM/Vac Ca^{2+} ATPase = plasma membrane/vacuolar Ca^{2+} transporting ATPase; ER Ca^{2+}ATPase = endoplasmic reticulum Ca^{2+} ATPase; GR Ca^{2+}ATPase = Golgi reticulum P-type Ca^{2+} ATPase (BEG141_c10704); Mm Ca^{2+} carrier = mitochondria membrane Ca^{2+}-binding carrier; CCaMK = Ca^{2+}/calmodulin protein kinase.

Transcripts of all the selected *G. intraradices* genes encoding Ca^{2+}-related proteins were present in the extracts from arbuscule-containing cortical root cells, except for the plasma membrane/vacuolar calcium transporting ATPase (BEG141_c3514) which was only detected in non-arbusculated tissues (intercellular hyphae) (Fig. 7.3A, B). The mitochondria membrane calcium-binding carrier (BEG141_c23149) was only weakly expressed in arbuscules and it was necessary to increase the number of PCR cycles and PCR products to detect transcripts (Fig. 7.3B). Transcripts of BEG141_c23149 and of the two vacuolar Ca/Mn transporters (BEG141_c17763 and BEG141_lrc1694) were specific to arbuscules whilst the genes BEG141_c2781 (endoplasmic reticulum P-type Ca^{2+} ATPase), BEG141_c10704 (Golgi reticulum P-type Ca^{2+} ATPase) and BEG141_lrc 995 (nuclear CCaMK) were also expressed in non-arbusculated tissues (intercellular hyphae) (Fig. 7.3A, B). None of the Ca^{2+}-related genes of *G. intraradices* appeared to be expressed in vesicles (results shown for BEG141_c23149 and BEG141_c3514; Fig. 5.14. C).

7.3. *G. intraradices* gene expression in *P. sativum L.* wild-type and mutant genotypes

G. intraradices BEG 141 gene expression was monitored in colonized roots of wild-type *P. sativum cv.* Finale and the mutant *Pssym36*. As the mutant *Pssym36* is defective for arbuscule and vesicle formation (see chapter 4.2), fungal gene expression is expected to be principally located in the intercellular hyphae.

Gene expression was monitored by Q-PCR relative to the α subunit of the fungal translation elongation factor 1 (*TEF*) house-keeping gene. The two symbiosis–related *G. intraradices* genes *DESAT* and *GiPT* were used as controls for fungal activity. Expression of these two genes was significantly down-regulated in *G. intraradices*-colonized roots of the *Pssym36* mutant as compared to wild type pea cv Finale, and to a much greater extent for *DESAT* than *GiPT* (Fig 7.4).

For the selected Ca^{2+}-related genes of *G. intraradices*, only BEG141_c17763 encoding the vacuolar Ca/Mn transporter 1 showed significantly enhanced expression in mutant as compared to wild type colonized roots. Transcripts of the BEG141_c23149 (mitochondria membrane calcium-binding carrier) were not detected in colonized roots of the *Pssym36* mutant and expression of BEG141_c3514 (plasma membrane/vacuolar calcium transporting ATPase) was not detected in either the wild-type or mutant. No

difference was observed in expression of the other fungal genes between the two pea genotypes (Fig. 7.4).

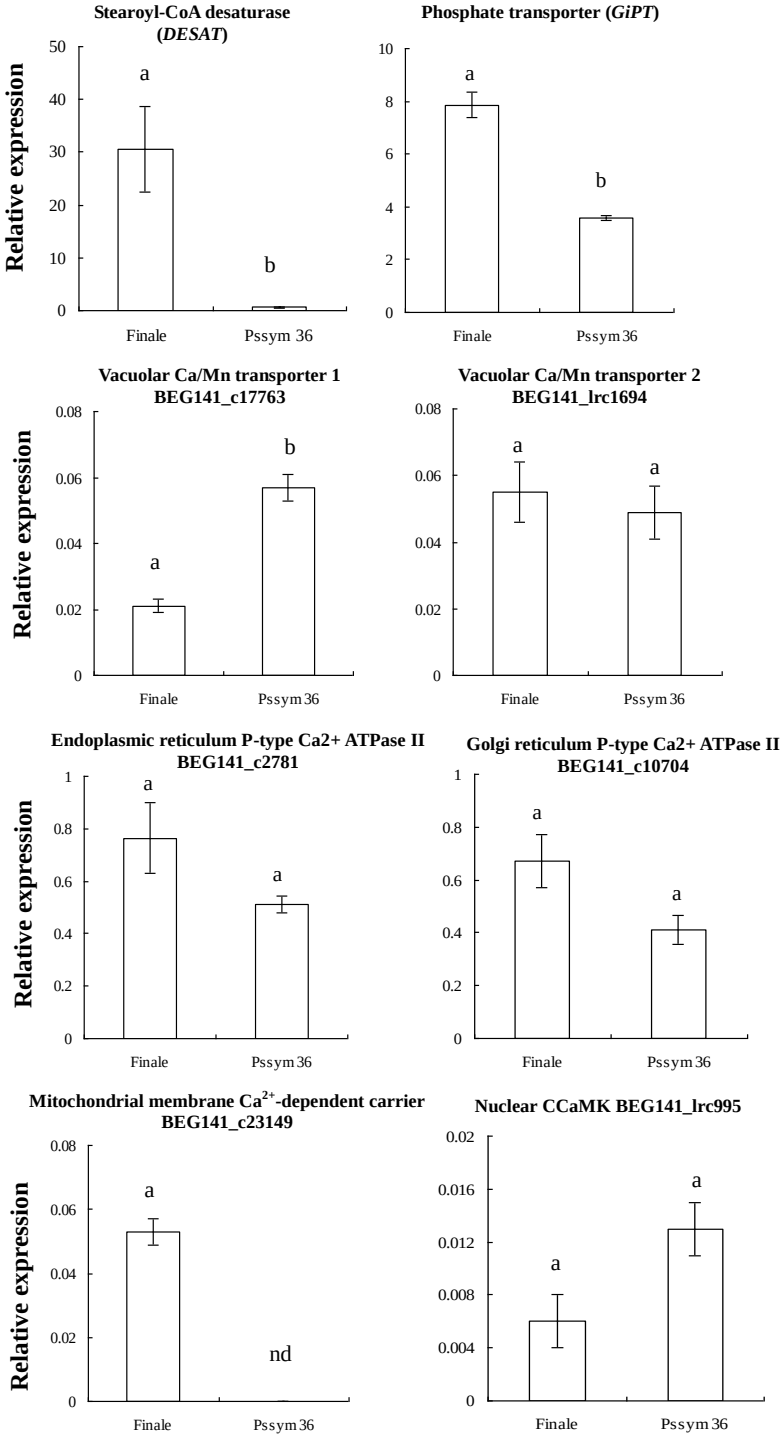


Fig. 7.4. Expression of *G. intraradices* BEG141 genes (relative to *TEF*) profiled by Q-PCR. Experiments were carried out on RNAs extracted from roots of *P. sativum* genotypes Finale and *Pssym36*. Data represent means of values from three independent biological experiments. Bars indicate standard errors of means and different letters indicate significant differences between values ($P \geq 0.05$) using one-way analysis of variance (Tukey's pairwise comparisons test); n.d. = not detected.

7.4. Discussion and conclusions

The three approaches used to localize transcripts of the different *G. intraradices* genes gave complementary information concerning gene expression topography. The technique of *in situ* RT-PCR showed *DESAT, LSU* (as reported by Seddas et al., 2009) and *TEF* expression in spores, but only *LSU* activity was detected in mycelium in roots and no transcripts of the Ca^{2+}-related genes could be located in any fungal structures. The reason for these results may be two-fold: technical, or gene expression may be too low to detect under the present conditions. *In situ* RT-PCR also gave a very weak signal and important background for the fungal gene Gm152 (see fig. 3.5 in Chapter 3).

Using microdissection and RT-PCR to target *G. intraradices* transcripts in tissues of mycorrhizal *M. truncatula* roots, on the contrary, clearly showed that activity of all four marker genes (*DESAT, GiPT, TEF, LSU*) is associated both with arbuscules and with intercellular hyphae in non-arbuscular, vesicle-free root tissues. As reported by Seddas et al. (2008), *DESAT* transcripts were detected not only in arbuscules but also in vesicles. In contrast, expression of phosphate transporter genes from *G. versiforme* (*GvPT*) and *G. intraradices* (*GiPT*) has been detected predominantly in the extraradical mycelium, the initial site of phosphate aquisition from the soil (Harrison and van Buuren, 1995; Maldonado-Mendoza et al., 2001). However, as for *G. intraradices* BEG141, the phosphate transporter gene from *G. mosseae* (*GmosPT*) also shows activity in arbuscules where it has been suggested that the AM fungus may somehow control the amount of phosphate delivered to the plant by re-absorbing Pi released from neighbouring plant cells (Benedetto et al., 2005; Balestrini et al., 2007; Tisserant et al., 2012). These observations were supported by monitoring of gene expression in *G. intraradices*-colonized roots of *P. sativum* which showed that, as compared to wild type cv Finale, the expression of *GiPT* was present but significantly down-regulated in the *Pssym36* mutant where AM fungi penetrate and colonize roots forming intercellular hyphae, but complete arbuscule formation is prevented. The incomplete arbuscule development results in the absence of the main functional symbiotic interface between the fungal and plant cells thus reducing nutrient exchange. This could explain the repression not only of *GiPT* but also of *DESAT* in the *Pssym36* mutant which confirms the observations by Kutznetsova et al. (2010) who concluded that this could result from reduced biosynthesis of fatty acids by the fungus due to limited uptake of plant carbon in the absence of a functional arbuscule interface. Since

transcripts of these two marker genes can also be detected by microdissection and RT-PCR in non-arbusculated tissues, that is in intercellular hyphae, it is suggested that carbon is also transferred to intercellular hyphae from cortical cells and that Pi can be re-absorbed from plant cells via the intercellular space.

For the selected Ca^{2+}-related genes of *G. intraradices*, most of the transcripts could be detected in arbuscules and/or intercellular hyphae by laser microdissection and RT-PCR. Expression of the mitochondria membrane calcium-binding carrier gene (BEG141_c23149) in arbusculated tissues of mycorrhizal *M. truncatula* roots and the lack of transcripts in intercellular hyphae or roots of the *Pssym36* pea mutant clearly indicate that it is specifically active in functional arbuscules. The two vacuolar Ca/Mn transporter genes (BEG141_c17763, BEG141_lrc1694) show the same arbuscular location using laser microdissection but differ by their expression profiles in the *Pssym36* mutant. From the microdissection results, these two genes are only expressed in arbuscules whilst both are active in the *Pssym36* mutant. Since transcripts could not be detected in intercellular hyphae by laser microdissection, this may indicate a function not only in normal but also in aborted arbuscules or that different host plants may somehow stimulate different expression profiles. For example, up-regulation of the vacuolar calcium ion transporter 1 (BEG141_c17763) in *Pssym36* roots may reflect the perception of a stress by the AM fungus in the mutant, as was suggested to explain the over-expression of the fungal alkaline phosphatase gene in the same pea genotype (Kuznetsova et al., 2010). Three of the *G. intraradices* genes, BEG141_c2781 (endoplasmic reticulum P-type Ca^{2+} ATPase), BEG141_c10704 (Golgi reticulum P-type Ca^{2+} ATPase) and BEG141_lrc 995 (nuclear CCaMK), were expressed in both arbuscules and intercellular hyphae; no significant effect was observed of the *Pssym36* mutation in pea roots, suggesting a possible function in the general development of the fungus within host tissues. In contrast, transcripts of the plasma membrane/vacuolar Ca^{2+}-transporting ATPase (BEG141_c3514) were only weakly detected in intercellular hyphae in mycorrhizal *M. truncatula* roots, and not in colonized pea roots, indicating no function in arbuscule formation or function.

CHAPTER 8

Functional characterization of three *G. intraradices* BEG141 genes

8.1. Full length gene sequencing and phylogenetic analyses

Three genes with interesting expression profiles and potentially involved in calcium homeostasis were selected for functional analyses. These genes showed similar responses in the pre-symbiotic stage of *G. intraradices* BEG141 development but different expression profiles during colonization of *M. truncatula* roots. They putatively code for the vacuolar calcium ion transporter 2 (VCX1) (BEG141_lrc1694), an endoplasmic reticulum calcium ATPase (PMR1) (BEG141_c2781), and a nuclear CCaMK (CMK1) (BEG141_ lrc995). Full length coding sequences of the selected genes were obtained by 3' and 5' end RACE. Homology searches were carried out with the full length sequences by BLAST using NCBI databases (http://blast.ncbi.nlm.nih.gov/). The phylogenetic analyses, applying the neighbor-joining method and including sequences from distinct eukaryotic organisms, are presented in Figs. 8.1 to 8.3. The phylogeny trees of VCX1 and CCaMK separate the fungal and plant homologues into two different clades (Figs. 8.1, 8.2). As expected, the three genes clustered with fungal proteins.

The *G. intraradices* VCX1 (BEG141_lrc1694) encodes for 403 amino acids and contains eleven predicted transmembrane spanning domains. Comparisons with the amino acid sequence databases showed that the vacuolar calcium ion transporter 2 possesses 52 % similarity to a *Scheffersomyces stipitis* (XP_001383222) Ca^{2+}/H^{+} antiporter. All of the Vcx1 homologues presented in Fig. 8.1B possess two sodium/calcium exchanger super family (Na_Ca_ex; PFAM 01699) domains playing a role in cellular cation homeostasis by transporting Ca^{2+} and Na^{+} into the vacuole. Moreover, prediction of transmembrane (TM) regions revealed that all these *Vcx1* proteins had 10 or 11 predicted TM domains.

The endoplasmic reticulum calcium ATPase (PMR1) (BEG141_c2781) from *G. intraradices* encodes for 998 amino acids and is closely related to P-type ATPases. It has 68 % similarity to a *Laccaria bicolor* (XP_001878234) Ca-transporting ATPase, and is predicted to encode eight transmembrane domains (Fig. 8.2B). As compared to members of the P-type II ATPase gene family in other fungi (Corradi and Sanders, 2006), this endoplasmic reticulum calcium ATPase is closely related to type II A (SERCA, or sarco/endoplasmic reticulum Ca^{2+}-ATPase). P-type IIA ATPase (SERCA ATPase) transfers Ca^{2+} from the cytosol of the cell into the endoplasmic reticulum lumen. The PMR1 homologues all possess :

1) the N terminus of the cation ATPase (Cation_ATPase_N, PFAM PF00690.21) which represents the conserved N-terminal region found in several classes of

cation-transporting P-type ATPases, including those that transport H^+, Na^+, Ca^{2+}, Na^+/K^+, and H^+/K^+

2) an E1-E2_ATPase (PFAM PF00122.15) which catalyzes auto- (or self-) phosphorylation of a key conserved aspartate residue within the pump; in addition, they all appear to interconvert between at least two different conformations, denoted by E1 and E2;
3) the hydrolase domain (HAD_like; PFAM PF00702.21) of the haloacid dehalogenase-like (HAD) superfamily which includes L-2-haloacid dehalogenase, epoxide hydrolase, phosphoserine phosphatase, P-type ATPase and many others, which all use a nucleophilic aspartate in their phosphoryl transfer reaction;
4) the C terminus of the cation ATPase (Cation_ATPase_C; PFAM PF00689) involved in Na^+/K^+, H^+/K^+, Ca^{2+} and Mg^{2+} transport.

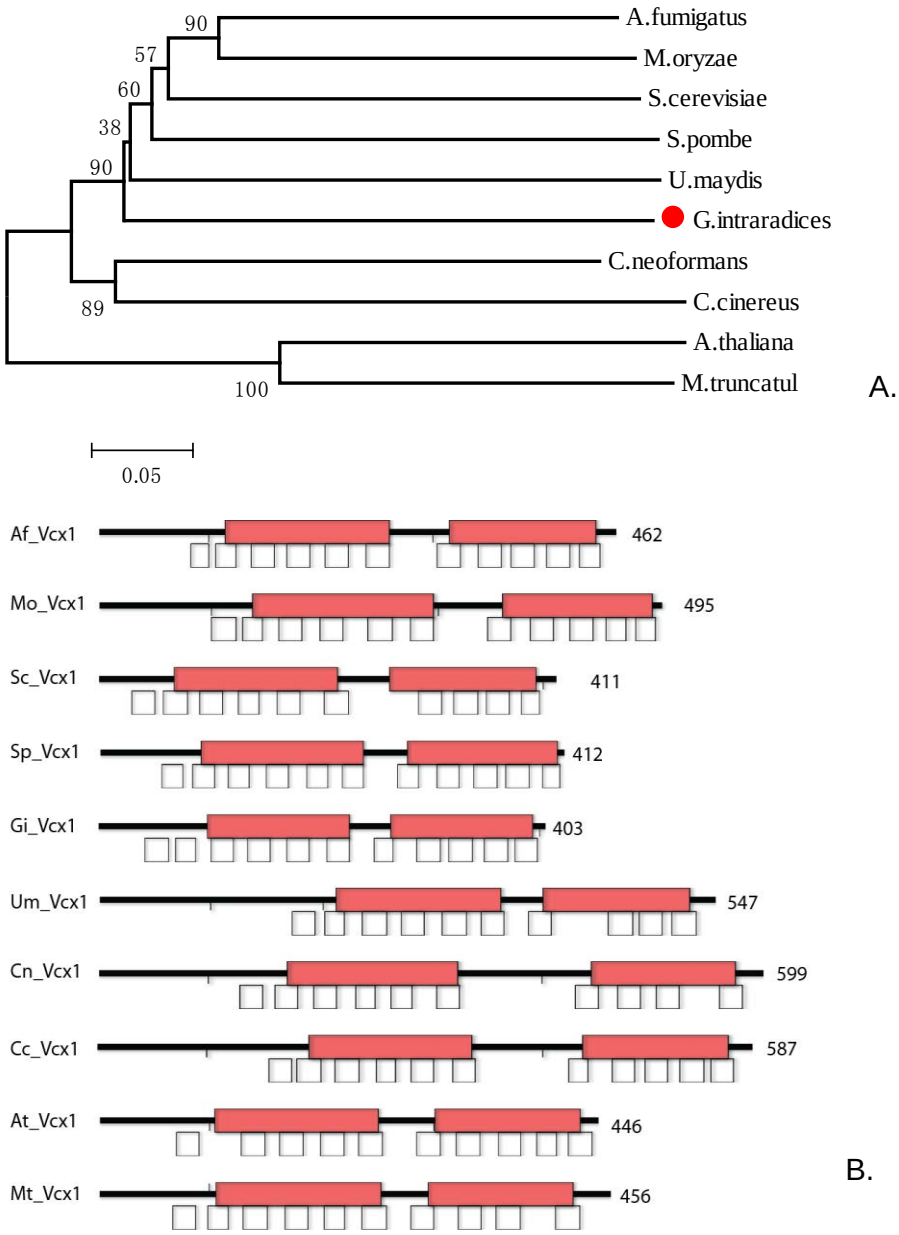


Fig. 8.1. A. Phylogenetic analysis of VCX1 cation/proton exchangers from different eukaryotic organisms: *S. cerevisiae* (NP_010155.1), *S. pombe* (O59768), *C. cinereus* (XP_001832277), *C. neoformans* (XP_566450), *A. fumigatus* (XP_750174.2), *M.oryzae* (EHA48361), *U. maydis* (XP_761279), *A. thaliana* (Q945S5) and *M. truncatula* (NP_003604703). The bar marker indicates the difference in percent. *G. intraradices* used in this study is indicated with a red point. B. Domain architecture of Vcx1 homologs from different organisms. The sodium/calcium exchanger superfamilly (PFAM 01699) domain is represented in plain boxes, and the transmembrane domains in white boxes. The lengths (in amino acids) of each of the proteins are indicated on the right. Af_Vcx1: *A. fumigatus* (XP_750174.2); Mo_Vcx1: *M.oryzae* (EHA48361); Sc_Vcx1: *S. cerevisiae* (NP_010155.1); Sp_Vcx1: *S. pombe* (O59768); Gi_Vcx1: *G. intraradices* BEG141 (this study); Um_Vcx1: *U. maydis* (XP_761279); Cn_Vcx1: *C. neoformans* (XP_566450); Cc_Vcx1: *C. cinereus* (XP_001832277); At_Vcx1: *A. thaliana* (Q945S5) and Mt_Vcx1_*M. truncatula* (XP_003604703).

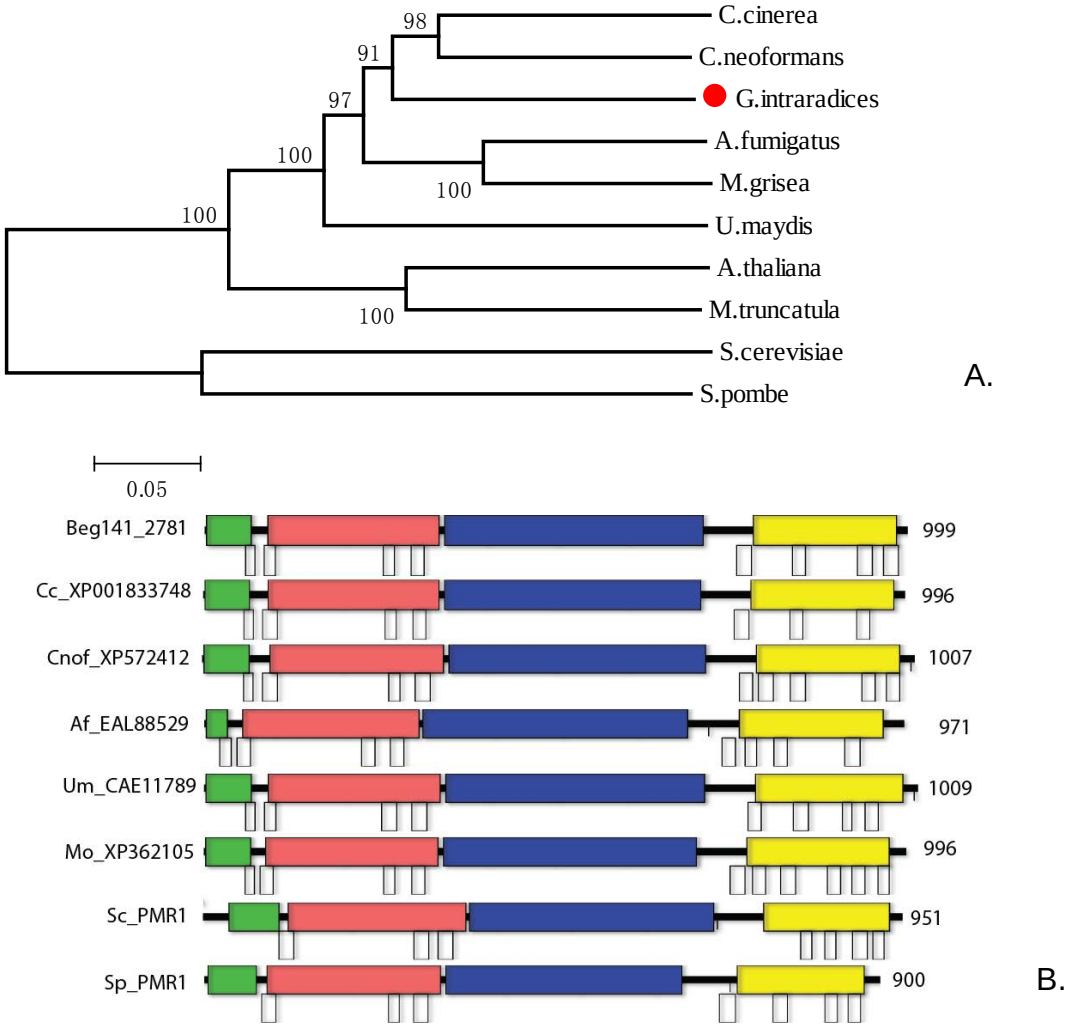


Fig. 8.2. A. Phylogenetic analysis of *G. intraradices* BEG141 endoplasmic reticulum calcium ATPase in relation to ortholog proteins from other eukaryotic organisms: *C. cinereus* (XP_001833748), *C. neoformans* (XP_572412), *A. fumigatus* (EAL88529.1), *M.oryzae* (XP362105), *U. maydis* (CAE11789.1), *A. thaliana* (AAF75073.1), *M. truncatula* (AAL35972), *S. cerevisiae* (CAA96880), and *S. pombe* (NP_595098). The bar marker indicates the difference in percent. *G. intraradices* used in this study is indicated with a red point. B. Domain structure of endoplasmic reticulum calcium ATPase ortholog proteins from different eukaryotic organisms. White boxes correspond to transmembrane domains, green boxes to the N terminus of the cation ATPase pfam PF00690.21, rose boxes to E1-E2_ATPase pfam PF00122.15, blue boxes to the hydrolase domain PFAM PF00702.21 and yellow boxes to the C terminus of the cation ATPase PFAM PF00689. The lengths (in amino acids) of each of the proteins are indicated on the right.. Gi_Beg141_2781: *G. intraradices* BEG141; Cc_XP_001833748: *C. cinereus*; Cnof_XP_572412: *C. neoformans*; Af_EAL88529.1: *A. fumigatus*; Mo_XP362105*: M.oryzae*; Um_CAE11789.1: *U. maydis*; Sc_Pmr1m: *S. cerevisiae* (CAA96880); Sp_Pmr1: *S. pombe* (NP_595098).

Finally, the nuclear CCaMK from *G. intraradices* includes an open reading frame encoding for 440 amino acids and shows similarity (48 %) to a calcium/calmodulin-dependent protein kinase of *Capsaspora owczarzaki* (EFW47030). It contains a protein kinase, catalytic domain (PKc_like super family, cl09925). The protein kinase superfamily is mainly composed of the catalytic domains of serine/threonine-specific and tyrosine-specific protein kinases which catalyze the transfer of the gamma-phosphoryl group from ATP to hydroxyl groups in specific substrates such as serine, threonine, or tyrosine residues of proteins.

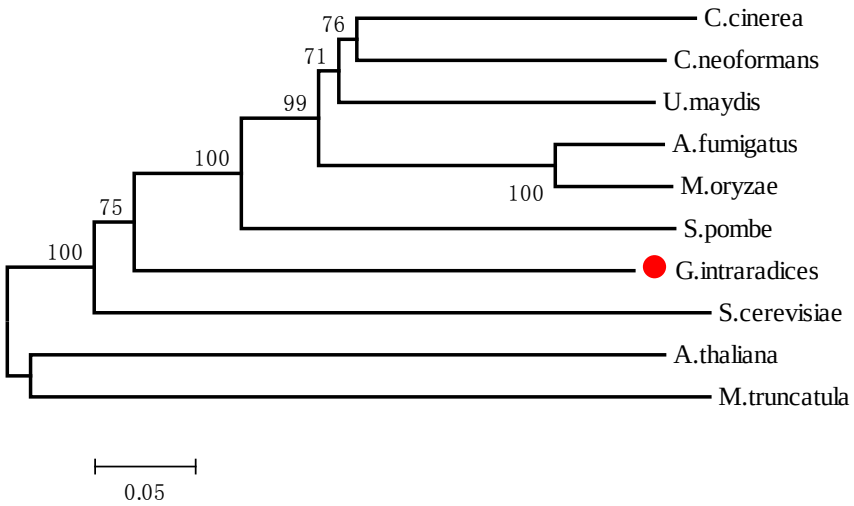


Fig. 8.3. Phylogenetic analysis results of calcium/calmodulin-dependent protein kinases from distinct eukaryotic organisms, as follows: *S. cerevisiae* (NP_116669), *S. pombe* (NP_593464), *C. cinereus* (BAF75875), *C. neoformans* (XP_572924), *A. fumigatus* (XP_754664), *M.oryzae* (ACB41780), *U. maydis* (XP_761691), *A. thaliana* (AED90798) and *M. truncatula* (XP_003628124). The bar marker indicates the difference in percent. *G. intraradices* used in this study is indicated with a red point.

8.2. Yeast complementation assays

8.2.1. Growth tests

For phenotypic characterization, the wild-type yeast (W303), knockout (YDL128W, K667 and YGL167C), and complemented transformations (with gene or empty vector) strains were grown on YPD or SD medium (+/-uracil) to a cell density of OD_{600}=0.6-0.8. The cell suspensions were serially diluted 10 fold, and 2.5 µl of each dilution was spotted on YPD or SD agar supplemented with $CaCl_2$ (50, 100, 200, 400, and/or 600, 800mM).

The plates were incubated for 2 days at 30°C, 35°C or 37°C and photographed. The results are presented in Figs.8.4 to 8.8. For the knockout strain *cmk1*Δ (YFR014C), no obvious calcium-related phenotypes were mentioned in the previous studies.

8.2.2 Complementation of *vcx1* mutants

In order to confirm the function of the vacuolar *Vcx1* gene from *Glomus intraradices* (GiVCX1/BEG141_lrc1694), complementation of a VCX1 deficient yeast strain (YDL128W) was performed. However, the *vcx1* mutant did not display Ca^{2+} sensitivity (Figs. 8.4 and 8.5) nor calcineurin-dependent Ca^{2+} sensitivity using the calcineurin inhibitor cyclosporine (Fig. 8.6). Kmetzsch et al. (2010) described the effect of calcineurin on a mutant of *Cryptococcus neoformans* vcx1Δ which was strongly inhibited in its growth with cyclosporine at 35°C. It was expected to replicate this phenotype in the yeast mutant for the gene *vcx1* (YDL128W) and thus test complementation, but the phenotype described by Kmetzsch et al. (2010) showing lack of growth in the presence of calcium could not be reproduced. In *S. cerevisiae* calcineurin negatively regulates the activity of Vcx1, but increases positively the transcription of two Ca^{2+} ATPases of the vacuole (PMC1) and the Golgi (PMR1) via the factor Crz1 transcription. So the use of calcineurin inhibitors like cyclosporine A or FK506, or of the mutant *cnb1* is not an absolute way to repress the Ca^{2+} regulation. What emerges from the experiments by Cunningham and Fink (1996) or Cagnac et al. (2010) is that there are one or more regulatory elements by which calcineurin plays a role in resistance to Ca^{2+}, most likely counterparts of PMC1 and PMR1.

For this reason, the yeast strain K667 which is triply mutated for the genes *pmc1*, *cnb1* and *vcx1* and cannot grow in concentrations of Ca^{2+} higher than 20 to 30 mM (according to Cagnac et al. 2010) was used. Because the yeast strain K677 lacks a functional calcineurin (CNB1), the endogenous vacuolar Ca^{2+}-ATPase (PMC1) and the vacuolar antiporter H^+/Ca^{2+} (VCX1), it is unable to uptake calcium into the vacuole and therefore to grow in the presence of high calcium concentrations (Cunningham and Fink 1996). This phenotype can be reverted when complemented by a functional homolog of the VCX1 gene (Hirschi et al. 1996; Cheng 2005; Cagnac et al. 2010). A successful complementation was not achieved; the K667 yeast strain transformed with the full length encoding sequence of VCX1from *G. intraradices* (GiVCX1/BEG141_lrc1694), was unable to grow on high calcium levels, like the untransformed K667 strain. Several hypotheses could be formulated to explain this result. VCX1 of *Saccharomyces cerevisiae*

and *G. intraradices* have predicted phosphorylation sites, and according to mass spectrometry phosphopeptide sequencing, serine 13 of yeast VCX1 is phosphorylated (Gruhler et al. 2005). The function and the conditions of this phosphorylation event are unknown (Gruhler et al. 2005). As the amino acids surrounding this serine (S13) differ between the two organisms, it is possible that the equivalent residue is not phosphorylated in the case of *G. intraradices*, and that this could hamper the activity of GiVCX1/BEG141_lrc1694, thereby not allowing a complete complementation. Another cause of lack of complementation could arise from differences in codon usage between *G. intraradices* and *S. cerevisiae*.

8.2.3 Complementation of a pmr1 mutant

A PMR1 deficient yeast strain (YGL167C) showing Ca^{2+} sensitivity (Szigeti et al., 2005) was acquired for complementation with GiPMR1/BEG141_c2781. However, the phenotype of the *pmr1* mutant from Open Biosystems (Thermo Scientific) was not correct as it was not sensitive to high levels of environmental Ca^{2+} (Fig. 8.7). Also, the YGL167C yeast strain transformed with PMR1/BEG141_c2781 of *G. intraradices* and the empty vector showed no differences in growth, although transformation was successful because the YGL167C yeast strain complemented with GiPMR1/BEG141_c2781was able to grow on SD agar without uracil (Fig. 8.8), but it did not show a Ca^{2+} sensitive phenotype in high concentrations of Ca^{2+} (as reported for yeast PMR1 by Szigeti et al., 2005). Consequently, it was not possible to conclude to the function of the GiPMR1 encoding gene.

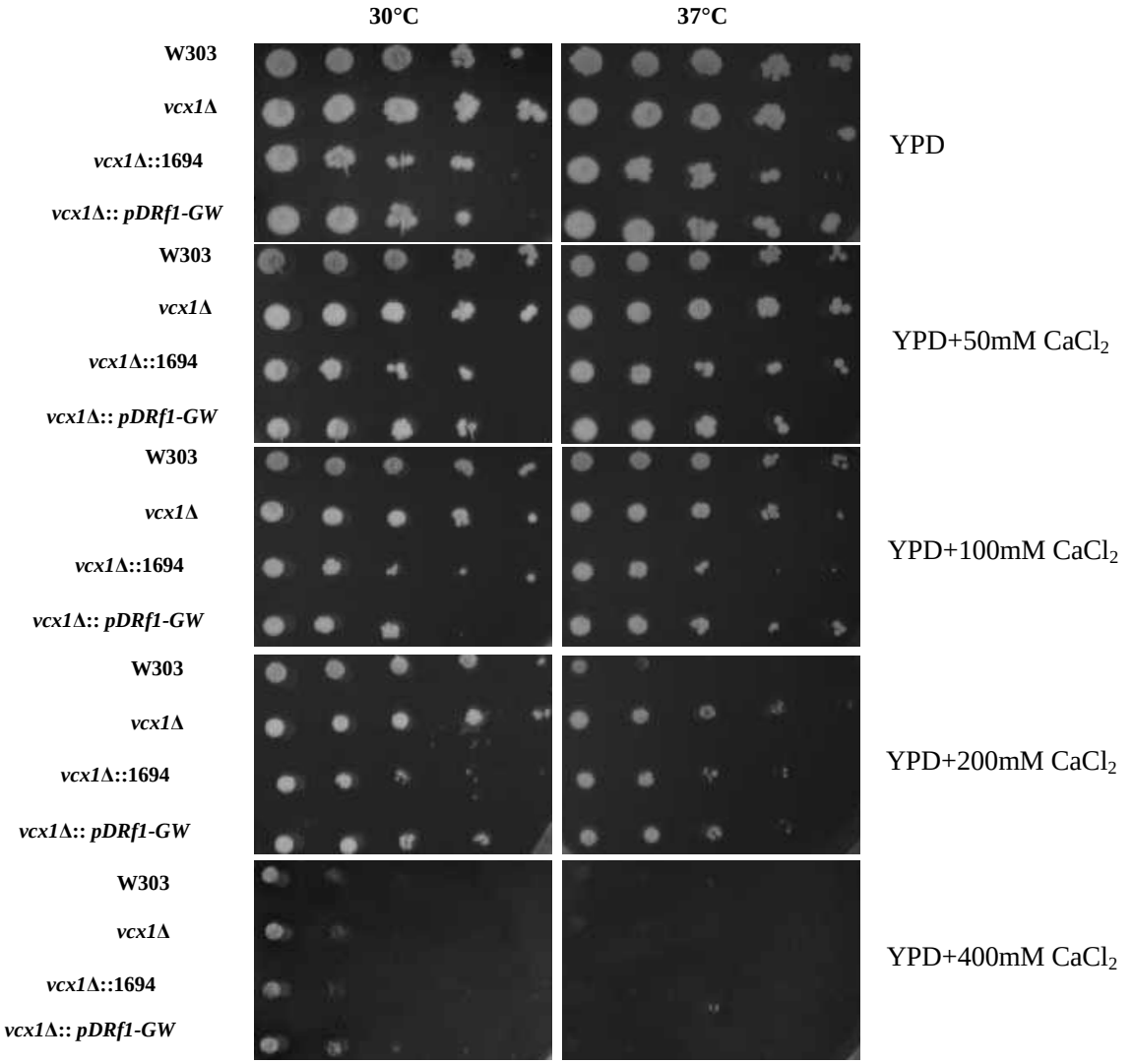


Fig. 8.4.The *vcx1* yeast mutant did not display Ca^{2+} sensitivity. Ten-fold serial dilutions of wild-type W303, *vcx1* mutant YDL128W (*vcx1*Δ), *vcx1*::VCX1-complemented (*vcx1*Δ::1694) and *vcx1*::empty vector-complemented (*vcx1*Δ:: *pDRf1-GW*) cells were plated in YPD agar containing 50-400 mM $CaCl_2$.The plates were incubated for 2 days at 30°C or 37°C, as indicated. As control, cells were grown in YPD agar only.

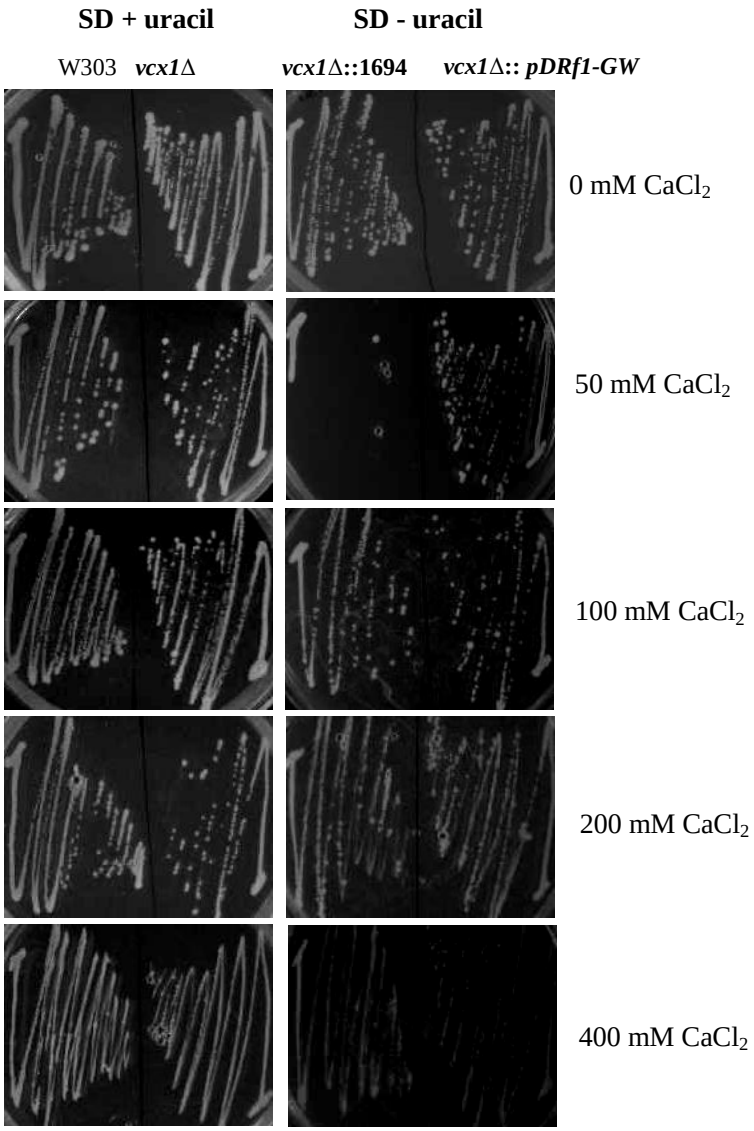


Fig. 8.5.The *vcx1* yeast mutant did not display Ca^{2+} sensitivity. Ten-fold serial dilutions of wild-type W303, *vcx1* mutant YDL128W (*vcx1*Δ), *vcx1*::VCX1-complemented (*vcx1*Δ::1694) and *vcx1*::empty vector-complemented (*vcx1*Δ:: *pDRf1-GW*) cells were plated in SD +/- uracil (with/without uracil) agar containing 50-400 mM $CaCl_2$. The plates were incubated for 2 days at 30°C or 37°C, as indicated.

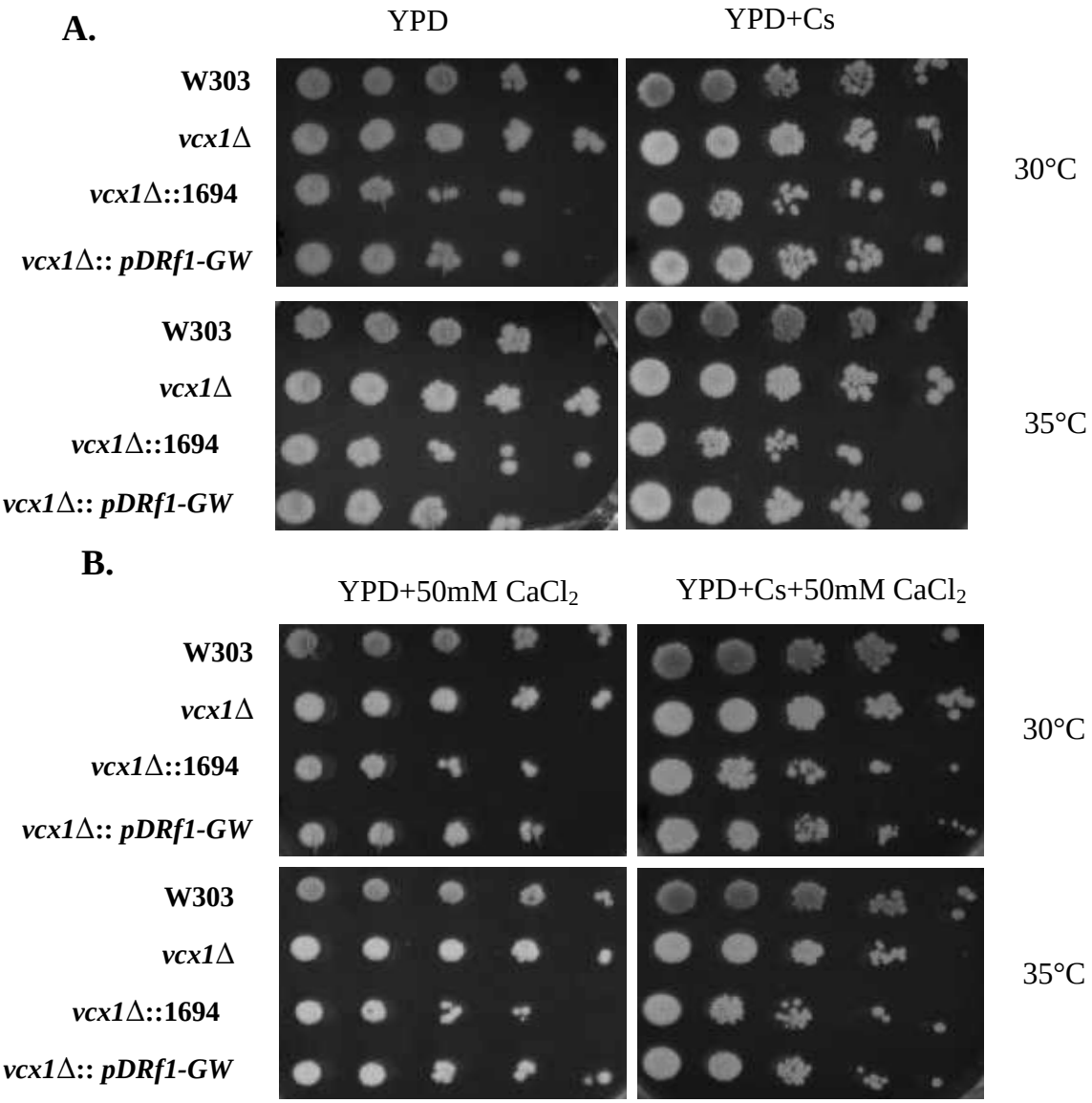


Fig. 8.6.The *vcx1* yeast mutant did not display calcineurin-dependent Ca^{2+} sensitivity. Ten-fold serial dilutions of wild-type W303, *vcx1* mutant YDL128W (*vcx1*Δ), *vcx1*::VCX1-complemented (*vcx1*Δ::1694) and *vcx1*::empty vector-complemented (*vcx1*Δ:: *pDRf1-GW*) cells were plated in YPD agar containing 100 µg/ml of Cyclosporine (Cs) (A), 50 mM $CaCl_2$ with 100 µg/ml of Cs (B).The plates were incubated for 2 days at 30°C or 35°C, as indicated. As control, cells were grown in YPD agar only.

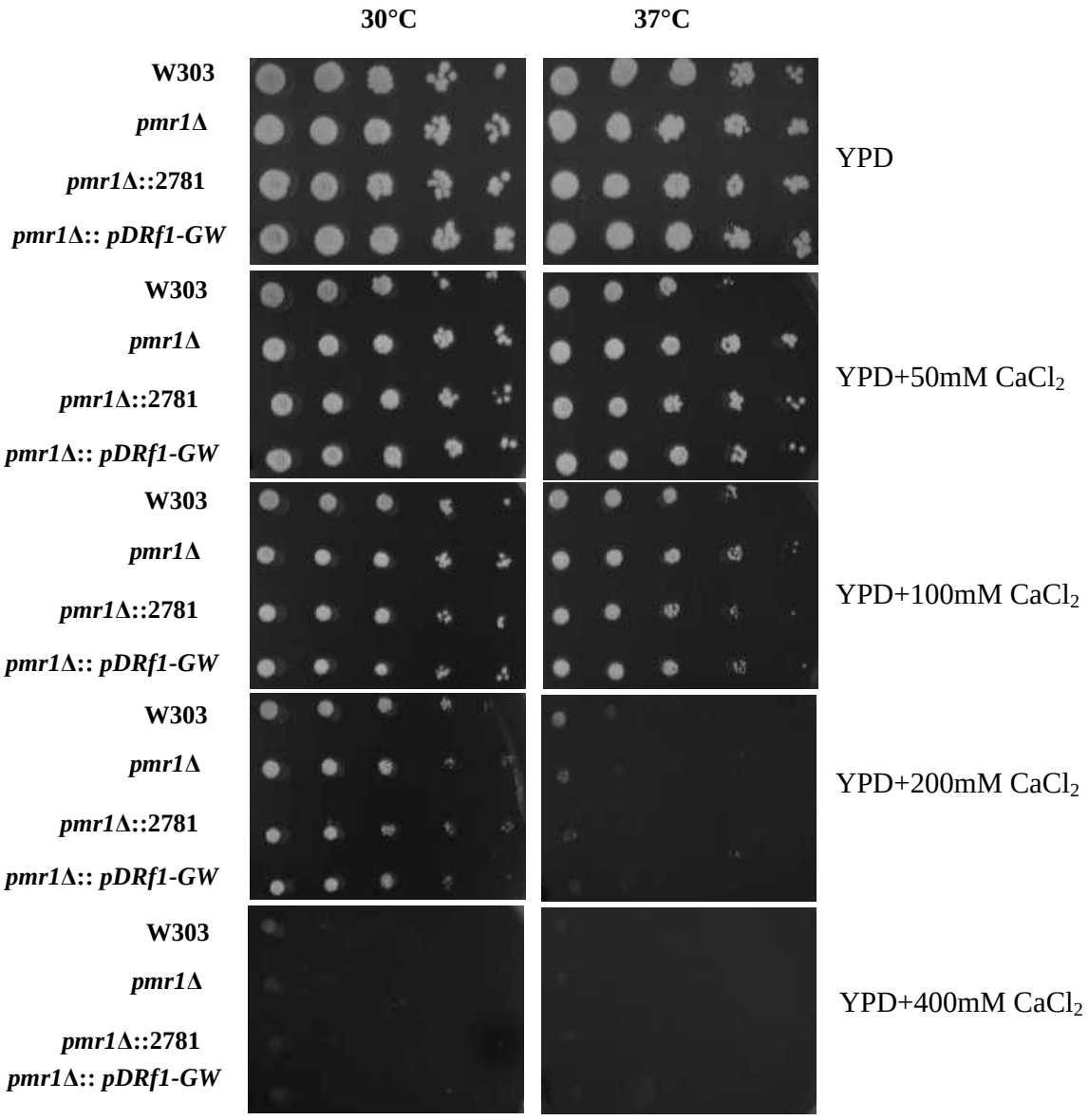


Fig. 8.7.The *pmr1* yeast mutant did not display Ca^{2+} sensitivity. Ten-fold serial dilutions of wild-type W303, *pmr1* mutant YGL167C (*pmr*Δ), *pmr1*::PMR1-complemented (*pmr*Δ::2781) and *pmr1*::empty vector-complemented (*pmr1*Δ:: *pDRf1-GW*) cells were plated in YPD agar containing 50-400 mM $CaCl_2$.The plates were incubated for 2 days at 30°C or 37°C, as indicated. As control, cells were grown in YPD agar only.

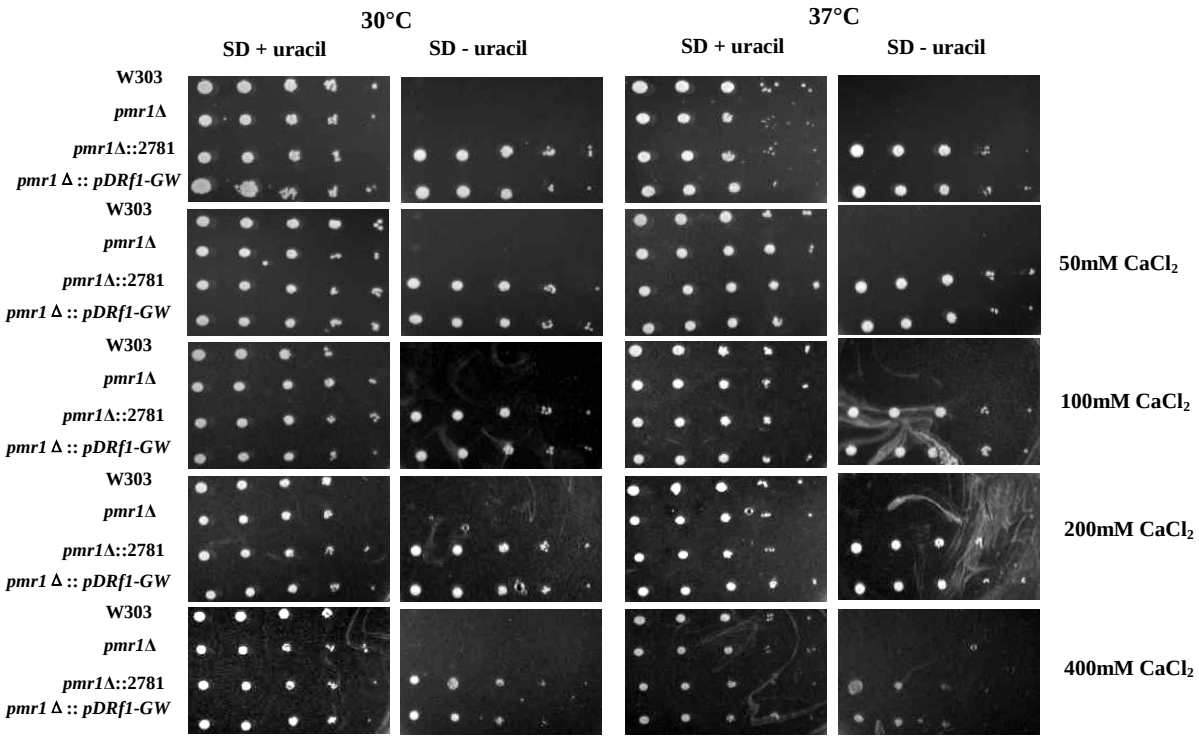


Fig. 8.8. The *pmr1* yeast mutant did not display Ca^{2+} sensitivity. Ten-fold serial dilutions of wild-type W303, *pmr1* mutant YGL167C (*pmr*Δ), *pmr1*::PMR1-complemented (*pmr*Δ::2781) and *pmr1*::empty vector-complemented (*pmr1*Δ:: *pDRf1-GW*) cells were plated in SD +/- uracil (with/without uracil) agar containing 50-400 mM $CaCl_2$. The plates were incubated for 2 days at 30°C or 37°C, as indicated.

8.3. Discussion and conclusions

Complete coding sequences for three genes from *G. intraradices* BEG141 have been identified which are putatively important in Ca^{2+} homeostasis and/or Ca^{2+}-based signaling: a tonoplast calcium ion transporter 2 (GiVCX1/BEG141_lrc1694), an endoplasmic reticulum calcium ATPase (GiPMR1/BEG141_c2781), and a nuclear CCaMK (GiCMK1/BEG141_ lrc995). Unfortunately, the yeast complementation assays in this study were inconclusive because the *vcx1* mutant YDL128W and the *pmr1* mutant YGL167C did not show an expected Ca^{2+} sensitive phenotype, and the triple K667 mutant of yeast, which cannot grow in the presence of Ca^{2+}, was not rescued after transformation with the BEG141_lrc1694 attB-pDONR plasmid. However, the phylogenetic trees clearly showed that full length BEG141_lrc1694 has a high homology with *vcx1* and BEG141_c2781 with *pmr1*, and that the *G. intraradices* genes have a domain structure

typical of homologs in other eukaryotes. The lack of complementation could be due to differences in the codon usage between yeast and *G.* intraradices. The *G. intraradice vcx1*and *pmr1* show 48 % and 33 % identity to yeast *vcx1* and *pmr1*, respectively. In another study, heterologous complementation with the *G. intraradices* transcription factor gene *GintSTE12* successfully restored pathogenicity of a *Colletotrichum lindemuthianum clste12*Δ mutant even though the level of similarity was not high (45%) (Tollot et al., 2009). This illustrates the possibility of investigating gene function of AM fungi where corresponding mutants exist in fungi other than yeast, which is not at present the case for VCX1 or PMR1.

The role of calcineurin in the regulation of Pmc1, Pmr1 and Vcx1, and vice-versa, in organisms like yeast is well-known. Ca^{2+}signaling involves Ca^{2+}spiking which is induced by external environmental stimuli. In response to these changes, Ca^{2+} binds to and activates the universal Ca^{2+} sensor protein calmodulin (CaM) which in turn may activate various proteins, including the phosphatase calcineurin. Activation of calcineurin leads to transcriptional induction of the vacuolar Pmc1 and the Golgi Pmr1 genes, both Ca^{2+} pumps responsible for depleting the cytosolic Ca^{2+} to maintain the low levels for growing (Ton and Rao, 2004), whilst the vacuolar Vcx1 Ca^{2+}/H^{+} exchanger is inhibited by activation of calcineurin. Thus, Pmc1 and Vcx1 independently transport cytosolic Ca^{2+} into vacuoles, the major Ca^{2+} cell store (Cunningham, 2011). In fine, removal from the cytoplasm of Ca^{2+} necessary for calcineurin activation by calmodulin inhibits calcineurin activity and downstream Ca^{2+}-dependent transcriptional and translational events.

CHAPTER 9

General discussion and conclusions

Ca^{2+} is a key secondary messenger in cell physiology and signalling. The Ca^{2+} channels, pumps and transporters, Ca^{2+} sensors, and signal transducers are conserved essential components of the cellular Ca^{2+} signaling machinery which can underlie Ca^{2+} homeostasis in cells by regulating movement of ions between the extracellular environment, cells and subcellular compartments, and so provide mechanisms for generating Ca^{2+} signals (Dodd et al., 2010). In this study, AM fungal genes coding Ca^{2+}-related proteins were targeted in order to investigate the regulation or role of Ca^{2+} in the molecular responses of the fungal partner during processes leading to the establishment and functioning of the mycorrhizal symbiosis.

Two genes investigated from *G. mosseae* (putatively encoding a MAP3k-like protein kinase and a P-type ATPase) were up-regulated in the presence of host root exudates from *A. sinicum* and, based on *in situ* RT-PCR, the latter appeared to be active in extraradicular hyphae. More detailed studies on seven *G. intraradices* identified Ca^{2+}-related genes, which putatively encode six membrane proteins and one nuclear kinase. The full-length coding sequences obtained for three of them confirmed a putative function already described in other fungi (PMR1-like endoplasmic reticulum calcium ATPase, VCX1-like vacuolar Ca/Mn transporter, CCaMK).

None of the genes from *G. intraradices* responded positively to root exudates from the host plant *M. truncatula* but expression profiles during symbiotic interactions suggest different functions in fungal development or function. Four of the fungal genes are active during appressoria development and up-regulated during root colonization. They are putatively linked to Ca^{2+} homeostasis or perception during AM symbiosis development and code for the PMR1-like endoplasmic reticulum Ca^{2+} ATPase, a Golgi reticulum P-type ATPase, the VCX1-like vacuolar Ca/Mn transporter 1 and a nuclear CCaMK. The expression of these four genes during appressoria development also on roots of the mycorrhiza-resistant *M. truncatula* mutant *Mtdmi3*, as well as in *G. intraradices*-colonized roots of the mycorrhiza-defective pea mutant *Pssym36*, suggests a possible function in the general development of the fungus. Expression of the remaining three genes putatively linked to Ca^{2+} homeostasis is directly related to the development of intraradical structures in mycorrhizal roots. These encode a mitochondria membrane Ca^{2+}-dependent carrier, a vacuolar Ca/Mn transporter (2) and a PMC1-like plasma membrane/vacuolar Ca^{2+}-transporting ATPase. Their expression profile suggests a role in the functional symbiosis since transcripts are only detected at the arbuscule stage of *G. intraradices* in roots of wild type *M. truncatula*, and none is activated in interactions with the mycorrhiza-resistant *M.*

truncatula mutant *Mtdmi3* or during intercellular hypha development in roots of the mycorrhiza-defective pea mutant *Pssym36* (except vacuolar Ca/Mn transporter 2). Targeted localization of transcripts by microdissection and RT-PCR indicated that the mitochondria membrane Ca^{2+}-dependent carrier and vacuolar Ca/Mn transporter genes are in fact only active in arbuscules formed in wild type *M. truncatula* roots, whilst those encoding PMR1-like endoplasmic reticulum Ca^{2+} ATPase and nuclear CCaMK are expressed both in arbuscules and intercellular hyphae, and the plasma membrane/ tonoplast Ca^{2+}-transporting ATPase gene only in the latter.

Endoplasmic reticulum, vacuoles and mitochondria have important functions in Ca^{2+} homeostasis which is regulated through membrane-bound proteins. The P-type II ATPase gene family codes for proteins with an important role as ion pumps in adaptation of the cell to variations in external K^+, Ca^{2+} and Na^{2+} concentrations. During Ca^{2+}-signalling in animal cells, a P-type II ATPase (SERCA pump) regulates Ca^{2+} levels by effluxing the ion into the endoplasmic reticulum which serves as an intracellular Ca^{2+} store (Berridge et al., 2003). The *Pmr*1-like endoplasmic reticulum and the Golgi reticulum P-type ATPase genes of *G. intraradices* showed low activity in the pre-symbiotic stage as compared to their expression levels during fungal development within roots of the wild-type *M. truncatula* genotype. It suggests that they may regulate the intracellular Ca^{2+} homeostasis when *G. intraradices* comes into contact with plant cells, and thus be involved in the regulation of a Ca^{2+}-based signaling process. In contrast, the *Pmc*1-like plasma membrane/vacuolar Ca^{2+}-transporting ATPase gene was inhibited with spore germination and specifically activated in the full symbiosis during intercellular hypha development, where it could be putatively linked to cation mediation.

Ca^{2+}/H^+ antiporters have a role in promoting intracellular calcium ion sequestration into organelles via the exchange of calcium ions for hydrogen ions across the membrane. The significant differences in the spatio-temporal expression of the *G. intraradices* genes encoding the two vacuolar calcium ion transporters 1 and 2 suggest independent functions in the symbiotic process during mycorrhiza interactions. Neither of the genes responded to root exudates but both were expressed in arbuscules. However, the genes showed different expression profiles in that only the former was also active at the appressoria stage which may indicate different implications according to the stage of symbiosis development. Expression of the *Vcx*1-like vacuolar calcium ion transporter 1 gene was detected with appressorium development on both wild-type and mutant *M. truncatula* roots, and it increased when arbuscules formed in roots. In comparison, expression of the calcium ion

transporter 2 was only detected with arbuscule formation which corresponded to its transcript location. Vacuoles represent a major organelle for Ca^{2+} storage in highly vacuolated cells, like those of fungi and plants, where the ion is sequestered in the form of complexes with polyphosphate (Cunningham, 2011; Pittman, 2011). AM fungi are in fact characterized by an extensive vacuolar system which is considered central for the accumulation and transfer of phosphate within the hyphae (Smith and Gianinazzi-Pearson, 1988). High concentrations of Ca^{2+} and polyphosphate have been co-localized in vacuoles of arbuscules suggesting a role of Ca^{2+} in phosphate sequestration in fungal tissues (Strullu and Gourret, 1981). In *G. intraradices*, the action of the two vacuolar Ca^{2+} ion transporters 1 and 2, together with the PMC1-like plasma membrane/vacuolar Ca^{2+}-transporting ATPase, may contribute to this phenomenon.

Mitochondrial carriers transfer molecules across the mitochondrial membranes involved in energy transfer. The *G. intraradices* gene coding for the mitochondrial Ca^{2+}-dependent carrier protein was inhibited by wild type *M. truncatula* root exudates and weakly activated in intraradical mycelium at the late stage of arbuscule formation, which may reflect an eventual role in symbiosis functioning. Mitochondria couple cellular metabolic state with Ca^{2+} transport processes, that is they control not only their own intra-organelle Ca^{2+} level but also more generally impact on cellular concentrations and therefore Ca^{2+} related signaling events. For example, Ca^{2+} channeling between mitochondria and the endoplasmic reticulum collaborate in the regulation of cytosolic Ca^{2+} that results from influx and extrusion through plasma membrane Ca^{2+} ATPases (Szabadkai and Duchen, 2008). Indeed, the cooperation of these Ca^{2+} related proteins located in different organelles forms a complex calcium signaling network and maintains cytosolic calcium at concentrations compatible with growth.

CCaMK proteins are involved in signalling pathways leading to gene regulation. Expression of the *G. intraradices* nuclear *CCaMK* gene was unaffected by root exudates during presymbiotic fungal development but the gene was clearly up-regulated during root colonization in the symbiotic stage. Interestingly, this gene followed very similar patterns of expression and transcript localization from appressoria to root colonization as the *Pmr1*-like endoplasmic reticulum Ca^{2+}-ATPase gene, suggesting a possible role of the *G. intraradices* nuclear CCaMK in Ca^{2+} perception following fungal responses to plant signals.

Several studies on plant pathogenic fungi have indicated the involvement of Ca^{2+}-related processes in interactions with hosts. For example, it has been reported that a P-type

ATPase (*PDE1*) of the rice blast fungus *Magnaporthe grisea* is necessary for penetration of host tissues, hypha development and pathogenicity (Balhadere and Talbot, 2001). Also, an endoplasmic sarcoplasmic/reticulum Ca^{2+}-ATPase (*Eca1*) identified in the plant pathogen *Ustilago maydis* restores growth of a yeast mutant defective in calcium homeostasis (Adamíková et al., 2004). In the fungal pathogen *Magnaporthe grisea*, a calcium/calmodulin-dependent signaling system is involved in appressorium formation. CCaMK activity is modulated by calmodulin isoforms and in *M. grisea* calmodulin gene expression is induced concomitantly with appressorium formation (Lee and Lee, 1998; Liu and Kolattukudy, 1999).

Calcium is well known as an important signaling molecule in plant responses to various environmental stimuli. Abiotic stress signals, such as salinity, osmotic stress, drought, oxidative stress or low temperature, and biotic signals, for example from pathogens or symbionts, serve as elicitors for the plant cells. These different signals induce Ca^{2+} elevation in the cytosol and other cellular compartments independently, including the nucleus and mitochondria. Calcium efflux from the cytosol into organelles allows replenishment of internal stores, and a return to resting calcium levels, which may contribute to shaping the specific and distinct calcium signatures (Mahajan and Tuteja, 2005; Boudsocq and Sheen, 2010). Calcium influxes the cytosol via Ca^{2+}-permeable channels and effluxes out of the cytosol through energy-dependent Ca^{2+}-ATPases and transporters. In *Arabidopsis*, Ca^{2+} pumps, including the endoplasmic reticulum (ER)-type Ca^{2+}-ATPases (ECA or type IIA) and the auto-inhibited Ca^{2+}-ATPases (ACA or type IIB) are proposed to be involved in calcium signaling in response to abiotic stresses. For instance, *AtECA1* and *AtECA3* have an important role in tolerance to Mn^{2+} stress; *ECA1* expression restores growth of yeast *pmr1* mutants on Mn^{2+}-containing medium. Also, the vacuolar Ca^{2+}/H^{+} antiporter *CAX1*, which is induced by cold, has been shown to negatively regulate the cold-acclimation response in *Arabidopsis* by repressing the expression of CBF/DREB1 genes and their downstream targets. Moreover, a nuclear CCaMK from pea roots (*PsCamPK*) is up-regulated in roots in response to low temperature and increased salinity (Pandey et al., 2002). In legume plants, CCaMKs play a critical role in signaling and gene regulation in interactions with root symbionts where a plant CCaMK is a prime candidate for the response to calcium signatures that are induced by AM fungi or Nod factors (Lévy et al., 2004; Mitra et al., 2004).

A hypothesis can be formulated for Ca^{2+} homeostasis and signaling in *G. intraradices* based on the data from the present thesis research together with what is known from

studies on yeast. In yeast (Fig.9.1), Ca^{2+} enters the cytosol via the plasma membrane channel complex Cch1/Mid1. In response to changes in Ca^{2+} levels, Ca^{2+} binds to and activates the universal Ca^{2+} sensor protein calmodulin which in turn activates the serine/threonine phosphatase calcineurin and multifunctional Ca^{2+}/CaM-dependent protein kinases (CaMKs). Dephosphorylation by activated calcineurin induces the transcriptional regulator Crz1/Tcn1, leading to nuclear translocation and transcriptional activation of target genes including the vacuolar *Pmc*1 and the Golgi *Pmr*1 genes, both encoding Ca^{2+} pumps ATPases in the tonoplast and responsible for depleting the cytosolic Ca^{2+} to maintain low levels that are compatible for yeast growth (Ton and Rao, 2004). The vacuolar Ca^{2+}/H^{+} exchanger *Vcx*1 gene is inhibited by activation of calcineurin so that the Pmc1 and Vcx1 proteins transport cytosolic Ca^{2+} independently into vacuoles, the major Ca^{2+} cell store in the fungal cells (Cunningham, 2011). In addition, Vcx1 inhibits calcineurin by removing Ca^{2+} (necessary for calcineurin activation by calmodulin) from the cytoplasm, so that Vcx1 and calcineurin form a double-negative feedback interaction: the Vcx1-off/calcineurin-on state leads to activation of the *Pmc*1 and *Pmr*1 genes to reduce cytosolic Ca^{2+} levels, switching on a Vcx1-on/calcineurin-off state. This dynamic process of homeostasis will be turned on and off during Ca^{2+} spiking.

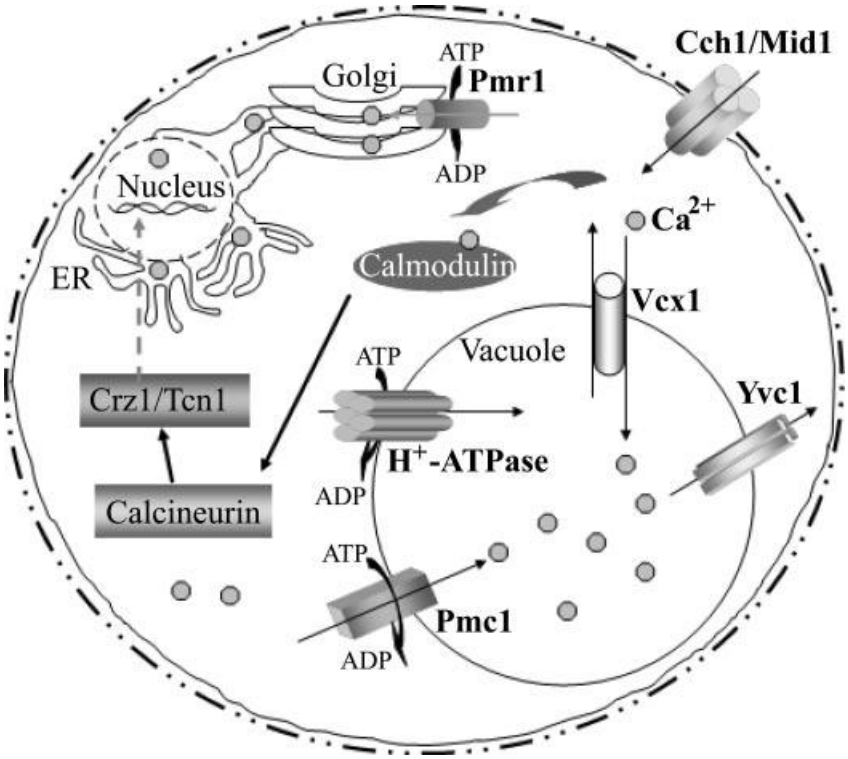


Fig. 9.1. Ca^{2+} signaling and transport pathways in *Saccharomyces cerevisiae* (taken from Ton and Rao, 2004). Ca^{2+} enters the cytosol via the plasma membrane channel complex Cch1/Mid1 or the vacuolar transient receptor potential-like channel Yvc1 in response to diverse environmental cues. Ca^{2+} / calmodulin binding activates the protein phosphatase calcineurin, which results in activation of the transcription factor Crz1/Tcn1, leading to its nuclear translocation and the transcription of target genes. Ca^{2+} is primarily removed from the cytosol by P-type ATPases in the Golgi (Pmr1) and vacuole (Pmc1), and by the vacuolar H^+/Ca^{2+} exchanger Vcx1.

The theoretical sub-cellular localization of the different Ca^{2+}-related genes of the AM fungus *G. intraradices* BEG141 is presented in Fig.9.2. It can be hypothesized that in *G. intraradices*, in response to cytoplasmic Ca^{2+} concentration changes, the Ca^{2+} sensor protein calmodulin can bind Ca^{2+} to activate the CCaMK (BEG141_lrc995) and calcineurin which regulates phosphorylation (coding sequences exist in the MIRA2 transcriptome database for calmodulin [step3_rep_c86] and calcineurin [step3_c3932] of *G. intraradices* DAOM197198). After dephosphorylation, the expression of the PMC1-like vacuolar (BEG141_c3514) and PMR1-like endoplasmic reticulum (BEG141_c2781) or Golgi (BEG141_c10704) Ca^{2+}-ATPases is induced via activation of transcription factors. These Ca^{2+} pumps can transport cytosolic Ca^{2+} into the vacuole and Golgi or endoplasmic reticulum to reduce cytoplasmic Ca^{2+} levels, which can in turn switch on the VCX1-like vacuolar Ca^{2+}/H^+ exchanger (BEG141_lrc1694).

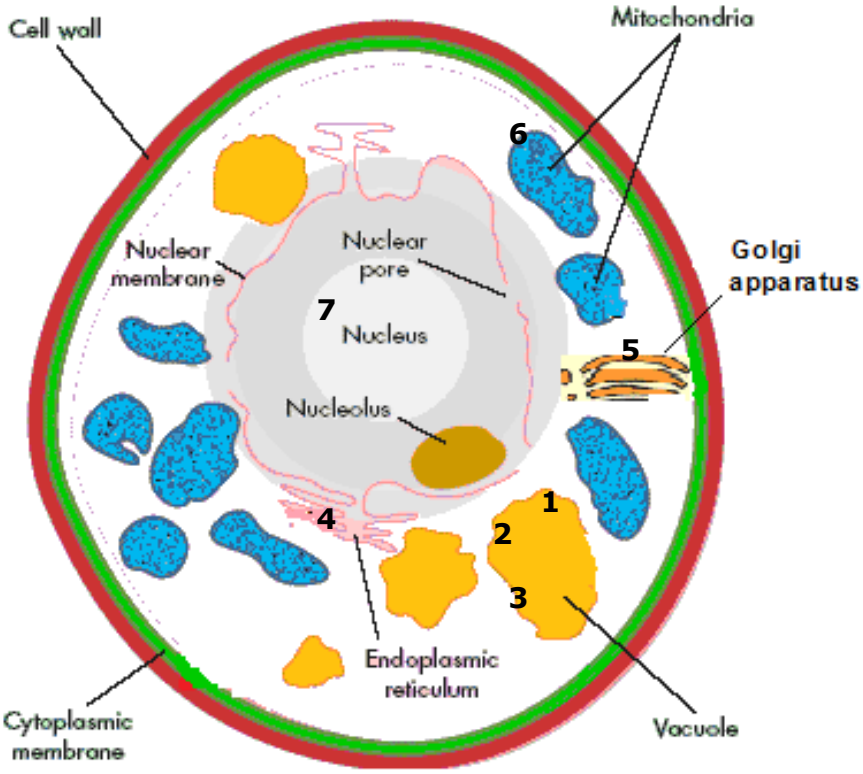


Fig. 9.2. The supposed sub-cellular localization of the different Ca^{2+}-related genes of the AM fungus *G. intraradices* BEG141: 1. Vacuolar calcium ion transporter 1; 2. Vacuolar calcium ion transporter 2; 3. Vacuolar calcium transporting ATPase; 4. Endoplasmic reticulum calcium ATPase; 5. Golgi reticulum calcium transporting ATPase; 6. Mitochondria membrane calcium-binding carrier; 7. Nuclear calcium/calmodulin-dependent protein kinase (CCaMK).

However, yeast complementation assays to obtain valid experimental evidence for *G. intraradices* gene function were unfortunately unsuccessful in the present study. In order to gain insight into the role of the different genes in the mycorrhizal symbiosis, an alternative approach for functional analysis should be developed. Heterologous complementation using fungi other than yeast has recently been reported to investigate gene function of AM fungi. For example, insertion of the *G. intraradices* transcription factor gene *GintSTE12* into a *clste12*Δ mutant of *Colletotrichum lindemuthianum* restores pathogenicity in the fungal pathogen, providing evidence for the possible existence of common genetic elements regulating penetration of plant tissues by symbiotic and pathogenic fungi (Tollot et al., 2009). Likewise, expression of the *G. intraradices* gene *SP7*, which interacts with a plant pathogenesis-related transcription factor, in the rice blast fungus *Magnaporthe oryzae*

attenuates root decay symptoms caused by the biotrophic pathogen (Kloppholz et al., 2011). Such an approach, together with the use of microdissection to localize the gene expression, offers new perspectives for the detailed analysis of fungal developmental processes that occur during functional differentiation in symbiotic arbuscular mycorrhiza interactions.

In conclusion, the present study of Ca^{2+}-related genes in *G. mosseae* and *G. intraradices* provides the first insight into the network of Ca^{2+} pumps and transporters which may be involved in regulating cytosolic Ca^{2+} in an AM fungus, and consequently in processes of homeostasis regulating changes in Ca^{2+} concentration that drive downstream CCaMK-dependent signaling events that are essential to the establishment and/or functioning of the mycorrhizal symbiosis.

References

Adamíková, L., Straube, A., Schulz, I., and Steinberg, G. (2004). Calcium signaling is involved in dynein-dependent microtubule organization. Molecular Biology of the Cell **15,** 1969-1980.

Aloui, A., Recorbet, G., Gollotte, A., Robert, F., Valot, B., Gianinazzi-Pearson, V., Aschi-Smiti, S., and Dumas-Gaudot, E. (2009). On the mechanisms of cadmium stress alleviation in *Medicago truncatula* by arbuscular mycorrhizal symbiosis: A root proteomic study. Proteomics **9,** 420-433.

Ané, J.M., Kiss, G.B., Riely, B.K., Penmetsa, R.V., Oldroyd, G.E.D., Ayax, C., Lévy, J., Debellé, F., Baek, J.M., and Kalo, P. (2004). *Medicago truncatula DMI1* required for bacterial and fungal symbioses in legumes. Science Signalling **303,** 1364-1367.

Balestrini, R., Gomez-Ariza, J., Lanfranco, L., and Bonfante, P. (2007). Laser microdissection reveals that transcripts for five plant and one fungal phosphate transporter genes are contemporaneously present in arbusculated cells. Molecular Plant-Microbe Interactions **20,** 1055-1062.

Balhadère, P.V., and Talbot, N.J. (2001). *PDE1* encodes a P-Type ATPase involved in appressorium-mediated plant infection by the rice blast fungus *Magnaporthe grisea*. The Plant Cell Online **13,** 1987-2004.

Balestrini, R., and Lanfranco, L. (2006). Fungal and plant gene expression in arbuscular mycorrhizal symbiosis. Mycorrhiza **16,** 509-524.

Benedetto, A., Magurno, F., Bonfante, P., and Lanfranco, L. (2005). Expression profiles of a phosphate transporter gene (*GmosPT*) from the endomycorrhizal fungus *Glomus mosseae*. Mycorrhiza **15,** 620-627.

Berridge, M.J., Bootman, M.D., and Roderick, H.L. (2003). Calcium signalling: dynamics, homeostasis and remodelling. Nature Reviews Molecular Cell Biology **4,** 517-529.

Bonfante, P., and Genre, A. (2010). Mechanisms underlying beneficial plant–fungus interactions in mycorrhizal symbiosis. Nature Communications **1,** 1-11.

Bonfante, P., and Requena, N. (2011). Dating in the dark: how roots respond to fungal signals to establish arbuscular mycorrhizal symbiosis. Current Opinion in Plant Biology **14,** 451-457.

Borges-Walmsley, M.I., and Walmsley, A.R. (2000). cAMP signalling in pathogenic

fungi: control of dimorphic switching and pathogenicity. Trends in Microbiology **8,** 133-141.

Boudsocq, M., and Sheen, J. (2010). Stress signaling II: calcium sensing and signaling. Abiotic Stress Adaptation in Plants: Physiological, Molecular and Genomic Foundation, 75-90.

Brechenmacher, L., Weidmann, S., van Tuinen, D., Chatagnier, O., Gianinazzi, S., Franken, P., and Gianinazzi-Pearson, V. (2004). Expression profiling of up-regulated plant and fungal genes in early and late stages of *Medicago truncatula-Glomus mosseae* interactions. Mycorrhiza **14,** 253-262.

Breuninger, M., and Requena, N. (2004). Recognition events in AM symbiosis: analysis of fungal gene expression at the early appressorium stage. Fungal Genetics and Biology **41,** 794-804.

Buee, M., Rossignol, M., Jauneau, A., Ranjeva, R., and Bécard, G. (2000). The pre-symbiotic growth of arbuscular mycorrhizal fungi is induced by a branching factor partially purified from plant root exudates. Molecular Plant-Microbe Interactions **13,** 693-698.

Cagnac, O., Aranda-Sicilia, M.N., Leterrier, M., Rodriguez-Rosales, M.P., and Venema, K. (2010). Vacuolar cation/H^+ antiporters of *Saccharomyces cerevisiae*. Journal of Biological Chemistry **285,** 33914-33922.

Cappellazzo, G., Lanfranco, L., Fitz, M., Wipf, D., and Bonfante, P. (2008). Characterization of an amino acid permease from the endomycorrhizal fungus *Glomus mosseae*. Plant Physiology **147,** 429-437.

Catoira, R., Galera, C., De Billy, F., Penmetsa, R.V., Journet, E.P., Maillet, F., Rosenberg, C., Cook, D., Gough, C., and Dénarié, J. (2000). Four genes of *Medicago truncatula* controlling components of a Nod factor transduction pathway. The Plant Cell Online **12,** 1647-1666.

Chabaud, M., Genre, A., Sieberer, B.J., Faccio, A., Fournier, J., Novero, M., Barker, D.G., and Bonfante, P. (2011). Arbuscular mycorrhizal hyphopodia and germinated spore exudates trigger Ca^{2+} spiking in the legume and nonlegume root epidermis. New Phytologist **189,** 347-355.

Cheng, N.H., Pittman, J.K., Shigaki, T., Lachmansingh, J., LeClere, S., Lahner, B., Salt, D.E., and Hirschi, K.D. (2005). Functional association of *Arabidopsis* CAX1 and CAX3 is required for normal growth and ion homeostasis. Plant Physiology **138,** 2048-2060.

Clapham, D.E. (2007). Calcium signaling. Cell **131,** 1047-1058.

Corcoran, E.E., and Means, A.R. (2001). Defining Ca^{2+}/calmodulin-dependent protein kinase cascades in transcriptional regulation. Journal of Biological Chemistry **276,** 2975-2978.

Corradi, N., and Sanders, I.R. (2006). Evolution of the P-type II ATPase gene family in the fungi and presence of structural genomic changes among isolates of *Glomus intraradices*. Bmc Evolutionary Biology **6,** 21.

Cunningham, K.W., and Fink, G.R. (1996). Calcineurin inhibits VCX1-dependent H^+/Ca^{2+} exchange and induces Ca^{2+} ATPases in *Saccharomyces cerevisiae*. Molecular and Cellular Biology **16,** 2226-2237.

Cunningham, K.W. (2011). Acidic calcium stores of *Saccharomyces cerevisiae*. Cell Calcium **50,** 129-138.

Dahan, J., Wendehenne, D., Ranjeva, R., Pugin, A., and Bourque, S. (2010). Nuclear protein kinases: still enigmatic components in plant cell signalling. New Phytologist **185,** 355-368.

Del Arco, A., Agudo, M., and Satrustegui, J. (2000). Characterization of a second member of the subfamily of calcium-binding mitochondrial carriers expressed in human non-excitable tissues. Biochemical Journal **345,** 725-732.

Dodd, A.N., Kudla, J., and Sanders, D. (2010). The language of calcium signaling. Annual Review of Plant Biology **61,** 593-620.

Dumas-Gaudot, E., Valot, B., Bestel-Corre, G., Recorbet, G., St-Arnaud, M., Fontaine, B., Dieu, M., Raes, M., Saravanan, R.S., and Gianinazzi, S. (2004). Proteomics as a way to identify extra-radicular fungal proteins from *Glomus intraradices* - RiT-DNA carrot root mycorrhizas. FEMS Microbiology Ecology **48,** 401-411.

Ebbole, D.J. (2007). *Magnaporthe* as a model for understanding host-pathogen interactions. Annual Review of Phytopathology **45,** 437-456.

Farmer, M., Li, X., Feng, G., Zhao, B., Chatagnier, O., Gianinazzi, S., Gianinazzi-Pearson, V., and Van Tuinen, D. (2007). Molecular monitoring of field-inoculated AMF to evaluate persistence in sweet potato crops in China. Applied Soil Ecology **35,** 599-609.

Franken, P., Lapopin, L., Meyer-Gauen, G., and Gianinazzi-Pearson, V. (1997). RNA accumulation and genes expressed in spores of the arbuscular mycorrhizal fungus, Gigaspora rosea. Mycologia **89,** 293-297.

Geisler, M., Frangne, N., Gomes, E., Martinoia, E., and Palmgren, M.G. (2000). The

ACA4 gene of *Arabidopsis* encodes a vacuolar membrane calcium pump that improves salt tolerance in yeast. Plant Physiology **124,** 1814-1827.

Genre, A., and Bonfante, P. (2007). Check-in procedures for plant cell entry by biotrophic microbes. Molecular Plant-Microbe Interactions **20,** 1023-1030.

Genre, A., Chabaud, M., Faccio, A., Barker, D.G., and Bonfante, P. (2008). Prepenetration apparatus assembly precedes and predicts the colonization patterns of arbuscular mycorrhizal fungi within the root cortex of both *Medicago truncatula* and *Daucus carota*. The Plant Cell Online **20,** 1407-1420.

Gianinazzi-Pearson, V. (1996). Plant cell responses to arbuscular mycorrhizal fungi: getting to the roots of the symbiosis. The Plant Cell **8,** 1871-1883.

Gianinazzi-Pearson, V., Branzanti, B., and Gianinazzi, S. (1989). In vitro enhancement of spore germination and early hyphal growth of a vesicular-arbuscular mycorrhizal fungus by host root exudates and plant flavonoids. Symbiosis **7,** 243-255.

Gianinazzi-Pearson, V., Séjalon-Delmas, N., Genre, A., Jeandroz, S., and Bonfante, P. (2007). Plants and arbuscular mycorrhizal fungi: cues and communication in the early steps of symbiotic interactions. Advances in Botanical Research **46,** 181-219.

Gietz, R.D., Schiestl, R.H., Willems, A.R., and Woods, R.A. (1995). Studies on the transformation of intact yeast cells by the LiAc/SS‐DNA/PEG procedure. Yeast **11,** 355-360.

Gollotte, A., van Tuinen, D., and Atkinson, D. (2004). Diversity of arbuscular mycorrhizal fungi colonising roots of the grass species *Agrostis capillaris* and *Lolium perenne* in a field experiment. Mycorrhiza **14,** 111-117.

Govindarajulu, M., Pfeffer, P.E., Jin, H.R., Abubaker, J., Douds, D.D., Allen, J.W., Bucking, H., Lammers, P.J., and Shachar-Hill, Y. (2005). Nitrogen transfer in the arbuscular mycorrhizal symbiosis. Nature **435,** 819-823.

Gruhler, A., Olsen, J.V., Mohammed, S., Mortensen, P., Færgeman, N.J., Mann, M., and Jensen, O.N. (2005). Quantitative phosphoproteomics applied to the yeast pheromone signaling pathway. Molecular & Cellular Proteomics **4,** 310-327.

Harrison, M.J., and van Buuren, M.L. (1995). A phosphate transporter from the mycorrhizal fungus *Glomus versiforme*. Nature **378,** 626-629.

Heupel, S., Roser, B., Kuhn, H., Lebrun, M.H., Villalba, F., and Requena, N. (2010). Erl1, a novel era-like GTPase from *Magnaporthe oryzae*, is required for full root virulence and is conserved in the mutualistic symbiont *Glomus intraradices*. Molecular Plant-Microbe Interactions **23,** 67-81.

Hewitt, E.J., Bureaux, C.A., and Royal, F. (1966). Sand and water culture methods used in the study of plant nutrition (2nd revised edn). Commonwealth Bureau of Horticulture and Plantation Crops, East Malling. Technical Communication. London, pp 547.

Hirschi, K.D., Zhen, R.G., Cunningham, K.W., Rea, P.A., and Fink, G.R. (1996). CAX1, an H^+/Ca^{2+} antiporter from *Arabidopsis*. Proceedings of the National Academy of Sciences USA **93,** 8782-8786.

Hoagland, D.R., and Arnon, D.I. (1950). The water-culture method for growing plants without soil. Circular. California Agricultural Experiment Station **347,** 32-37.

Javot, H., Pumplin, N., and Harrison, M.J. (2007). Phosphate in the arbuscular mycorrhizal symbiosis: transport properties and regulatory roles. Plant, Cell and Environment **30,** 310-322.

Kahl, C.R., and Means, A.R. (2003). Regulation of cell cycle progression by calcium/calmodulin-dependent pathways. Endocrine Reviews **24,** 719-736.

Karandashov, V., and Bucher, M. (2005). Symbiotic phosphate transport in arbuscular mycorrhizas. Trends in Plant Science **10,** 22-29.

Kloppholz, S., Kuhn, H., and Requena, N. (2011). A secreted fungal effector of *Glomus intraradices* promotes symbiotic biotrophy. Current Biology **21,** 1204-1209.

Kmetzsch, L., Staats, C.C., Simon, E., Fonseca, F.L., de Oliveira, D.L., Sobrino, L., Rodrigues, J., Leal, A.L., Nimrichter, L., Rodrigues, M.L., Schrank, A., and Vainstein, M.H. (2010). The vacuolar Ca^{2+} exchanger Vcx1 is involved in calcineurin-dependent Ca^{2+} tolerance and virulence in *Cryptococcus neoformans*. The Eukaryotic Cell **9,** 1798-1805.

Kosuta, S., Chabaud, M., Lougnon, G., Gough, C., Denarie, J., Barker, D.G., and Becard, G. (2003). A diffusible factor from arbuscular mycorrhizal fungi induces symbiosis-specific *MtENOD11* expression in roots of *Medicago truncatula*. Plant Physiology **131,** 952-962.

Krüger, M., Krüger, C., Walker, C., Stockinger, H., and Schüßler, A. (2012). Phylogenetic reference data for systematics and phylotaxonomy of arbuscular mycorrhizal fungi from phylum to species level. New Phytologist **193,** 970-984.

Küster, H., Vieweg, M.F., Mantey, K., Baier, M.C., Hohnjec, N., and Perlick, A.M. (2007). Identification and expression regulation of symbiotically activated legume genes. Phytochemistry **68,** 8-18.

Kuznetsova, E., Seddas-Dozolme, P.M.A., Arnould, C., Tollot, M., van Tuinen, D.,

Borisov, A., Gianinazzi, S., and Gianinazzi-Pearson, V. (2010). Symbiosis-related pea genes modulate fungal and plant gene expression during the arbuscule stage of mycorrhiza with *Glomus intraradices*. Mycorrhiza **20,** 427-443.

Lanfranco, L., and Young, J.P.W. (2012). Genetic and genomic glimpses of the elusive arbuscular mycorrhizal fungi. Current Opinion in Plant Biology **15,** 454-461.

Lee, S., and Lee, Y. (1998). Calcium/calmodulin-dependent signaling for appressorium formation in the plant pathogenic fungus *Magnaporthe grisea*. Molecules and Cells **8,** 698.

Lévy, J., Bres, C., Geurts, R., Chalhoub, B., Kulikova, O., Duc, G., Journet, E.P., Ane, J.M., Lauber, E., Bisseling, T., Denarie, J., Rosenberg, C., and Debelle, F. (2004). A putative Ca^{2+} and calmodulin-dependent protein kinase required for bacterial and fungal symbioses. Science **303,** 1361-1364.

Liu, Y.G., and Chen, Y. (2007). High-efficiency thermal asymmetric interlaced PCR for amplification of unknown flanking sequences. BioTechniques **43,** 649-656.

Liu, Z.M., and Kolattukudy, P.E. (1999). Early expression of the calmodulin gene, which precedes appressorium formation in *Magnaporthe grisea*, is inhibited by self-inhibitors and requires surface attachment. Journal of Bacteriology **181,** 3571-3577.

López-Pedrosa, A., González-Guerrero, M., Valderas, A., Azcón-Aguilar, C., and Ferrol, N. (2006). *GintAMT1* encodes a functional high-affinity ammonium transporter that is expressed in the extraradical mycelium of *Glomus intraradices*. Fungal Genetics and Biology **43,** 102-110.

Loqué, D., Lalonde, S., Looger, L.L., von Wiren, N., and Frommer, W.B. (2007). A cytosolic trans-activation domain essential for ammonium uptake. Nature **446,** 195-198.

Mahajan, S., and Tuteja, N. (2005). Cold, salinity and drought stresses: An overview. Archives of Biochemistry and Biophysics **444,** 139-158.

Maillet, F., Poinsot, V., André, O., Puech-Pagès, V., Haouy, A., Gueunier, M., Cromer, L., Giraudet, D., Formey, D., Niebel, A., Martinez, E.A., Driguez, H., Bécard, G., and Dénarié, J. (2011). Fungal lipochitooligosaccharide symbiotic signals in arbuscular mycorrhiza. Nature **469,** 58-63.

Maldonado-Mendoza, I.E., Dewbre, G.R., and Harrison, M.J. (2001). A phosphate transporter gene from the extra-radical mycelium of an arbuscular mycorrhizal fungus *Glomus intraradices* is regulated in response to phosphate in the environment. Molecular Plant-Microbe Interactions **14,** 1140-1148.

Mansilla, M.C., Banchio, C.E., and Mendoza, D. (2008). Signalling pathways controlling fatty acid desaturation. Lipids in Health and Disease**,** 71-99.

Martin, F., Gianinazzi-Pearson, V., Hijri, M., Lammers, P., Requena, N., Sanders, I.R., Shachar-Hill, Y., Shapiro, H., Tuskan, G.A., and Young, J.P.W. (2008). The long hard road to a completed *Glomus intraradices* genome. New Phytologist **180,** 747-750.

Massoumou, M., van Tuinen, D., Chatagnier, O., Arnould, C., Brechenmacher, L., Sanchez, L., Selim, S., Gianinazzi, S., and Gianinazzi-Pearson, V. (2007). *Medicago truncatula* gene responses specific to arbuscular mycorrhiza interactions with different species and genera of Glomeromycota. Mycorrhiza **17,** 223-234.

Mazars, C., Bourque, S., Mithofer, A., Pugin, A., and Ranjeva, R. (2009). Calcium homeostasis in plant cell nuclei. New Phytologist **181,** 261-274.

McAinsh, M.R., and Pittman, J.K. (2009). Shaping the calcium signature. New Phytologist **181,** 275-294.

Mitra, R.M., Gleason, C.A., Edwards, A., Hadfield, J., Downie, J.A., Oldroyd, G.E.D., and Long, S.R. (2004). A Ca^{2+}/calmodulin-dependent protein kinase required for symbiotic nodule development: Gene identification by transcript-based cloning. Proceedings of the National Academy of Sciences USA **101,** 4701-4705.

Morandi, D., Prado, E., Sagan, M., and Duc, G. (2005). Characterisation of new symbiotic *Medicago truncatula* (Gaertn.) mutants, and phenotypic or genotypic complementary information on previously described mutants. Mycorrhiza **15,** 283-289.

Nash, M.S., Young, K.W., Challiss, R.A.J., and Nahorski, S.R. (2001). Intracellular signalling: receptor-specific messenger oscillations. Nature **413,** 381-382.

Navazio, L., and Mariani, P. (2008). Calcium opens the dialogue between plants and arbuscular mycorrhizal fungi. Plant Signaling & Behavior **3,** 229-230.

Oldroyd, G.E.D., Harrison, M.J., and Udvardi, M. (2005). Peace talks and trade deals. Keys to long-term harmony in legume-microbe symbioses. Plant Physiology **137,** 1205-1210.

Oldroyd, G.E.D., and Downie, J.A. (2006). Nuclear calcium changes at the core of symbiosis signalling. Current Opinion in Plant Biology **9,** 351-357.

Oldroyd, G.E.D., Harrison, M.J., and Paszkowski, U. (2009). Reprogramming plant cells for endosymbiosis. Science **324,** 753-754.

Pandey, S., Tiwari, S.B., Tyagi, W., Reddy, M.K., Upadhyaya, K.C., and Sopory, S.K.

(2002). A Ca^{2+}/CaM-dependent kinase from pea is stress regulated and in vitro phosphorylates a protein that binds to *AtCaM5* promoter. European Journal of Biochemistry **269,** 3193-3204.

Parniske, M. (2008). Arbuscular mycorrhiza: the mother of plant root endosymbioses. Nature Reviews Microbiology **6,** 763-775.

Pfaffl, M.W. (2001). A new mathematical model for relative quantification in real-time RT–PCR. Nucleic acids research **29,** e45-e45.

Pittman, J.K., Edmond, C., Sunderland, P.A., and Bray, C.M. (2009). A cation-regulated and proton gradient-dependent cation transporter from *Chlamydomonas reinhardtii* has a role in calcium and sodium homeostasis. Journal of Biological Chemistry **284,** 525-533.

Requena, N., Breuninger, M., Franken, P., and Ocon, A. (2003). Symbiotic status, phosphate, and sucrose regulate the expression of two plasma membrane H^+-ATPase genes from the mycorrhizal fungus *Glomus mosseae*. Plant Physiology **132,** 1540-1549.

Rho, H.E.E.S., Jeon, J., and Lee, Y.H. (2009). Phospholipase C‐mediated calcium signalling is required for fungal development and pathogenicity in *Magnaporthe oryzae*. Molecular Plant Pathology **10,** 337-346.

Roussel, H., Van Tuinen, D., Franken, P., Gianinazzi, S., and Gianinazzi-Pearson, V. (2001). Signalling between arbuscular mycorrhizal fungi and plants: identification of a gene expressed during early interactions by differential RNA display analysis. Plant and soil **232,** 13-19.

Sanchez, L., Weidmann, S., Arnould, C., Bernard, A.R., Gianinazzi, S., and Gianinazzi-Pearson, V. (2005). *Pseudomonas fluorescens* and *Glomus mosseae* trigger *DMI3*-dependent activation of genes related to a signal transduction pathway in roots of *Medicago truncatula*. Plant Physiology **139,** 1065-1077.

Satrústegui, J., Pardo, B., and del Arco, A. (2007). Mitochondrial transporters as novel targets for intracellular calcium signaling. Physiological Reviews **87,** 29-67.

Schüβler, A., Schwarzott, D., and Walker, C. (2001). A new fungal phylum, the Glomeromycota: phylogeny and evolution. Mycological Research **105,** 1413-1421.

Scotto–Lavino, E., Du, G., and Frohman, M.A. (2007). 3′ end cDNA amplification using classic RACE. Nature Protocols **1,** 2742-2745.

Seddas, P.M.A., Arnould, C., Tollot, M., Arias, C.M., and Gianinazzi-Pearson, V. (2008). Spatial monitoring of gene activity in extraradical and intraradical

developmental stages of arbuscular mycorrhizal fungi by direct fluorescent in situ RT-PCR. Fungal Genetics and Biology **45,** 1155-1165.

Seddas, P.M.A., Arias, C.M., Arnould, C., van Tuinen, D., Godfroy, O., Benhassou, H.A., Gouzy, J., Morandi, D., Dessaint, F., and Gianinazzi-Pearson, V. (2009). Symbiosis-related plant genes modulate molecular responses in an arbuscular mycorrhizal fungus during early root interactions. Molecular Plant-Microbe Interactions **22,** 341-351.

Siciliano, V., Genre, A., Balestrini, R., Cappellazzo, G., deWit, P.J.G.M., and Bonfante, P. (2007). Transcriptome analysis of arbuscular mycorrhizal roots during development of the prepenetration apparatus. Plant Physiology **144,** 1455-1466.

Smith, S.E., and Gianinazzi-pearson, V. (1988). Physiological Interactions between Symbionts in Vesicular-Arbuscular Mycorrhizal Plants. Annual Review of Plant Physiology and Plant Molecular Biology **39,** 221-244.

Smith, F.A., and Smith, S. (1997). Transley review No 96. Structural diversity in (vesicular)–arbuscular mycorrhizal symbioses. New Phytologist **137,** 373-388.

Smith, S.E., and Read, D.J. (2008). Mycorrhizal symbiosis (Third Edition). Academic Press, London, pp 800.

Steinkellner, S., Lendzemo, V., Langer, I., Schweiger, P., Khaosaad, T., Toussaint, J.P., and Vierheilig, H. (2007). Flavonoids and strigolactones in root exudates as signals in symbiotic and pathogenic plant-fungus interactions. Molecules **12,** 1290-1306.

Strullu, D., Gourret, J., Garrec, J., and Fourcy, A. (1981). Ultrastructure and electron-probe microanalisis of the metachromatic vacuolar granules occurring in taxus mycorrhizas. New Phytologist **87,** 537-545.

Szabadkai, G., and Duchen, M.R. (2008). Mitochondria: The hub of cellular Ca^{2+} signaling. Physiology **23,** 84-94.

Szigeti, R., Miseta, A., and Kellermayer, R. (2005). Calcium and magnesium competitively influence the growth of a PMR1 deficient *Saccharomyces cerevisiae* strain. FEMS Microbiology Letters **251,** 333-339.

Tamasloukht, M.B., Séjalon-Delmas, N., Kluever, A., Jauneau, A., Roux, C., Bécard, G., and Franken, P. (2003). Root factors induce mitochondrial-related gene expression and fungal respiration during the developmental switch from asymbiosis to presymbiosis in the arbuscular mycorrhizal fungus *Gigaspora rosea*. Plant Physiology **131,** 1468-1478.

Tamasloukht, M.B., Waschke, A., and Franken, P. (2007). Root exudate-stimulated RNA accumulation in the arbuscular mycorrhizal fungus *Gigaspora rosea*. Soil Biology and Biochemistry **39,** 1824-1827.

Tisserant, E., Kohler, A., Dozolme-Seddas, P., Balestrini, R., Benabdellah, K., Colard, A., Croll, D., Da Silva, C., Gomez, S.K., Koul, R., Ferrol, N., Fiorilli, V., Formey, D., Franken, P., Helber, N., Hijri, M., Lanfranco, L., Lindquist, E., Liu, Y., Malbreil, M., Morin, E., Poulain, J., Shapiro, H., van Tuinen, D., Waschke, A., Azcón-Aguilar, C., Bécard, G., Bonfante, P., Harrison, M.J., Küster, H., Lammers, P., Paszkowski, U., Requena, N., Rensing, S.A., Roux, C., Sanders, I.R., Shachar-Hill, Y., Tuskan, G., Young, J.P.W., Gianinazzi-Pearson, V., and Martin, F. (2012). The transcriptome of the arbuscular mycorrhizal fungus *Glomus intraradices* (DAOM 197198) reveals functional tradeoffs in an obligate symbiont. New Phytologist **193,** 755-769.

Tollot, M., Hoi, J.W.S., van Tuinen, D., Arnould, C., Chatagnier, O., Dumas, B., Gianinazzi-Pearson, V., and Seddas, P.M.A. (2009). An *STE12* gene identified in the mycorrhizal fungus *Glomus intraradices* restores infectivity of a hemibiotrophic plant pathogen. New Phytologist **181,** 693-707.

Ton, V.K., and Rao, R. (2004). Functional expression of heterologous proteins in yeast: insights into Ca^{2+} signaling and Ca^{2+}-transporting ATPases. American Journal of Physiology-Cell Physiology **287,** C580-C589.

Trouvelot A, Kough JL, Gianinazzi-Pearson V. (1986). Mesure du taux de mycorrhization VA d'un systeme radiculaire. Recherche des methodes d'estimation ayant une signification fonctionnelle. In: V. Gianinazzi-Pearson and S. Gianinazzi (Eds.), The Mycorrhizae: Physiology and Genetic, INRA Press, Paris, 217-221.

Vadassery, J., and Oelmüller, R. (2009). Calcium signaling in pathogenic and beneficial plant microbe interactions: what can we learn from the interaction between *Piriformospora indica* and *Arabidopsis thaliana*. Plant Signaling & Behavior **4,** 1024-1027.

Wakelam, M.J.O. (1998). Diacylglycerol–when is it an intracellular messenger? Biochimica et Biophysica Acta **1436,** 117-126.

Weidmann, S., Sanchez, L., Descombin, J., Chatagnier, O., Gianinazzi, S., and Gianinazzi-Pearson, V. (2004). Fungal elicitation of signal transduction-related plant genes precedes mycorrhiza establishment and requires the *dmi3* gene in *Medicago truncatula*. Molecular Plant-Microbe Interactions **17,** 1385-1393.

Zézé, A., Dulieu, H., and Gianinazzi-Pearson, V. (1994). DNA cloning and screening of a partial genomic library from an arbuscular mycorrhizal fungus, *Scutellospora castanea*. Mycorrhiza **4,** 251-254.

Acknowledgements

This thesis was completed within the context of a postgraduate education and training agreement between Huazhong Agricultural University, Wuhan, China (President Professor Deng Xiu Xin), and the University of Burgundy, Dijon, France (President Professor Sophie Béjean). I am grateful to the National Natural Science Foundation of China for financial support of the 1st year research period in Wuhan, and to the Chinese Ministry of Education (State Scholarship) for travelling costs and living expenses during the 2nd and 3rd year period in Dijon.

I am greatly indebted to Professor Bin Zhao (State Key Laboratory of Agricultural Microbiology, Huazhong Agricultural University), and Dr. Vivienne Gianinazzi-Pearson (UMR INRA/CNRS/Burgundy University, INRA centre, Dijon) who jointly supervised my research work. My sincere thanks go to Professor Bin Zhao for his valuable suggestions and comments on my work, the organization of the research in China, and for a chance to do further study in France. Many thanks also go to Ms. Hui Lin, Nianwu Tang and all the colleagues of the State Key Laboratory of Agricultural Microbiology, for their help and concern.

I am particularly grateful to Drs. Vivienne Gianinazzi-Pearson and Diederik van Tuinen who supervised my scientific progress, greatly helped me to organize and conduct research in France, and advised me in the English writing of the thesis and articles. I express my thanks for their continual guidance, encouragement and support both in solving different problems of work organization and life in a different country. I express my gratitude particularly to Ms. Christine Arnould (Microscope Centre and Pôle IPM, Dijon) for her help and guidance in the research with laser cell microdissection and *in situ* RT-PCR method, and to Ms. Anne Colombet and Ms. Valérie Monfort-Pimet, members of the Dijon laboratory, for their help in conducting experiments with mycorrhiza. Most sincere thanks to all the colleagues of the Pôle IPM and UMR PME: Dr. Silvio Gianinazzi, Prof. Daniel Wipf, Ms. Odile Chatagnier, Dr. Eliane Dumas-Gaudot, Joan Doidy, Soukayna Hayek, Virginie Molinier, Ivan Sanchez-Castro, Léonardo Casieri, Herbert Stockinger and all the other members for the chance to work together, their friendly support and concern.